OBESITY AND ITS INFLUENCE ON KNEE JOINT CONTACT FORCES IN INDIVIDUALS WITH MODERATE KNEE OSTEOARTHRITIS

by

Pouya Amiri

Submitted in partial fulfilment of the requirements
for the degree of Master of Applied Science

at

Dalhousie University
Halifax, Nova Scotia
August 2014

DEDICATION PAGE

To my family…

TABLE OF CONTENTS

LIST OF TABLES

LIST OF FIGURES

ABSTRACT

Obesity is known as a major risk factor for the development and progression of knee OA. It has been proposed to affect the joint through linked mechanical and metabolic factors. However, its precise role in the pathomechanics of the disease is still not well understood. Given the importance of altered mechanical environment in both initiation and progression of knee OA, it is crucial to examine if and how obesity may affect the joint mechanically.

This thesis is a continuing work of our group on the role obesity and its influence on joint mechanics. Previous work in our group showed that obese individuals walk with altered pattern of knee joint loading and furthermore, obesity may expose the joint to higher absolute contact forces, found through an inverse dynamics model. Following the previous work by our group, in this thesis we used the method of principal component analysis to examine the role of obesity and its interaction with moderate knee OA on the neuromuscular patterns of major knee muscles. Our results showed that obese individuals walk with altered muscular activity, which was associated with delayed and prolonged activation of gastrocnemius muscles and sustained activation of the quadriceps muscles. This may result in sustained loading of the joint, proposed to be detrimental to joint integrity.

Following our first study on the neuromuscular patterns of major knee muscles, we implemented an electromyography driven model to incorporate the real EMG activity of knee muscles to estimate muscle forces and subsequently tibiofemoral joint contact forces. The model was validated against existing literature and then were calibrated for an asymptomatic obese and a healthy weight subject in order to find their medial, lateral, and total joint contact forces. This case study demonstrated the ability of the model to take into account the real activation patterns of the muscles in the estimation of muscle and knee joint contact forces. Furthermore, it was demonstrated the obese individual walked with higher absolute tibiofemoral joint contact forces compared to the healthy weight subject. This result will be further investigated by applying the model a large cohort with a range of BMI in the future.

LIST OF ABBREVIATIONS USED

OA	osteoarthritis
EMG	electromyography
PCA	principal component analysis
JSN	joint space narrowing
BMI	body mass index
BW	body weight
GRF	ground reaction force
ROM	range of motion
DOF	degree of freedom
KL	kellgren Lawrence
MVIC	maximum voluntary isometric contraction
PC	principal component
ANOVA	analysis of variance
HW	healthy weight
OB	obese
OV	overweight
AMTI	advanced mechanical technology incorporation
MTU	musculotendon
AP	anteroposterior
PD	proximal/distal
CC	contractile component
PEC	parallel elastic component
SEC	series elastic component
ODE	ordinary differential equation
RMSE	root mean squared error
VL	vastus lateralis
VM	vastus medialis
VI	vastus intermedius
RF	rectus femoris
SM	semimembranosus
ST	semitendinosus
BFLH	biceps femoris long head
BFSH	biceps femoris short head
LG	lateral gastrocnemius
MG	medial gastrocnemius
LH	lateral hamstrings
MH	medial hamstrings

ACKNOWLEDGEMENTS

I would like to first thank my supervisor Dr. Janie Astephen Wilson for her support and enthusiasm during this work. Dr. Wilson taught me how to organize an appropriate research plan, resulting in valuable findings. I would like to thank the research group at the Dynamics of Human Motion Lab, especially Jereme Outerleys who has been helping me a lot for data processing in the lab. Finally, I would like to thank my family for their love and support.

CHAPTER 1 INTRODUCTION

1.1 INTRODUCTION

Knee osteoarthritis (OA) is a progressive joint disease associated with a huge personal and societal burden. Numerous interrelated factors are involved in the initiation and progression of the disease. Although, a great deal of effort has been dedicated to develop effective treatment options for knee OA, still there is no cure for the disease, due to the existence of numerous risk factors, and their complex interactions. Unfortunately, the last treatment option available is total knee replacement, which is highly invasive and undesirable.

A broad range of risk factors such as age, sex, and joint trauma are associated with the initiation and progression of knee OA, over a few of which we have control. Obesity is the most important modifiable risk factors associated with knee OA. It is believed that obesity endangers the joint environment through linked mechanical and metabolic factors. Mechanically, obesity has been proposed to expose the joint to excessive loading, resulting in injurious stress, which is known as the major player in the initiation and progression of OA. Metabolically, obesity has been reported to destabilize joint homeostasis through the overexpression of some hormones, which weakens the structural integrity of the joint and makes it vulnerable to mechanical loading. Although, altered metabolism of joint is an important factor, mechanical insult is the main initiator of the disease, and as long as the abnormal biomechanic environment of the joint is not taken care of, the joint will not heal. The huge amount of endeavor to develop pharmaceutical interventions to ameliorate the diseased joint, although, has been successful in treating the symptoms, but not in halting or slowing the progression, because these treatments often do not address underlying pathomechanics of the disease. Keeping this in mind, one of the keys to understanding the influence of obesity in the pathomechanics of OA is to examine joint biomechanics

for alterations due to increased weight and body size (not only due to increased loading, but also due to altered pattern of the joint loading and kinematics of the gait).

Knee OA and obesity induce altered gait kinematics and kinetics, and neuromuscular patterns during self-selected gait, compared to normal gait. Although, modified gait characteristics have been widely characterized for knee OA, there is still a lack of information over the role of obesity in biomechanics of walking, specifically its effect on joint loading. Previous work in our group showed that obese individuals walk with altered pattern of the knee joint loading [1] and furthermore, obesity may expose the joint to higher absolute contact forces found through an inverse dynamics model [2]. However, there has not been any studies, examining the neuromuscular alterations due to obesity and its interaction with knee OA. Furthermore, to take into account possibly altered neuromuscular activities in the estimation of the knee joint contact forces, a model capable of incorporating the measured activity of the muscle should be developed. Considering muscles are main determinants of joint contact loading, this will give us a better understanding of the potential role of muscles in the production of possibly large forces inside the joint that may predispose the joint toward knee OA initiation or progression. Therefore, the main objectives of this thesis were to first examine the alterations in the neuromuscular patterns of knee periarticular muscles and then implement an EMG-driven model to estimate medial, lateral, and total tibiofemoral joint contact forces and demonstrate the utility of the model to examine the role of obesity on knee joint contact loading.

1.2 OBJECTIVES

Although, there is a consensus over the role of obesity as one of the most important modifiable risk factor associated with knee OA, the mechanism through which it affects the joint is still unclear. Both mechanical and metabolic factors seem to contribute to the disease; however, it has been widely accepted that an altered mechanical

environment of the joint is the major player in knee OA. Therefore, there is a need to closely inspect the mechanical environment of the knee in obese individuals to determine any possible alteration that may be contributing to the disproportionate rate of OA development in the obese. This thesis is a continuing work of our group on the role obesity and its influence on joint mechanics.

1.3 Objective 1: Alteration in Neuromuscular Patterns of Knee Muscles

Altered joint loading due to obesity and OA suggests that the muscles spanning the knee joint actuate the joint differently compared to a healthy joint. This can be due to alteration in muscle activity or muscle physiological properties. Furthermore, it has been proposed that obese individuals may have the ability to adopt neuromuscular patterns different from healthy weight individuals, helping them to achieve lower loads on their knees. Therefore, the first objective was *to examine the interacting role of obesity and moderate knee osteoarthritis on neuromuscular patterns of the periarticular knee musculature during self-selected gait*. Principal component analysis was used to examine not only differences in activation magnitudes, but also patterns throughout the gait cycle, as EMG patterns have been implicated in the knee OA disease process in previous research by our team. It was hypothesized that obesity and moderate knee OA both are associated with altered lower limb muscle activity. It was further hypothesized that neuromuscular changes occur in association with the interaction between obesity and moderate knee OA disease presence.

1.4 Objective 2: Implementing an EMG-Driven Model of Knee to Calculate Medial, Lateral, and Total Tibiofemoral Joint Contact Forces and Performing a Case Study to Examine the Effect of Obesity on the Joint Contact Forces

Due to the importance of contact load distribution on the joint in knee OA, particularly in understanding the role of obesity in knee OA initiation and progression, there is a

need to develop a model that is capable of estimating the amount of the loads applied to the medial and lateral compartments of the knee, using experimental three dimensional gait and EMG data. The model should be able to incorporate actual activation patterns of muscles, which may be subject specific, or altered due to pathology or obesity. Therefore, the second objective was to *implement an electromyography driven musculoskeletal model to estimate total, medial and lateral tibiofemoral contact forces during self-selected gait and perform a case study to examine the influence of obesity on knee joint contact forces.* It was hypothesized that obesity would result in higher tibiofemoral joint contact forces due to increased body mass.

1.5 STRUCTURE OF THESIS

This thesis is organized into five chapters. Chapter 2 gives a literature review on OA, obesity, and musculoskeletal modeling for tibiofemoral joint contact calculation. Chapter 3 contains the results of our analysis on the effect of obesity and its interaction with knee OA on the neuromuscular patterns of major knee periarticular muscles (objective 1). Chapter 4 explains the details of different steps of the implementation of an EMG-driven model, the validation of the model against literature values, and a case study, performed to examine the effect of obesity on knee joint contact forces (objective 2). Finally, chapter 5 summarizes the thesis and it implications and limitations, followed by concluding remarks and direction for future research.

CHAPTER 2 BACKGROUND

2.1 KNEE OSTEOARTHRITIS

Osteoarthritis (OA) is a degenerative joint disease, which results in loss of articular cartilage, joint space narrowing, bony changes, pain and impaired mobility [3]. It is a leading cause of disability world-wide [4], resulting in a huge societal burden, both in terms of personal suffering and use of healthcare system [5]. The prevalence of OA is increasing with an alarming rate in Canada [6], with Nova Scotia having the highest rate in the country [7].

OA is a complex musculoskeletal disease, emanating from different interrelated biological, mechanical, and structural factors [8]. It is defined as a group of overlapping distinct diseases with different etiologies, with similar biologic, morphologic, and clinical outcomes, affecting the entire joint, including articular cartilage, subchondral bone, ligaments, capsules, synovial membrane, and periarticular muscles [9]. OA is the result of the disruption of a joint's normal stable environment, and believed to start due to a mechanical insult [10]. Andriacchi et al. proposed a framework for the initiation and progression of OA after an ACL (anterior cruciate ligament) injury, stating the process can start by a change in the normal kinematics of the joint, resulting in a spatial shift of the load bearing area on cartilage and its subsequent fibrillation, which is then followed by enhanced friction forces, causing matrix breakdown [8]. Following the start of the insult to the joint, which does not necessarily mean insult to articular cartilage [11], other pathways also come to action to halt degeneration and heal the joint [10]. Subchondral bone, which is responsible for attenuation of the transferred load to the joint through its viscoelastic properties, starts to remodel and thicken [10]. This newly nonmineralized bone instead of improving the joint capacity to withstand external loads, causes the thinning of articular cartilage, and can worsen the state of the joint [12]. Furthermore, the breakdown of the cartilage is mediated by matrix metalloproteinases, whose production is induced by cytokines released by chondrocytes

in response to injurious mechanical loads [10]. Beyond the direct effect of mechanical insult, capsule/synovium of the joint with OA may have an additive effect, resulting in enhanced release of chemical substances and contribute to faster degradation of the damaged cartilage [10]. The procedure explained above applies to secondary knee OA. However, there is a huge range of demographical risk factors for the development of knee OA, such as Obesity, Sex, Age, race, etc. The mechanism through which each individual factor contributes to the disease is different, however, the outcomes and symptoms are similar.

2.1.1 Gait analysis

Gait analysis is a valuable tool that gives us the ability to examine the biomechanics of human gait and understand the underlying mechanisms of normal and pathological walking [13]. Modern gait analysis uses motion capture and force platform to provide important information about the kinematics and kinetics of walking. To explain, the three-dimensional movement of body segments are tracked by passive or active markers, attached to each segment, and ground reaction force (GRF), which is usually the only external force, acting on the body during normal walking, is measured using a force platform [14]. A simplified model of the body, composed of segments, articulating relative to each other is considered and the measured marker data are used to calculate the joint angles in each instance in time during the gait. This step, called inverse kinematics, can be performed using different methods, including Cardan/Euler [15], Joint Coordinate System [15], and Helical axis methods [16]. Afterward, the body segment physical properties are estimated usually based on regression equations obtained through cadaver studies (anthropometrics) [14]. Finally, inverse kinematics outputs, GRF, and anthropometric data altogether are used as input to Newton's equations to estimate the moments and forces that produce the movement (inverse dynamics). Obtained moments and forces are the result of muscles, ligaments and articular contact forces. Among obtained variables through inverse kinematic and dynamic analysis, knee flexion-extension angle, net resultant knee flexion-extension and net resultant knee abduction/adduction moments have been used in literature as

important parameters, providing us with a better understanding of knee mechanics and especially possible alterations due to knee OA and obesity.The knee is the joint most commonly afflicted by OA [17], and most frequently associated with disability and symptoms [18]. Gait analysis is considered to be a very important marker, revealing information about the in vivo function of the joint [8]. Furthermore, walking is the most common dynamic daily activity, loading the knee joint [19] and one of the most common functional deficits reported by those suffering from knee OA [20]. Therefore, numerous gait studies investigated the effect of knee OA on the biomechanics of walking. Most commonly reported changes are slower walking speed and decreased stride length [21, 22], decreased knee flexion angles [21-23], and moments [22, 24], and increased peak knee adduction moment [19, 21, 22, 24]. The knee adduction moment has been shown to be associated with severity [24], progression [25], and symptoms of knee OA [26]. It is considered to be a measure of the relative distribution of load on the medial and lateral compartments of the knee [27], explaining the in vivo environment of the joint. These alterations due to the disease, however, have not been reported in all studies, specifically in individuals with moderate stages of knee OA. Some studies found no difference in the peak knee adduction moment [28, 29], walking speed [28, 29], and knee flexion angle between asymptomatic and individuals with moderate knee OA [28]. This may have happened due to differences in demographics and severity of knee OA and the methodological differences among studies. Some of the mentioned studies used multivariate objective analysis method, principal component analysis (PCA), allowing them to examine amplitude and temporal differences among waveforms, rather than only comparing peak and mean parameters subjectively [22, 30-33].

2.1.2 Electromyography

Muscles are primary structures that cause body movement. However, inverse dynamics and kinematics do not provide us with sufficient insight to the muscle activity. Electromyography (EMG) is an experimental technique concerned with the development, recording and analysis of myoelectric signals, resulting from the

propagation of action potentials through muscle fibers [34]. EMG is essentially superposed action potentials of active motor units innervating muscle fibers and can be measured using especial electrodes through skin in the form of voltages (called raw EMG) [35]. The voltage usually varies between ±5 millivolt, with frequency contents between 6 and 500 Hz [34]. Raw EMG data can give us some information such as the periods that the muscle are on or off; however, for quantitative amplitude analysis usually raw EMG signals are processed to increase the reliability and validity of findings [14, 35]. Raw EMG signal is first full wave rectified (all negative values are converted to positive values) and then smoothened (using different methods, such moving average, low pass filter, etc) and the results are called linear enveloped EMG wavforms [34]. Obtained EMG signal (millivolt scaled) strongly depend on the experimental condition, such as electrode placement, and cannot be used for other purposes, such as force estimation, comparison among different muscles, or subjects. One solution to overcome this problem is normalizing obtained signals to a reference value. The most popular method to obtain a reference value for the normalization is to perform maximum voluntary contractions (MVC), with the aim of eliciting maximal activity of muscles that can be used as the reference values [34]. Linear enveloped EMG waveforms are usually normalized to MVC values and then can be used for comparison purposes among different muscles or among different cohorts (e.g. asymptomatic group against knee OA group) or use as input to other algorithms such as an EMG-driven model to estimate muscle forces. EMG waveforms have been used in literature in different studies to characterize muscle activities during normal human movement [36] and alterations that happen in different pathologies such as cerebral palsy [37, 38], and knee OA [39].

Alterations in the activity of lower limb muscles have been reported in individuals with moderate knee OA during walking [40]. Increased lateral muscle co-contraction has been shown in individuals with knee OA regardless of severity, joint alignment, or laxity.[33, 39, 41-43]. Alterations were also reported in the amplitude of the EMG activity of muscles, including higher activity for vastii [43-45] and hamstrings muscles [44-46]; although, the EMG amplitude of gastrocnemius muscles were not changed in

the presence of moderate knee OA [46, 47]. The duration of the activity of gastrocnemius muscles were reported not to be affected by moderate knee OA [31, 46, 48], while vastus lateralis and rectus femoris [31, 39, 48], and hamstrings activity [31, 39] durations were reported to be higher for individuals with moderate knee OA. These altered muscle activity patterns in individuals with knee OA may have deleterious effects on joint loading and stability and further modeling studies should be performed to examine how the joint contact forces are altered in the presence of these alterations in muscle activity.

Joint damage occurs when the structures protecting the joint fail, and this happens when there is an impairment of joint protectors or when transarticular loads go beyond the physiological limits [49]. Based on this, risk factors can be viewed as factors that endanger the joint integrity and those causing excessive loading [49], especially high load rates [10]. Different systemic risk factors, such as age, female sex, genetic predisposition, higher insulin-like growth factor-1, accompanied by local risk factors, such as malalignment, mis-shapened joints, proprioceptive deficiencies, meniscal damage, and muscle strength may result in joint vulnerability [5]. On the other hand, obesity and occupational activities, for example, cause excessive loading of the joint [5].

2.2 OBESITY

Based on what is called by World Health Organization as a global epidemic of obesity, increased rate of obesity and overweight will cause a devastating impact on the health of societies [50]. In Canada as part of this global epidemic, the rate of obesity increased from 11.5% and 15.7% reported in 1978 to 22.9% and 23.2% for men and women in Canadian population, showing a sharp increase [51]. Furthermore, it is reported the prevalence of childhood overweight has increased dramatically in economically developed countries [52], which is unfortunate due its influence on young people's psychosocial development and long-term effects on mortality and morbidity [53]. Obesity increases the risk of a number of chronic diseases.

Body mass index (BMI) is usually used as a variable to assess obesity. Although, it has been considered as a convenient and almost effective measure of obesity in children and adolescents [35], there are some limitations with it. In two review studies it was found that BMI as measure of obesity has high specificity but low sensitivity to detect excess adiposity and fails to identify over a quarter of children and half of the people with excess body fat percentage [36, 37], especially when BMI is less than 30 kg/m2 [38]. Furthermore, it is not an appropriate measure for individuals with muscular bodies such as body builders [39]. Using other method such as bioelectric impedance can give us a better understanding of individuals' body fat [38]. In this thesis, due to its wide use we used BMI to categorize our subjects into different groups.

Obesity is known to be the most important modifiable risk factor for knee OA [54-59]. The potential role of obesity in the initiation of knee OA is doubtless [60, 61]; however, there is controversy over its effect on the structural progression of knee OA; some studies reported significant progression [62, 63], while others did not [64, 65], and this seems to be the results of two reasons. First, the usual criterion used to assess the progression of the disease is joint space narrowing (JSN), which has been proposed to be insensitive to the changes happening in the joint and produce variable results [66]. Second, the effect of obesity is modified due to the coexistence of other risk factors, associated with knee OA, most importantly knee malalignment [66], which is itself a major risk factor for the disease, imposing its effect by changing the internal loading of the joint [67]. It has been reported that the effect of body mass on progression may depend on the extent of malalignment [65, 66, 68]; however, how the two factors interact is not known. Felson et al. reported that BMI does not have any effect on disease progression for neutral or severe malaligned knee; however, can affect knees with moderate malalignment [66]. Niu et al. stated that high BMI increases the risk of progression for knees with neutral alignment, but not varus malalignment. Furthermore, BMI can have small effects on the progression of valgus aligned knees [65]. Therefore, it is needed to consider knee alignment, when examining the effect of obesity in the progression of knee OA.

Although the true mechanism of the obesity in knee OA is not known, the role of both mechanical [49] and metabolic processes [69] are widely accepted. However, how these two interact and which one precedes the other one, is not known. Grotle et al. suggested knee OA is correlated to the OA of hand and wrist [70], while Pottie et al. reported the correlation between obesity and OA of non-load bearing joints [71]. These two studies suggest that there may be systemic risk factors associated with knee OA. Adipose tissue is an endocrine organ, capable of releasing substances such as cytokines and adipocytokines (for example, leptin, resistin, and adiponectin). The overexpression of these substances may destabilize the homeostasis of the joint and result in cartilage degeneration [69].

The other hypothesis emphasizes on increased knee joint loading as the primary effect of obesity, causing knee OA [49]. Based on the framework proposed by Andriacchi, the initiation of knee OA is the result of altered joint kinematics, causing the load bearing area of the joint to be changed, which then followed by high shear forces emanating from compressive forces, resulting in the breakdown of articular cartilage [8]. It has been shown that obese people walk with increase total energy expenditure, showing altered movement strategies [72]. These modified gait behaviors may result in a change in the kinematic environment of the knee, followed by large compressive loads due to higher body weight, consistent with Andriacchi's framework.

Considering the proposed hypothesis on the mechanical role of obesity in knee OA, gait analysis can be used as a valuable tool to examine the in vivo mechanics of the joint in obese individuals. Alteration in gait biomechanics in obese people may be categorized as "mass driven" or "behavioral" adaptations [73]. "Mass driven" adaptations refer to direct, intuitive consequences of increased BMI, such as increased ground reaction force (GRF). On the other hand, "behavioral" adaptations refer to the indirect results of increased weight, over which the person has options, for example, smaller stride length. Both kinds of adaptations happen due to weight alteration, either gaining or losing mass. Modified kinematic gait parameters seem to be behavioral adaptations, accompanying weight alteration. Different studies showed higher BMI was associated

with slower velocity, shorter stride length, increased double support time, and decreased knee range of motion (ROM), and maximum knee flexion angle in stance phase [56, 74-77]. On the other hand, weight loss in obese people was associated with opposite results, including increased swing time, stride length, gait speed, hip ROM, maximum knee flexion, and ankle plantar flexion [73, 78, 79]. Some studies reported similar kinematics of obese and lean individuals [80, 81]. Messier et al. showed ankle and hip kinematic variables were not associated with BMI, while knee maximum extension is dependent on BMI [82]. Interestingly, DeVita et al. proposed altered gait kinematics in obese individuals may be viewed as a compensatory mechanism to prevent knee from high repetitive loading during gait by keeping the moment at a constant level [83]. They claim there is an inverse linear relationship between step length and BMI, realizing constant or even decreased knee flexion moment in obese people [83]. Similar statements have been proposed in two other studies, investigating the gait of pregnant women during pregnancy and 1 year after labor [84], and the gait of individuals, carrying backpack [85], lending support to the idea. Based on DeVita et al., the ability of obese individuals to cope with increased weight may be the real risk factor associated with knee OA [83]. Furthermore, the fact that not all obese people develop knee OA, shows the possibility of the ability of some obese individuals to modify their knee mechanical environment through 'behavioral' adaptations.

Kinetic alterations associated with obesity are less intuitive, compared to kinematics. This is especially evident in the alterations shown in previous studies in knee flexion moment. DeVita et al. reported obese individuals possess smaller sagittal plane peak knee normalized moment (/body weight) compared to lean individuals during their self-selected speed, and when walking with the same speed, they had the same normalized moment as lean individuals [83]. Furthermore, only BMI larger than 30 kg/m^2 resulted in a decrease in normalized knee sagittal moment, suggesting BMI of 30 kg/m^2 as a start point for the appearance of new neuromuscular patterns to lower knee joint loading [83]. Gushu et al. also reported obese children have the same normalized knee flexion moment (/body weight*height) as lean individuals [77]. Increased weight due to pregnancy [84] and carrying back pack [85] also did not result in increased normalized

knee flexion moment. This complication may happen due to the interaction between alteration in weight and its subsequent modified kinematics, having opposing effects on gait biomechanics. DeVita et al. stated that altered kinematics, reflected as decreased velocity, accompanied by increased peak vertical GRF maintained the knee moment at almost a constant value [83]. However, Browning et al. reported that sagittal plane absolute (not normalized, in Nm) knee moments increased due to obesity, as a result of greater peak vertical GRF and the same kinematics as lean individuals [80]. They also showed decreased velocity resulted in decreased knee joint flexion moments [80], confirming the effect of velocity on joint sagittal plane moments. However, both studies reported increased ankle plantar flexion moment due to increased obesity, possibly because of the necessity of larger forces to propel the heavier body [80, 83, 84].

On the other hand, some of the weight loss studies suggested absolute knee sagittal moment did not change after reduction in BMI [73, 86, 87]. In a study by Hortobagyi et al. obese individuals underwent massive weight loss of 33.6% of their initial weight through metabolic surgery; however, interestingly, their absolute knee and hip moment in sagittal plane did not change, ankle moment decreased, and normalized knee flexion moment increased 77.4% probably due to 7.9% increase in the walking speed [73]. All these studies strengthen the hypothesis proposed by DeVita, stating that there may be some compensatory mechanisms associated with weight modification, trying to achieve the same amount of sagittal plane knee moment.

Alteration in knee adduction moment with obesity is also not clear. The results of different studies regarding absolute knee adduction moment for people with high BMI have been different, suggesting higher moment [80], and the same moment [77]; while the latter showed normalized knee adduction moment (/body weight*height) was higher for obese individuals. This differences could have happened due to different mean BMI of the groups included in the studies, as the former included a cohort of females and males with mean BMI of 37.0 and 34.1 kg/m^2, respectively; while the other study had two groups with different mean BMI of 18.0 and 29.9 kg/m^2.

In weight loss studies, the results based on the way the knee adduction moment is presented is different; absolute knee adduction moment decreased after weight loss [73, 86], and stayed the same [88], while normalized moment was reported to decrease after weight loss [86, 87]. It also has been suggested that there may be a limit of weight loss, after which further weight reduction does not result in any further decrease in knee adduction moment [73, 87]. There is only one study reporting normalized knee rotation moment, showing decreased peak moment associated with weight loss [87]. Furthermore, in a study by our research group here at Dalhousie, Harding et al. used PCA to analyze the effect of obesity and OA and their interaction on biomechanics of gait. They found alterations in gait biomechanics due to obesity are in the patterns of knee joint loading rather than only peak and mean parameters. Their results showed obese individuals had lower late stance normalized extension moment, and more constant normalized knee adduction and rotation moments during stance [1].

Given the associations found in previous work between the knee adduction moment, and initiation, progression, and severity of knee OA, taken together previous study suggests that a higher BMI is associated with altered mechanics that may be detrimental to the mechanical integrity of the knee joint, and also that weight loss may improve mechanics in a favorable direction, supporting the notion that weight loss could be considered as an effective treatment option for knee OA. However, when prescribing weight loss and exercise as a treatment for knee OA, it must be noted that decreased BMI usually results in increased velocity which otherwise increases GRF, counteracting the effect of weight loss on knee joint loading [73]. More works needs to be done to understand how the myriad of joint-level changes that may accompany weight loss affect the amount, frequency and duration of joint loading to fully understand mechanical repercussions of the treatment.

2.3 KNEE JOINT CONTACT MODELING

Given the crucial importance of the internal mechanical environment of knee in the initiation and progression of knee OA, determining articular contact loading in the knee joint can further our understanding of the pathomechanics of the disease. The first method is the direct measurement of contact forces using instrumented prosthesis [89]; use of this method is limited to individuals who are implanted with total knee replacement, which is highly invasive and undesirable; furthermore, these people usually develop different neuromuscular patterns after the surgery [32]. Therefore, considering muscles as primary contributors to joint loading [90], the loading environment of the knee may be altered.

Another approach is the use of musculoskeletal modeling, which can be employed to predict articular contact, muscle and ligament forces, and tissue-level stress and strain, which are major quantities in biomechanical studies [89]. Musculoskeletal modeling makes us capable of developing subject specific analysis in order to explore different treatment options, reduce the level of subjectivity in treatment planning process, usually seen in clinical settings, and optimize clinical outcomes on an individual patient basis [89]. The most significant barrier against wide use of these models in clinical settings, is the lack of validation studies, proving the developed computational model predicts biomechanical quantities accurately [89]. The use of instrumented prosthesis opens an opportunity to directly measure articular contact forces and thus offers an opportunity to indirectly validate modeling approaches, determining articular contact forces through calculated muscle forces [91]; however, this can be done only on a specific group of individuals who are candidates for knee replacement, which is usually the last treatment option available. Therefore, in earlier stages of the disease, when there is a need to develop interventions to ameliorate the mechanical loading on the joint and halt the progression of the disease, the only possible approach is the use of computational methods. To do so, muscle forces must be first estimated, which can then be used to

predict articular contact forces; however, the problem is the redundancy present in musculoskeletal system, making the unique computational prediction of muscle forces impossible [90]. Furthermore, direct measurements of muscle forces in vivo is limited to minimally invasive measurements in superficial tendons [92], or the measurements of the muscle forces using force transducer placed on tendons in operation room and removed at the end of surgery [93], which are also not feasible in clinical settings [91]. To complicate matters, determination of tibiofemoral contact forces itself is an indeterminate problem, because at least two regions of contact exists [89]. Despite these limitations, musculoskeletal modeling has been used in different studies and in some cases successful in predictions. Three different methods have been employed in research studies to predict mentioned biomechanical quantities; namely reduction methods, optimization methods, and EMG driven methods [89], all of which try to resolve the redundancy in musculoskeletal system.

One possible solution to solve the redundancy problem in musculoskeletal system is the use of reduction method, seeking to reformulate the muscle force estimation problem so that the number of unknown muscle forces equals the number of equations available from inverse dynamics [89]. This is usually done by removing the unknown muscle forces or combining the muscles that do the same function [89]. In spite of its simplicity, in some studies it turned out to predict total knee joint contact forces, sufficiently close to their true values [94, 95]; however, it is not able to capture coactivation among muscles [89] and therefore, is not appropriate for examining joint loading in knee OA, as it has been shown that individuals even with moderate levels of knee OA walk with increased co-contraction of lower limb muscles [31].

Optimization based methods resolve the redundancy problem of musculoskeletal system by usually minimizing (or maximizing) a performance criterion [91]. They can be inverse or forward dynamic simulations, based on the method the equations of motion of the skeletal system are used, and can be static or dynamic optimization, based on the way the optimization index is formulated [91].

Inverse dynamic based optimization solves equations of motion algebraically, using experimental kinematics and GRF data as inputs to determine the resultant joint torques, which then are distributed among the muscles based on static optimization, in which an index at each instant is solved to find the muscle forces, without the need of the data in other time points [91]. The most common used index for lower extremity during gait is sum of cubed muscle stresses [96], expressed to maximize the endurance during walking [91]. Although, computationally efficient, inverse dynamic based optimization methods are strongly dependent on experimental data [97], in which inaccuracies due to the noises and other artifacts is inevitable; furthermore, the method is not capable of prediction of high muscle co-contractions in knee OA [98], and the typical indices used to find muscle forces may not be true in the presence of pathologies [91].

Forward dynamic based methods involve the integration of motion equations of the skeletal system, to predict the movement, which optimizes an index [91]. The method can be used to estimate muscle forces, to achieve experimental kinematic and kinetic data tracking [91]. Forward dynamics assisted data tracking employs a function of experimental data, usually second norm of the difference between predicted and experimental generalized coordinates, to estimate muscle activations through integration of motion equations [91]. This method has been used usually to reliably reproduce experimental data, and then exploring injuries by perturbing obtained optimal parameters [99]. The advantage of the method over inverse dynamic based methods are the possibility of incorporation of muscle activation behavior, and less dependency on the experimental data; however, unfortunately it is computationally demanding [91].

When there is no experimental data available or prediction of the musculoskeletal system under possible treatment options is needed, forward dynamic optimal methods can be used [91]. The performance criteria usually is a function of kinematic and muscle activations, and more importantly time dependent, making it a dynamic optimization problem [91]. Predictive simulations can be done to assess changes in

control of muscles and their forces as a result of therapeutic interventions, surgery and rehabilitation [100]. The limitations of the method are unknown objective functions for some tasks, computational complexity, and implementation difficulties [100].

Finally, EMG driven models exploit measured muscle EMG, in addition to measured kinematic and GRF data as input, to resolve muscle redundancy problem [89]. This method can be used in combination with forward dynamics, where prescribed muscle activation patterns are fed into a muscle model and associated movement of the skeletal system will be predicted [101]; or it can be used in combination with inverse dynamics data to calibrate unknown muscle parameters, in a way that predicted moment of the muscles around a joint matches corresponding inverse dynamics moment [102, 103]. The most important advantage of the method is the possibility of incorporating real activation patterns and co-contraction of muscles [91], which can be altered due to pathology, specifically knee OA [31]. The limitations include the need to measure EMG of muscles, and the lack of deep muscle EMG activities [89].

Most of the musculoskeletal models, which have been used to find the knee articular contact forces (Table 2-1), overestimated tibial contact forces [89]. While the results of published studies on total tibial contact forces based on the measurements done through the use of tibial instrumented implants, range from 1.8 to 3.0 body weight (BW), usually remaining between 2.0 to 2.5 BW, modeling studies reported the forces ranging from 1.8 to 8.1 BW, with the most estimates are between 3.0 to 3.5 BW [94, 95, 104-121]. These inaccuracies may be due to inaccurate moment arms or muscle parameters [89]. Only three studies used EMG driven models [119-121], while the others used reduction or optimization methods; and only 8 studies determined medial and lateral contact forces, among which two EMG driven studies, expressed the unloading of the lateral compartment of knee during mid-stance in individuals with OA [120, 121].

A few studies investigated the effect of weight loss on knee compressive contact forces through musculoskeletal modeling. Messier et al. used an inverse dynamic reduction method and found each pound of weight loss results in 4 pound decrease in knee

compressive forces (this study did not take to account the change in the velocity after the weight loss) [87]. Using the same model as Messier's, Aaboe et al. suggested each pound of weight loss results in 2 pound decrease in knee joint compressive forces (Linear regression analyses here was adjusted for changes in walking speed) [86]. In another study by Messier, older adults with knee OA enrolled in the Arthritis, Diet, and Activity Promotion Trial, and subsequently were divided into three different groups of no, low, and high weight loss groups (0%, >5%, <5%, respectively) and their knee compressive and shear forces were calculated based on the Messier's inverse dynamic approach. The results showed high weight loss group (10.2%) decreased their knee compressive forces significantly, which was found to be mostly mediated through the decreased co-activation of hamstring muscles (while quadriceps muscle did not change) [88]. Interestingly, in low weight loss group (2.6%) GRF decreased, while knee compressive forces increased [88], showing GRF is not necessarily a direct indicator of knee joint compressive forces. The study implies there should be certain thresholds for weight loss after which improvement in joint mechanical environment happens. In addition, one must note that discrepancies in the results of different obesity gait studies may be due to the inclusion of groups with different mean BMI.

In his thesis, Harding adopted the model proposed by Devita [73] and used it to examine the effect of obesity and OA and their interaction on compressive and shear contact forces of the knee [2]. He found that BMI did not have any effect on normalized shear, compressive, and muscle forces, while the presence of OA resulted in lower first peak of normalized shear forces, and lower normalized quadriceps and gastrocnemius muscle groups. On the other hand, comparing absolute force values, he found that there was no effect of the disease, while higher BMI resulted in higher second peaks of shear and compressive forces, as well as higher peak of hamstring and quadriceps muscle activity. Furthermore, significant interaction was found between OA presence and BMI for absolute force values of quadriceps muscle, stating that asymptomatic group has higher peak quadriceps muscles forces than OA group with higher BMI.

Kumar et al. used an EMG-driven model to examine the effect of OA on knee joint contact loading [120, 121]. In their first study, they used experimental kinematic, kinetic and EMG data of a healthy individual and a subject with knee OA. Their results showed the OA subjects had higher medial contact absolute load in both halves of the stance phase, and higher absolute lateral contact loads in the 1st half and lower in the 2nd half of the stance phase. They also found the healthy subject and individual with knee OA had 75 to 80% and 95 to 100% of the total load on their medial knee compartments, respectively. Finally, lateral unloading was observed for the OA subject in mid stance [120]. In their second study, they used the same model to study the knee joint contact loading of 12 control subjects and 16 individuals with knee OA. The results showed normalized medial and lateral contact forces were the same for the whole stance for OA and asymptomatic individuals; on the other hand, absolute medial contact load was higher for OA group through the first half of the stance phase (with the same lateral loading through this half). There was no difference in absolute medial and lateral contact loads between the groups in the 2nd half of stance phase. Furthermore, it was observed that half of OA individuals experienced lateral compartment unloading at mid stance. In addition, using linear regression, they found increased mass was associated with increased absolute medial loading [121].

2.4 SUMMARY OF MOTIVATION

Knee joint contact forces, especially medial joint contact forces are important variables, when we are dealing with knee OA. Knee adduction moment is usually considered to be an indication of medial joint contact forces; however, the medial joint contact forces are the results of an interaction between the knee adduction (external forces) and muscles (internal joint forces) [104, 119]. Therefore, higher knee adduction moment [77] or more constant knee adduction moment [2], reported for obese individuals do not necessarily mean the same alterations in knee joint contact forces. Modeling work should be performed to estimate the joint contact forces to be able to draw strong conclusions about the influence of obesity on knee joint contact forces. The model

should be able to use measured EMG activity of the muscles to predict muscle forces and calculate the knee joint contact forces. Therefore, in this thesis, due to importance of muscle activities, we first tried to examine any alteration in the activity of knee muscles due to obesity and then use these measured EMG activity in an electromyography-driven model to examine the joint contact forces.

Table 2-1 Results of different study on knee joint contact modeling (obtained and modified from [89])

Study	No. of Subjects	Total Force (xBW)	Medial Force (xBW)	Lateral Force (xBW)
Morrison [110]	12	2.1-4.0	-	-
Seireg and Arvikar [113]	1	6.7	-	-
Mikosz et al. [111]	1	5.0	-	-
Schipplein and Andriacchi [108]	1	3.2	-	-
Kuster et al. [109]	12	3.4-3.9	-	-
Wimmer and Andriacchi [116]	1	3.3	-	-
Komistek et al. [94]	1	2.3	-	-
Lu et al. [95]	2	2.2	-	-
Heller et al. [107]	4	3.3	-	-
Taylor et al. [115]	4	2.7-2.8	-	-
Shelburne et al. [104]	1	2.9	2.4	0.5
Thambyah et al. [105]	10	2.9-3.5	-	-
Shelburne et al. [112]	1	2.7	2.2	0.5
Kim et al.[106]	1	2.0-2.6	1.2-1.8	0.8-0.8
Lundberg et al. [117]	1	3.5	2.5	1.0
Wehner et al. [118]	1	3.3	-	-
Winby et al. [119]	1	3.0-4.4	2.0-3.0	1.0-1.4
Catalfamo et al. [122]	1	8.1	-	-
Lin et al. [114]	1	1.8-3.6	1.4-2.7	0.4-0.9
Kumar et al. [120]	2	-	2.1-3.1	1.2-1.9
Kumar et al. [121]	28	2.9-4.5	1.9-3.0	1.0-2.5

CHAPTER 3 Alteration in Activation Patterns of Knee Muscles during Gait due to Obesity

3.1 INTRODUCTION

Osteoarthritis (OA) is a degenerative joint disease, which results in loss of articular cartilage, bony changes, joint space narrowing, pain and impaired mobility [3]. The knee is the joint most often afflicted by OA [17, 123], and most frequently associated with disability and symptoms [18]. Numerous risk factors are associated with the initiation and progression of knee OA, among which obesity is known as the most important modifiable risk factor [54-57, 70, 71, 75]; however, its role in the initiation and progression of the disease is unclear [124, 125].

Obesity, as measured by Body Mass Index (BMI), affects the knee joint through linked mechanical [73, 88] and systemic risk factors [69, 71]. Mechanically, it may result in excessive joint loading [25, 73, 80], usually inferred from peak gait parameters, such as peak knee adduction moment [77, 80]; however, the patterns of knee joint loading may also alter in the presence of obesity [1]. These altered loading patterns during walking may deleteriously influence the joint through the application of force on some parts of articular cartilage, which are not adapted to high loads and this can induce cartilage break down and subsequent joint degeneration [8].

Muscles are primary contributors to the joint loading [90]; therefore, altered mechanical environment of the knee in the presence of OA and obesity may occur as a result of changed activation of the major muscles around the joint. Several studies reported altered muscular activity of the knee periarticluar muscles in the presence of knee OA; Increased cocontraction [33, 39, 41, 42, 47], increased EMG amplitude [31, 33, 48], and prolonged activation of the lateral muscles [31, 33, 39, 126] are typical alterations seen in the presence of knee OA, regardless of the disease severity, knee alignment or joint laxity [40]. These altered patterns toward higher activation of lateral muscles is proposed to be an attempt to reduce medial joint loading and increased knee joint active stiffness during the stance phase [31, 33, 39, 40, 48]; However, a modeling study

reported that this new compensatory mechanism may actually increase lateral contact forces, while preventing the medial forces from increasing, suggesting the increased lateral co-contraction can only improve the joint stability, but not the joint loading (it increases the total joint contact force) [127].

A few studies also examined the influence of obesity on activation patterns of lower limb muscles in healthy children [128, 129] and female adolescence [130], and reported no difference between obese and non-obese individuals. However, studies, investigating the effect of load carrying on lower limb muscle activity found increased activity of gastrocnemius [131-133], rectus femoris (RF) [132], and vastus lateralis (VL) [131, 134] and prolonged activity of biceps femoris (LH) [131] and VL [132]. This implies that the nature of obesity, as an undesirable multifaceted condition, is much more complicated than solely increased mass, and requires more investigation to be appropriately understood.

All of the above mentioned studies on the effect of obesity on EMG activity of lower limb muscles, used some discrete subjectively chosen variables, such as integrated EMG [131] or burst duration [129]. The emergence of principal component analysis (PCA), a multivariate statistical method, as a tool in the field of gait analysis has given the researcher the ability to examine the patterns of gait data [135]. PCA is essentially a transformation of the original waveforms to a new space that reveals features of the data that could not be seen before [136]. This technique has been used to examine gait kinetic and kinematic [1, 137-140] and electromyography [31, 33, 36, 46, 141] features. Hubley-Kozey et al. has used PCA to examine the effect of early to moderate knee OA and muscles and their interaction on EMG activation patterns of knee periarticular muscles [31]. Harding et al. [1] also employed PCA to examine the influence of knee OA and obesity and their interaction on the biomechanics of walking in a cross sectional study and reported altered gait patterns as a results obesity [1]; however, there is a lack of information regarding the role of obesity and its interaction with knee OA on the activity of knee periartiuclar muscles, which may play important roles in the observed biomechanical alterations. Therefore, the aim of this study was to examine the

effect of knee OA, obesity and their interaction on the major knee joint periarticular muscles, using PCA. It was hypothesized that the disease and obesity and their interaction alter the activation patterns of the knee muscles.

3.2 METHODS

3.2.1 Subjects

118 asymptomatic and 177 individuals with moderate knee OA participated in this study. The data used here were drawn from two knee OA progression studies and a study examining the effect of brace on knee biomechanics (progression studies were funded by CIHR (principal investigator: Cheryl Hubley-Kozey) and NSHRF (principal investigator: Janie Astephen Wilson); the brace study was funded by CIHR (principal investigator: Cheryl Hubley-Kozey). Asymptomatic subjects were recruited through university and hospital postings and had no history of knee pain. Individuals with knee OA were recruited from the Orthopedic and Sports Medicine Clinic of Nova Scotia and the Orthopaedic Assessment Clinic at the QEII Halifax Infirmary site. In line with our previous work, subjects were diagnosed with moderate knee OA based on a combination of their radiographs (anterioreposterior and lateral views), and a physical and clinical examination by an orthopaedic surgeon and included if they were not candidates for total knee replacement surgery [1, 31]. To be included in the moderate OA group, subjects had Kellgren and Lawrence (KL) score between 1 and 3 [142], showing mild to moderate joint changes. Subjects in both groups were included if they were over 35 years old, able to walk a city block, jog 5 meters and walk up stairs in a reciprocal manner. Exclusion criteria included history of cardiovascular disease, any neuromuscular disease such as Parkinson's Disease, stroke, etc, other forms of arthritis, gout, or history of trauma or surgery to the lower limb [31]. All individuals signed a written consent in accordance with the institutional ethics review board prior to testing.

Asymptomatic and OA group were divided into three body mass groups based on their BMI: healthy weight (20 kg/m^2<BMI< 25 kg/m^2), overweight (25 kg/m^2< =BMI<30 kg/m^2), and obese (BMI>=30 kg/m^2).

3.2.2 Gait Analysis

Three-dimensional gait and surface electromyography (EMG) testing were performed on all individuals. The aim of this study was to examine the muscle activation patterns; therefore, details pertaining to EMG data collection and processing is only explained here. The attachment points of the electrodes on the lower limb muscles, including RF, VL, vastus medialis (VM), LH, semimembranosus (MH), lateral and medial gastrocnemius (LG and MG) were initially determined based on standard anatomical landmarks (Figure 3-1, Table 3-1) [143]. Isolated movement, aimed at activating different muscles were performed by the subjects to validate the points chosen for electrode attachment [144]. Afterward standard preparation of skin was performed (shaving and cleaning with alcohol+water) and the silver/silver chloride pellet surface electrodes ,10 mm diameter, 20 mm interelectrode distance) were attached in a bipolar configuration (20 mm center-to-center) over the muscles on the attachment sites. A reference electrode was mounted on the shaft of tibia. Raw EMG signal of the muscles were pre-amplified (500x) and then further amplified (band-pass 10–1000 Hz), using an eight channel surface EMG system (AMT-8 EMG, Bortec Inc., Calgary, Alberta) with a common mode rejection ration of 115 dB (at 60 Hz), an input impedance of about 10 GOhms and a sampling rate of 2000 Hz. A second set of isolated movements were performed by the subjects to adjust the gains of the amplifier to ensure the collection of a good quality signal and minimize the cross talk [145]. For the calibration of EMG signals, a bias trial was performed while the subjects lied on a bed and completely relaxed.

EMG, three dimensional marker data and ground reaction force were collected, while the subjects were walking across a 6-meter walkway at a self-selected speed for a

minimum number of 5 trials. To ensure consistency, an infrared timing system was used to measure the walking speed during different trials and if a trial velocity was not within the 5% of the mean velocity of all trials it was discarded and another trial was performed. Three dimensional motion data were collected using an Optotrak-3020 motion capture system at 100 Hz (Figure 3-1) (Northern Digital Inc.,Waterloo, ON) and ground reaction forces were measured with a sampling rate of 2000 Hz, using an AMTI force platform (Advanced Mechanical Technology Inc.,Watertown, MA). These two sets of data were used to determine the gait event data (heel contact and toe-off) [31, 46].

(a) (b)

Figure 3-1 a) Electrode placement; b) ired markers

Table 3-1 Guidelines for muscle site, location and orientation utilized for the standardized placement of surface electrodes on the lower extremity, obtained from Rutherford et al. [146]

Muscle site	Location	Orientation
Lateral gastrocnemius (LG)	30% distance from lateral knee joint line to the tubercle of the calcaneous (ankle in neutral position)	Along lead line
Medial gastrocnemius (MG)	35% distance from medial knee joint line to the tubercle of the calcaneous (ankle in neutral position)	Along lead line
Vastus lateralis (VL)	25% distance from the lateral joint line of the knee to the ASIS	45° medial and inferiorly to lead line
Vastus medialis (VM)	20% distance from the medial joint line of the knee to the ASIS	45° lateral and inferiorly to lead line
Rectus femoris (RF)	50% distance ASIS to superior border of patella	Along lead line
Biceps femoris (LH)	50% distance from the ischial tuberosity to fibular head	Along lead line
Semitendinosus/semimembranosis (MH)	50% distance from the ischial tuberosity to the medial joint line of the knee	Along lead line

To elicit maximal voluntary EMG activity, needed to normalize the gait EMG data, 8 different maximum voluntary isometric contraction (MVIC) exercises were performed, each twice for a time period of 3 seconds, with a time interval of one minute in between (7 exercises were performed on a Cybex dynamometer (Lumex, NY)). These exercises were identified from a series of pilot studies to determine exercise positions that elicited maximal activation amplitudes from the seven muscle sites in a small test set [146]. The exercises include: 1) Seated knee extension in supine, with knee at 45° of flexion; 2) Simultaneous knee extension and hip flexion in the same position as 1; 3) Seated knee flexion in supine, with knee at 55° of flexion; 4) Knee extension in supine, at 15° of knee flexion; 5) Knee flexion in supine, at 15° of knee flexion; 6) Plantarfelxion in supine, with the ankle in neutral and knee close to full extension; 7) Heel rise while standing on only one foot; 8) Knee flexion in prone position, at 55° of knee flexion. Before each MVIC exercise a practice was performed and then the real exercises were performed by the subjects with the verbal encouragement of the clinician, while visual feedback of the torque production was also available. A gravity trial was performed for each MVIC task, while all lower limb muscles were completely relaxed.

3.2.3 EMG processing

The force platform and marker data were used to find the start and end of the gait cycle (heel strike to ipsilateral heel strike), and the end of the stance phase. The EMG data during the gait cycle then were band pass filtered between 20 and 500 Hz. The frequency spectra of the resulting signals were looked for possible unusual spikes, showing the presence of noise in the data and if any, a digital filter was used to remove the noise. EMG signals then were corrected for gain and bias, full wave rectified and low pass filtered using a second order non-recursive Butterworth low pass filter with a cut off frequency of 6 Hz [14]. A moving average algorithm with a window of 0.1 second was used to find the maximum EMG activity for each muscle during MVIC trials and the maximal values among all different exercises were used to amplitude normalized EMG waveforms. For each individual, EMG waveforms of at least five trials then were time normalized to the 100% of the gait cycle and ensemble averaged to yield the final waveforms for all muscles. Final waveforms for each muscle group were placed into the rows of three matrices, including a matrix for the three quadriceps ($\boldsymbol{X}_{885\times101}$), a matrix for the two gastrocnemius ($\boldsymbol{X}_{590\times101}$), and a matrix for the two hamstrings ($\boldsymbol{X}_{590\times101}$). The mean values corresponding to each time point (percentage of the gait cycle) were calculated and placed in the rows of a mean matrix with the same size as each matrix and then the covariance of the resulting matrix were calculated:

$$\boldsymbol{S}_{101\times101} = Cov(\boldsymbol{X}_{n\times101} - \overline{\boldsymbol{X}}_{n\times101}) \qquad \text{Equation 3-1}$$

In which $\boldsymbol{S}$, $\boldsymbol{X}$, and $\overline{\boldsymbol{X}}$ are the covariance matrix, EMG waveform matrix, and mean matrix. To find the directions explaining the highest variability in the data, eigenvalues and eigenvectors of the $\boldsymbol{S}$ were calculated [136]. This results in the following equation:

$$\boldsymbol{S} = \boldsymbol{T}\boldsymbol{\Lambda}\boldsymbol{T}^{\boldsymbol{T}} \qquad \text{Equation 3-2}$$

In which $\boldsymbol{T}$, the transform matrix, is a 101×101 matrix, containing eigenvectors in its columns and $\boldsymbol{\Lambda}$, the diagonal eigenvalues matrix, containing the variances for the new set of uncorrelated variables. The projection of the original waveforms on to the first k (k<101) eigenvectors ($\boldsymbol{U}_{101\times k}$) with the highest variability, will yield Z-score matrix ($\boldsymbol{Z}_{n\times k}$):

$$\boldsymbol{Z}_{n\times k} = (\boldsymbol{X}_{n\times 101} - \bar{\boldsymbol{X}}_{n\times 101})\boldsymbol{U}_{101\times k} \qquad \text{Equation 3-3}$$

Each row of $\boldsymbol{Z}$ contains the first k Z-scores for the corresponding subject.

Different methods exist to assess the ability of the chosen principal components (PC) to explain the salient feature of the waveforms [136]; however, the following equation was used to reconstruct the data and visual inspection was performed to make sure the selected PCs capture the main features of the waveforms:

$$\boldsymbol{X}_{n\times 101} = \bar{\boldsymbol{X}}_{n\times 101} + \boldsymbol{Z}_{n\times k}\boldsymbol{U}^{\boldsymbol{T}}_{k\times 101} \qquad \text{Equation 3-4}$$

After visually comparing the reconstructed and original waveforms, three first PCs for all muscle groups were chosen, in line with our previous works in order to capture the major modes of variability among the muscle groups [31, 48]. There are different methods to interpret obtained PCs [135], among which the representative extreme method is simple and effective, and has been used in many studies [30, 31, 33, 46, 48, 140].

3.2.4 Statistical Analysis

Two-way analysis of variance was performed on stride characteristics with the factors being, disease presence and BMI. Z-scores, corresponding to the first three eigenvalues of each muscle group, were calculated for all muscle groups (histograms also were obtained for the Z-scores to make sure they follow a normal distribution, APPENDIX

B) and three factor analysis of variance was used to examine the main effects and two and three way interactions among the factors, being disease, BMI, and muscle, separately for each muscle group (9 Z-scores in total). A Bonferroni post hoc procedure was performed to test for pairwise differences whenever there was a significant interaction or main effect (for a factor with more than 2 subgroups) ($\alpha = 0.05$).

3.3 RESULTS

Table 3-2 shows the demographics, anthropometrics and stride characteristics of all the groups. There were 59 healthy weight, 42 overweight, and 17 obese individuals in the asymptomatic group, and 18 healthy weight, 75 overweight, and 84 obese individuals in the knee OA group. OA groups were older and heavier compared to the asymptomatic groups.

Table 3-3 shows the results of the two-way ANOVA performed on the stride characteristics. OA group walked with shorter stride length and longer stride and stance times and percent compared to the asymptomatic group. OA group overall walked slower that the asymptomatic group. Obesity did not have any effect on walking velocity.

Three PCs captured 85.2% of amplitude and temporal variation for gastrocnemius and quadriceps, and 84% for Hamstrings muscles. The first PC for each muscle group captured the overall amplitude and shape of the EMG signals, while the other PCs contained subtle features of the temporal waveforms.

Table 3-2 Demographics, anthropometrics, and stride characteristics of healthy weight, overweight, obese, asymptomatic and moderate OA subject groups

	Asymptomatics			Moderate OA		
	HW	OV	OB	HW	OV	OB
Age (yrs)	49.4±8.9	48.0±8.7	48.8±10.5	56.7±7.0	58.1±8.3	57.6±8.7
Height (m)	1.67±0.09	1.70±0.09	1.69±0.10	1.71±0.11	1.74±0.08	1.72±0.1
Weight (kg)	64.5±7.8	79.8±9.0	95.2±15.9	68.5±9.2	84.0±9.1	103.7±16.9
BMI (kg/m^2)	22.6±1.6	27.5±1.5	33.2±3.5	23.4±0.7	27.8±1.3	34.8±4.0
Speed (m/s)	1.37±0.18	1.39±0.15	1.37±0.16	1.31±0.17	1.26±0.19	1.20±0.20
Stride length (m)	1.43±0.12	1.47±0.13	1.44±0.14	1.43±0.17	1.42± 0.15	1.35±0.16
Stride time (s)	1.06±0.08	1.07±0.09	1.06±0.07	1.10±0.08	1.14±0.12	1.13±0.10
Stance time (s)	0.66±0.06	0.67±0.06	0.68±0.05	0.69±0.05	0.73±0.080	0.74±0.07
Stance percent	62.4±1.7	63.0±1.1	63.8±1.4	62.4±1.6	63.9±1.70	65.0±1.8

Table 3-3 P-values for the ANOVA performed on stride characteristics (P_1, P_2, and P_{12} are the p-values corresponding to disease presence, BMI, and their interaction, respectively; bold values are the statistically significant ones.)

	P_1	P_2	P_{12}
Stride length	**0.019**	0.14	0.23
Stride time	**<0.001**	0.22	0.54
Stance time	**<0.001**	**0.014**	0.29
Stance percent	**0.003**	**0.000**	0.13
Speed	**<0.001**	0.27	0.30

3.3.1 Gastrocnemius

Figure 3-2 shows the first three PCs for the gastrocnemius muscles and the average waveforms of the original waveforms, corresponding to the 5 highest and 5 lowest Z-scores. PC1 captured minimal activity during early stance followed by a gradual rise in activity, peaking just prior to 50% of the gait cycle then rapidly decreasing until toe off

at 60%; PC2 captured a phase shift between in the activity of the muscles; and PC3 captured the difference between the EMG activity of early to late stance [31, 48].

Three factor ANOVA results for gastrocnemius muscles are shown in Table 3-4. A significant BMI by disease interactions was found for PC2 ($P<0.05$) (Table 3-4). Pairwise post hoc analysis ($\alpha = 0.05/15$) revealed OB asymptomatic individuals, had significantly lower Z-scores than all other five groups ($P<0.0026$), showing that higher BMI is associated with a delay in muscle activity. A BMI main effects was found for PC3 ($P<0.05$) (Table 3-4). Post hoc Bonferroni comparison ($\alpha = 0.05/3$) revealed obese individuals had significantly lower Z-scores compared to OV ($P=0.007$) and HW subjects ($P=0.0001$).

A significant disease by muscle interactions was found for PC1 ($P<0.05$). Pairwise Bonferroni comparisons ($\alpha = 0.05/6$) revealed a significantly higher PC1 score for asymptomatic MG compared to asymptomatic LG, OA MG, and OA LG ($P<0.0001$). Significant disease by muscle interactions was found for PC2 ($P<0.05$). Post hoc analysis ($\alpha = 0.05/6$) revealed higher score for MG OA compared to LG OA ($P=0.0010$), higher score for MG asymptomatic compared to LG asymptomatic ($P=0.0000$), and higher OA LG score than asymptomatic LG ($P=0.0011$). A disease main effect was found for PC3 ($P<0.05$) (Table 3-4) that showed OA individuals had significantly smaller Z-scores compared to asymptomatic individuals ($P=0.0003$).

Table 3-4 Results of three way ANOVA on the first three PC scores of gastrocnemius ($P<0.05$ is significant; significant results are shown in bold)

muscles	PC	BMI	Disease	Muscle	B and D	B and M	D and M	B and D and M
Gastrocnemius	1	0.98	**0.0000**	**0.00**	0.53	0.90	**0.03**	0.30
	2	**0.00**	**0.0104**	**0.00**	**0.02**	0.72	**0.04**	0.63
	3	**0.00**	**0.0000**	0.09	0.20	0.67	0.66	0.71

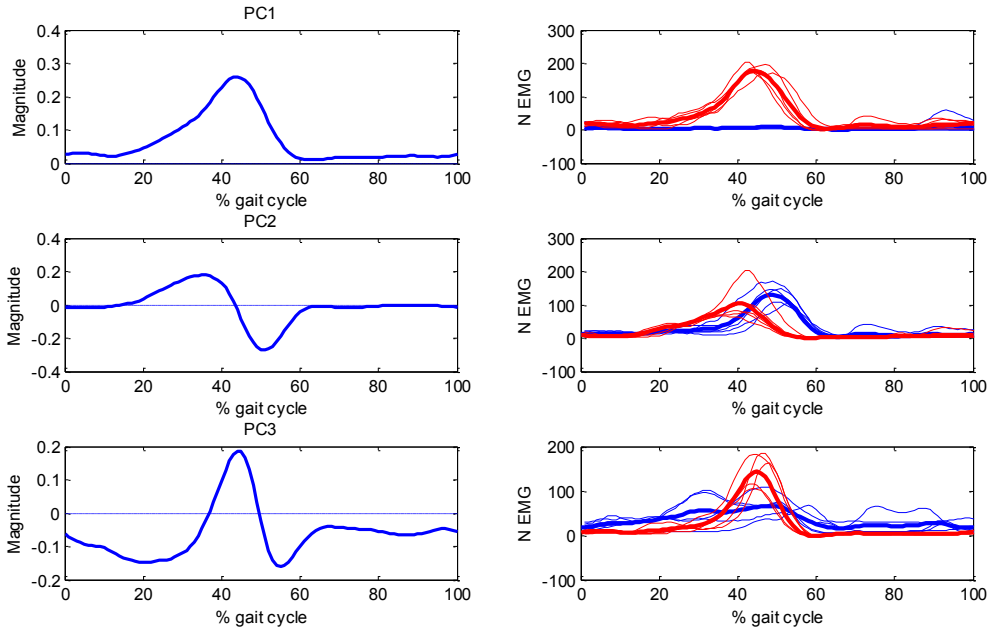

Figure 3-2 Gastrocnemius, PCs and the Original waveform, corresponding to the five highest (red) and five lowest (blue) Z-scores and their average waveforms

3.3.2 Hamstrings

Figure 3-3 shows the three first PCs for the hamstrings and the average waveforms of the original waveforms, corresponding to the 5 highest and 5 lowest Z-scores. PC1 captured high activity at initial foot contact, decreasing during the first 10–15% of the gait cycle, increasing again around 85% of the gait cycle, peaking prior to heel contact; PC2 captured the prolonged activation during stance phase, gradually decreasing until toe off and the continual increase in activity during late swing; PC3 captured the continual rise in activity prior to heel contact with the amplitude peaking just before heel contact [31, 48].

Three factor ANOVA results for hamstrings are shown in Table 3-5. Obesity did not have any effect on hamstrings PCs. However, a significant disease by muscle interaction was found for PC1 ($P<0.05$) (Table 3-5). Pairwise Bonferroni comparison ($\alpha = 0.05/6$) showed LH OA had higher PC1 score than MH OA and both hamstrings muscles of the asymptomatic group ($P<0.0001$). A disease main effect was found for

PC2 (P<0.005), which revealed that OA group had a higher Z-score compared to asymptomatic group. A disease main effect for PC3 (P<0.05) showed asymptomatic individuals had significantly higher Z-scores than OA group.

Table 3-5 Results of three way ANOVA on the first three PC scores of hamstrings (P<0.05 is significant; significant results are shown in bold)

muscles	PC	BMI	Disease	Muscle	B and D	B and M	D and M	B, D and M
Hamstrings	1	0.71	**0.00**	**0.00**	0.51	0.89	**0.05**	0.87
	2	0.07	**0.02**	0.26	0.40	0.70	0.38	0.40
	3	0.70	**0.00**	0.10	0.54	0.62	0.21	0.55

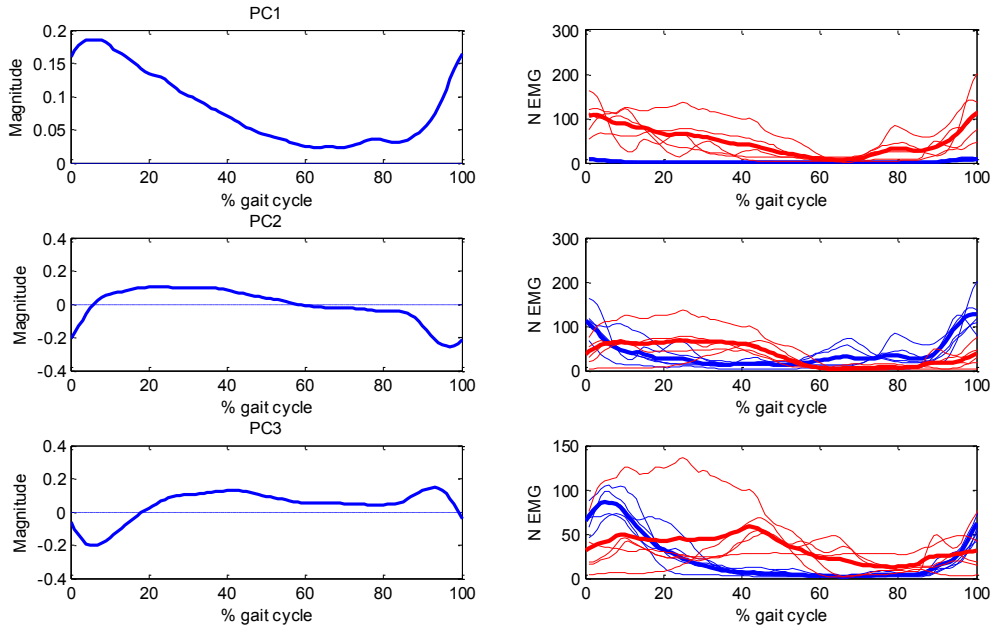

Figure 3-3 Hamstrings, PCs and the Original waveform, corresponding to the five highest (red) and five lowest (blue) Z-scores and their average waveforms

3.3.3 Quadriceps

Figure 3-4 shows the first three PCs for the quadriceps and the average waveforms of the original waveforms, corresponding to the 5 highest and 5 lowest Z-scores. PC1 captured a burst of activity during the loading phase peaking at approximately 10% of the gait cycle, gradually decreasing to a plateau after 30% of the gait cycle, then increasing prior to heel contact; PC2 captured an increase in amplitude during mid-

stance, reflecting that activity was present for a longer duration; PC3 captured burst in activity during late stance-early swing peaking at 70% of the gait cycle [31, 48].

Three factor ANOVA results for quadriceps muscles are shown in Table 3-6. BMI had a significant effect only on PC2 (Table 3-6). Post hoc comparisons ($\alpha = 0.05/3$) showed higher score for obese group compared to the other two groups (the two latter groups were the same).

A disease main effect was found for PC1 (P<0.05), showing OA group had higher scores compared to asymptomatic group. A muscle main effect also was found for PC1 (P<0.05). Post hoc analysis ($\alpha = 0.05/3$) revealed RF had lower score compared to the other two muscles (P<0.0001). A muscle main effect was found for PC2 (P<0.05) and post hoc analysis ($\alpha = 0.05/3$) showed higher score for RF compared the other two groups. A disease main effect was found for PC3 (P<0.05) showing higher score for asymptomatic compared to OA group, while a muscle main effect for PC3 (P<0.05) showed lower score for VL compared to both RF and VM.

Table 3-6 Results of three way ANOVA on the first three PC scores of quadriceps (P<0.05 is significant; significant results are shown in bold)

muscles	PC	BMI	Disease	Muscle	B and D	B and M	D and M	B and D and M
Quadriceps	1	0.30	**0.00**	**0.00**	0.54	0.99	0.40	0.97
	2	**0.00**	0.08	**0.00**	0.97	0.70	0.69	0.99
	3	0.91	**0.00**	**0.00**	0.60	0.70	0.24	0.98

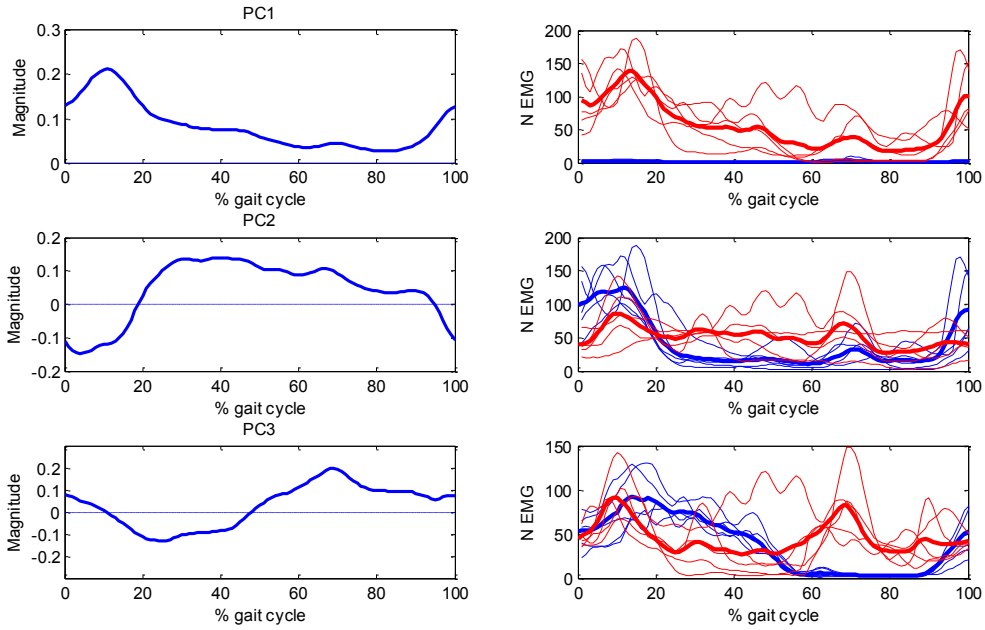

Figure 3-4 Quadriceps, PCs and the Original waveform, corresponding to the five highest (red) and five lowest (blue) Z-scores and their average waveforms

3.4 Discussion

The results of this cross sectional study revealed alterations in the activity of knee major muscles due to obesity, knee OA, and their interaction. It was found that obesity may be associated with prolonged and delayed activation of prolonged gastrocnemius (PC3, Figure 3-2, Table 3-4) and quadriceps (PC2, Figure 3-4, Table 3-6), which is in contrast to the results of the previous studies, reporting no effect of obesity on lower limbs muscle activity in children and adolescents [128-130]. Prolonged activation of gastrocnemius and quadriceps muscle group in obese individuals may be an attempt to enhance dynamic joint stability during the stance phase, possibly as a response to increased weight [74, 147]; however, on the other hand, this strategy potentially exposes the joint to higher cumulative contact loading, undesirable for the cartilage, and also may result in muscle fatigue, which disrupts the active mechanism for shock absorption in the knee joint [148]. The obtained results, regarding the effect of the disease on muscle activities were consistent with the previous studies [31, 39, 48].

3.4.1 Gastrocnemius

Obesity did not have any effect on the amplitude of the EMG of gastrocnemius (PC1, Table 3-4). This is consistent with the results of previous studies, which reported there was no difference in the EMG activity of gastrocnemius muscle of obese and nonobese female adolescents [130] and children [128, 129]. This is interesting because it has been shown that gastrocnemius muscles activity peaks at late stance to propel the body [114, 119], which necessitates the production of higher torques at the ankle joint and studies, interrogating the effect of load carriage on the lower limb joint, reported an increase in the activity of gastrocnemius muscles with loads up to 40% of BW and no change afterwards [132, 133].

Significant BMI by disease interaction for PC2 demonstrated that obese asymptomatic individuals had a delay in gastrocnemius muscle activity, compared to HW and OV group. Gastrocnemius muscle forces play an important role on the knee joint contact forces during late stance [114, 119]; therefore, this delayed activity and the resultant imbalance between flexors and extensors [149] may result in the disruption of the normal loading of the joint and expose the cartilage to high contact loads at inappropriate time intervals.

Obese individuals walked with smaller PC3 scores compared to both HW and OV group (Table 3-4). This shows the difference between early to late EMG activity of gastrocnemius for the OB group is less than the other two groups. Smaller change in the activity of the muscle through the stance phase also may be viewed as prolonged activity, probably to enhance joint stability, while having the adverse effect of prolonged loading of the knee joint. This can endanger the joint integrity and have deleterious effect on joint mechanical environment [150]. Interestingly, this only happened for the OB group and not the OV group, supporting the idea of existence of a threshold for BMI after which individuals with higher mass may start to adapt new gait and neuromuscular patterns [83].

The OA group recruited the medial gastrocnemius muscle (MG) to a lesser degree compared to the asymptomatic group, which is proposed to be a mechanism to reduce medial joint loading (and probably due to slower walking velocity) [31, 40, 48]. However, in a recent modeling study, the activation patterns, obtained using a static optimization, were perturbed to account for the activation patterns of OA individuals, i.e., decreased MG activation and increased lateral muscle activation, and the knee joint medial and lateral contact forces were obtained. The results demonstrated that these altered compensatory patterns produced higher lateral and almost the same medial joint loading, which may have the advantage of improving the joint stability, but not reducing medial joint loading [135]. Consistent with previous studies, PC2 showed MG muscles activity were shifted toward earlier time of the gait cycle compared to LG for both OA and asymptomatic groups [31, 48]. Furthermore, it was found through PC3 that OA individuals have smaller difference between early to late stance activity of their gastrocnemius muscles, that can be viewed as longer periods of activation for gastrocnemius muscles and corroborates the results of the previous studies, expressing increased cocontraction of shank muscles during the whole stance phase [39, 41, 47].

3.4.2 Hamstrings

There was no effect of BMI on hamstrings muscles activity, consistent with previous studies on children and adolescents [128-130]; although, the ANOVA results showed the BMI P-value for the PC2 to be 0.0679, which is close to be significant (Table 3-5).

Significant disease by muscle interaction for PC1 of the hamstrings, consistent with previous works, showed OA individuals recruited lateral more than the medial hamstrings [31, 48]. Increased lateral hamstring muscle activity was reported in OA individuals [44, 45], probably to increase joint stability through increased agonist-antagonist co-contraction [31, 40]. Increased PC2 scores for OA individuals compared to aymptomatic subjects, demonstrated the prolonged activity of hamstrings muscle in the OA group. Hubley-Kozey et al. [31] and Rutherford et al. [48] found this prolonged activity for only lateral hamstrings sites, while our results showed prolonged activity

for both medial and lateral sites. Furthermore, asymptomatic individual had higher PC3 scores compared to the OA group, stating the peak activity of their hamstrings muscle happens before the heel contact, while the negative score for the OA individuals show the peak hamstring activity after heel contact. This can be due to proprioceptive deficiencies in knee OA [151, 152].

3.4.3 Quadriceps

The only main effect of BMI was in PC2, revealing that the OB group had prolonged activity compared to both OV and HW groups. Interestingly, HW and OV group did not have any difference, again implying there could be a threshold for the new neuromuscular patterns to emerge [83]. Chori et al. reported backpack carriage equal to 20% of the body weight increased the duration of the activity of VL, MH, and gastrocnemius muscle in the gait of healthy subjects, and when the backpack weight increased to 50% of the body weight, only VL burst duration was furthered. They concluded this altered neuromuscular patterns in the presence of increased weight can be an attempt to maintain the same kinematics of gait [134]. The increase in the duration of VL activity due to load carrying was also reported in another study by Harman et al. [153]; they explained the EMG activity of the gastrocnemius muscle also was increased with a load up to 42% body weight, and further mass increase only resulted in increase in VL activity, suggesting that knee musculature is more important than ankle plantar flexor in attenuating higher loads during gait [153]. This prolonged activity of quadriceps muscle during stance phase may be an attempt to increase stability in response to the higher loads due to high body weight, which on the other hand may have adverse effects on the joint contact loading, resulting in the application of high loads on the cartilage and its break down. We should keep in mind that obesity is a complicated multifaceted condition and carrying some amount of mass for a short time does not necessarily resemble the influence of obesity and even its influence on psychological factors such as motivation may have drastic effect on the gait.

Statistical analysis on PC1 for the quadriceps showed increased overall activity for OA group compared to asymptomatic, consistent with previous studies [33, 48]; this increased activity is reported to be a feature emerging due to the disease, not due to different the walking velocities [48]. Furthermore, muscle effect for PC1 illustrated higher overall activity for VL and VM compared to RF, consistent with [31, 33, 48]. This confirm the differential recruitment of the agonist muscles [31]. Significant higher PC2 for RF compared to the vasti muscles, capturing longer duration of its activity, specifically in stance is consistent with previous studies [31, 39, 48]. Significant muscle and disease main effects were found for PC3, capturing a burst in the activity of the muscles in late stance-early swing, with no interaction between the two factors; this is in agreement with [48], however, different from [31], reporting an interaction between the disease and muscles. Lower PC3 scores for OA group in our results illustrates lower levels of activity during late stance-early swing, may happen due to the fact that there is not much demand for the stability of the joint in the swing phase and therefore OA individuals reduce their quadriceps activity, probably to reduce the pain. Furthermore, as found by the muscle main effect for PC3, higher RF activity in the late stance-early swing is associated with its biarticular nature [36].

There are some concerns with EMG measurement in the presence of high amount adipose tissues for obese individuals. It has been proposed that adiposity reduces the amplitude of the measured signal [154, 155] and increase crosstalk [145, 154]. However, first, it should be noted that only the first PC of each muscle group could be influenced by the amount of the adipose tissues, as these PCs explain the overall amplitude of the waveforms; therefore, we are not concerned about the results we obtained for the quadriceps and gastrocnemius muscle based on other PCs, as those PCs contain information about different points in the gait cycle and are relative in nature. Furthermore, crosstalk in EMG measurement is inevitable [145] and in the case of obese individuals this effect is more pronounced. However, we tried to maximize the amplitude and minimize crosstalk in our EMG signals by doing the followings: electrode placement based on standard protocols [143], using electrodes with small surface areas and short bipolar spacing [145], palpating electrode placements while the

subject were doing isolated tasks by an experienced kinesiologist [14], doing a second set of isolated movement to adjust the gains of the amplifier and make sure a signal with good quality and minimal crosstalk was being measured isolated movements [145].

Altered activation patterns due to obesity and knee OA were found in this cross sectional study; however, there is still unclear if these strategies ameliorate the mechanical environment of the joint and slow the progression of the disease, or degenerate the joint due to high and prolonged joint loading; longitudinal studies should be performed to further investigate the effect of these mechanisms. In addition, it has been proposed in two recent studies that there is relatively small correlation between the EMG measured during gait and the knee joint contact forces [156, 157]. Therefore, inferring based on measured electromyography may be misleading and in the case of this study, regarding the role of obesity, prolonged activation of gastrocnemius and quadriceps may not necessarily imply prolonged joint contact loading. Therefore, modeling studies, using measured activation patterns of the muscles, specific to the obesity may improve our understanding of its effect on mechanical joint loading. It should be also noted that although BMI is a frequently used metric, as a measure of body mass [66], it may not reflect the real body compositions, and mask some effects. Therefore, developing new parameters which are easy to use and able to characterize altered body mass distribution effectively is worthwhile.

3.5 Conclusions

This study identified alterations in the activity patterns of the lower limb muscles due to obesity, knee OA, muscles and their interactions. Obesity causes prolonged activation of quadriceps and gastrocnemius, which can results in prolonged knee joint contact loading. Longitudinal studies accompanied by modeling approaches should be performed to examine how, important risk factors, such as obesity, contribute to knee OA initiation and progression and possibly organize interventions to improve the joint mechanical environment to halt the progression of knee OA or even prevent its initiation.

CHAPTER 4 EMG-Driven Model for Knee Joint Contact Forces Estimation

4.1 INTRODUCTION

Osteoarthritis (OA) is theorized to be driven by high and prolonged forces within the joint [13]. However, net resultant joint moments which are calculated during typical biomechanical analysis, do not give us sufficient information regarding the internal loading within the joints, because they oversimplify the contribution of muscle forces. Specifically, knee adduction moment is known as an important variable which is associated with symptoms [26], severity [24] and progression [25] of knee OA and usually is considered as a measure showing the relative distribution of the joint contact forces, with higher knee adduction moment corresponding to the higher medial joint contact forces [27], implicated to be detrimental to joint integrity and resulting in OA initiation and progression. However, care should be taken when inferring conclusions based on this variable, as it is not always correlated with the joint contact forces [157-159]. In the data published in the knee grand challenge competition (https://simtk.org/home/kneeloads) from a subject who was implanted by an instrumented prosthesis in 2012 [160], it was shown that medial thrust gait (gait pattern that involved medializing the knee during stance phase) can reduce the knee adduction moment; however, the knee joint contact forces increased both on the medial and lateral compartment of the knee [159, 160]. Furthermore, individuals with pathologies such as knee OA or joint laxity may have altered lower limb –muscle activation patterns [31, 39, 40], in a way that is associated with increased co-contraction of lower limb muscles in order to improve the joint stability or possibly unloading the medial compartment of the knee joint [31, 40]. In such cases, real joint contact forces may be elevated, while the knee adduction moment does not change. Therefore, there is a need to measure the absolute values of medial and lateral knee joint contact forces to understand how OA affects the mechanical environment of the knee joint during gait.

Obesity is a major risk factor for knee OA, which has been reported to influence the knee joint through both altered loading patterns [1] and excessive loading of the joint [73, 80], specifically increased knee adduction moment [77, 80]. This increased loading usually is attributed to increased body mass; however, it has been shown that muscles contribute to the joint loading the most [90, 109], and in the last chapter, we showed that obese individuals walk with altered lower limb muscle activation patterns, i.e. prolonged activity of quadriceps and gastrocnemius (and probably hamstrings). However, EMG activity does not necessarily correlate with the knee joint contact forces [157, 158]. Therefore, there is a need to examine tibiofemoral contact forces during obese gait to understand the effect of obesity.

One method to measure knee joint contact forces is the use of instrumented prosthesis [89, 160]; however, this method is only applicable to the individuals who are candidates for total knee replacement [89, 91], and therefore cannot be used in earlier stages of knee OA, where conservative treatment options may slow the progression of knee OA. An alternative is to develop musculoskeletal models that give us the ability to examine a range of biomechanical variables which are not readily feasible to measure through experiments [89, 91]. EMG-driven modeling is a method that is used to solve the muscle redundancy problem and subsequently find tibiofemoral joint contact forces. In contrast to other methods, this method uses the measured activation patterns of muscles and therefore, is able to take into account the co-contraction seen in some pathologies, such as knee OA [91].

The aim of this study was to first implement an EMG-driven model which can be used to estimate medial, lateral and total knee joint contact forces during gait, and then use the model for one asymptomatic healthy weight and one asymptomatic obese subject (with similar self-selected walking velocities) in order to demonstrate how obesity might change the tibiofemoral joint contact forces during gait.

4.2 METHODS

4.2.1 Subject

Three individuals with asymptomatic knees were included in this study. The first subject was an overweight subject (BMI=26.3 kg/m^2, age: 40 years, speed=1.26 m/s) and his data was used to implement and validate the model. Second and third subjects were obese (BMI=30.1 kg/m^2, age: 53 years, speed=1.16 m/s) and healthy weight (BMI=22.6 kg/m^2, age: 49 years, speed=1.09 m/s), respectively (Table 4-1, Table 4-2). These two subjects were included to demonstrate in a small case study the influence of obesity on knee joint contact forces. The two subjects were matched as closely as possible for age, sex, and walking velocity, to minimize any confounding effects due to these factors on their gait patterns. They were also selected from an asymptomatic cohort to prevent the presence of the confounding effect of OA on joint contact forces and make the interpretation of the results possible.

4.2.2 Gait analysis

Three dimensional motion data were collected using a 2-camera bank Optotrak^{TM} 3020 motion capture system at 100 Hz (Northern Digital Inc., Waterloo, ON), while the subjects walked across a 6-meter walkway at a self-selected speed for a minimum number of 5 trials. Triads of infrared light emitting diodes were placed on the foot, shank, thigh and pelvis and individual diodes were placed on shoulder and three bony landmarks of the chosen leg, including, greater trochanter, lateral epicondyle, and lateral malleolus. A standing calibration trial was also performed, following by 8 different digitization trials (to digitize medial malleolus, second metatarsal, heel, tibial tuberosity, fibular head, medial epicondyle, right and left Anterior superior iliac spine). The obtained data during standing calibration and digitization trials were used to define the coordinate systems of each segment and to find the length of the segments in the model. Ground reaction forces (GRF) were measured with a sampling rate of 2000 Hz,

using an AMTI force platform (Advanced Mechanical Technology Inc., Watertown, MA). GRF and 3D motion data were used as inputs to an inverse dynamic model developed in Visual3D software to calculate the knee joint net resultant external moments. The net external flexion and adduction moments were obtained in knee joint coordinate system to be used later for the calibration of the muscle forces [161] (section 4.3.10) and estimating knee joint contact forces (section 4.3.12), respectively. The details of the EMG data collection during different exercises including gait and maximum voluntary isometric contractions are the same as the methods presented in the previous chapter of this thesis (3.2.2).

4.3 EMG-DRIVEN MODEL

The following steps were performed to implement an EMG-driven model. First, activations from EMG (4.3.1) and muscle-tendon lengths and moment arms from the marker data (as input to an anatomical model) (4.3.2) were obtained. Then these data were used as input to a Hill-type model for each muscle (containing force-length and force-velocity of the muscles) to find muscle forces (4.3.3 to 4.3.11). Muscle forces were calibrated through optimization (4.3.12) and then the calibrated forces were used as input to a 2D frontal plane model to find the medial, lateral, and total tibiofemoral contact forces (4.3.13).

4.3.1 EMG to activation

The first input to the muscle model was activation, which was found through measured EMG [103, 159, 162]. Activation for the following muscles were obtained: rectus femoris (RF), vastus lateralis (VL), vastus intermedius (VI), vastus medialis (VM), biceps femoris long and short head (BFLH and BFSH), semimembranosus and semitendinosus (SM and ST), lateral gastrocnemius (LG), and medial gastrocnemius MG using the following steps:

The force platform and marker data were used to find the start and end of the stance phase. The EMG data during the stance phase of the gait then were band pass filtered between 20 and 500 Hz. The frequency spectra of the resulting signals were examined for possible unusual spikes, showing the presence of noise in the data and if any, a digital filter was used to remove the noise. EMG signals then were corrected for gain and bias, full wave rectified and low pass filtered using a second order recursive Butterworth low pass filter with a cut off frequency of 6 Hz [14]. A moving average algorithm with a window of 0.1 second was used to find the maximum EMG activity for each muscle during MVIC trials and the maximal values among all different exercises were used to amplitude normalized EMG waveforms [30, 31, 33].

There is a time delay between the emergence of the EMG and the force in muscles, called electromechanical delay, *d*, and happens due to a) dynamic of muscle force production, depending on its chemical properties, and b) a transport problem, depending on factors such as the release of calcium into muscle membrane [162]. This value has been reported to be between 10 to 100 milliseconds [163]. The process of taking this electromechanical delay into account is called muscle activation dynamics [164]. The input is linear enveloped normalized EMG and the output is a variable called neural activation, *u* [164]. A first order nonlinear differential equation was proposed by Zajac to do this [164]; however, we used a second order discretized recursive filter, which is essentially a discrete representation of a second order differential equation. This differential equation itself is based on the fact that the response of a muscle fiber to an action potential can be best represented by a critically damped linear second-order differential system [165], and proposed to be more efficient [162]. As well, it addresses the difficulties other researchers have had to find muscle forces from processed EMG [103, 166]. Equation 4-1 was used to find *u*, at *n*th time step:

$$u(t) = M\frac{d^2e(t)}{dt^2} + B\frac{de(t)}{dt} + Ke(t) \quad \xrightarrow{backward\ difference} \quad u(n) = \alpha\, e\left(n - d \times emg_{frequency}\right) - \beta_1\, u(n-1) - \beta_2\, u(n-2) \qquad \text{Equation 4-1}$$

Where d is the electromechanical delay and α, β_1, and $\beta_2$are the coefficients governing the second order dynamics between EMG and muscle force [103]. e and $emg_{frequency}$ are the processed EMG and EMG sampling rate. In order to have a stable system the poles of the transfer function, with the e as input and u as output, must be less than 1 [162]:

$$|\gamma_1| and |\gamma_2| < 1 \qquad \text{Equation 4-2}$$

The relationships between the poles and coefficients in Equation 4-2 are:

$$\beta_1 = \gamma_1 + \gamma_2 \qquad \text{Equation 4-3}$$
$$\beta_2 = \gamma_1 \times \gamma_2$$

Therefore, choosing the poles, the coefficients were found. Furthermore, in order for the u not to go beyond unity, the following condition was met, through which α can be calculated:

$$\alpha = \beta_1 + \beta_2 + 1 \qquad \text{Equation 4-4}$$

A complicated relationship exists between the EMG and the muscle force, and the model used to characterize this relationship depends on a number of factors, such as the kinematics of the movement, and EMG acquisition and processing procedure [35]. Researchers characterized this relationship to be both linear [167] and curvilinear [167, 168]. Here we used a formulation which is nonlinear in low levels of activation and almost linear in higher levels of activation [103, 169]:

$$a(t) = \frac{e^{Au(t)} - 1}{e^{A} - 1} \qquad \text{Equation 4-5}$$

A is a nonlinear shape factor which can take values between 0 to -3, with 0 corresponding to linear relationship between force and EMG [162].

4.3.2 Anatomical model

The second input to the muscle model was musculotendon (MTU) lengths (musculotendon is a term used here to refer to the overall muscle-tendon structure, as they are in series and act as one entity). A three dimensional model, comprised of 7 segments, with 11 degrees of freedom (DOF), and 44 MTU compartments was used [170] in OpenSim, a freely available software for musculoskeletal modeling [171]. The model was developed based on muscle architecture data of 21 adult cadavers, recently collected by Ward et al. [172]. Using the Ward's dataset means the model was based on a cohesive set of experimentally measured data that is not pieced together from separate sources. The knee joint was modeled with one DOF in sagittal plane, while the anterior-posterior (AP) and proximal-distal (PD) relative motion between the femur, and the varus-valgus and rotation of the knee in the frontal plane are coupled to the DOF in the sagittal plane, using the equation from Walker et al. [173]. Here, in order to find the muscle moment arms in the frontal plane, the coupling between knee flexion and varus-valgus angle was removed, and a medial and a lateral contact point was defined. A standard frontal plane view radiograph of the subject was used to estimate the size of medial and lateral aspects of the proximal tibia and it was assumed the contact points are in the middle of each tibial aspect (Figure 4-1) [119]. Contact locations were fixed in the tibial frame to approximate translation with respect to the femur during knee flexion [119]. To find the scale factor needed to translate the lengths of each aspect of the tibia from radiograph to real tibia lengths, the distance between the medial and lateral epicondyle in the standing calibrations was compared to the frontal plane radiograph of the knee.

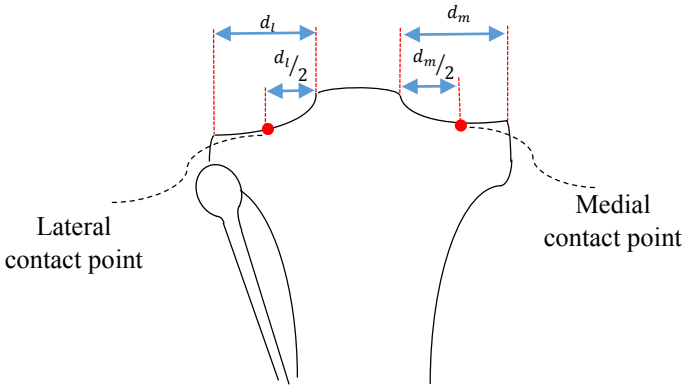

Figure 4-1 Schematic of the method used to find medial and lateral contact points on the head of tibia

Raw marker data, during the static calibration trials were used to uniformly scale the model segments to match the subjects (in OpenSim). Marker data during the stance phase of walking trials were then used as the input to the musculoskeletal model in OpenSim and an inverse kinematic step was performed, which gave as output the joint angles and subsequently MTU lengths and moment arms in the sagittal plane and frontal plane about the medial and lateral contact points, at each percent of the gait cycle.

4.3.3 Hill-type model

A general Hill-type model was used to model the muscles (Figure 4-2) [99, 103, 119, 162, 174]. There is a contractile component (CC), representing active properties of MTU, a parallel elastic component (PEC), showing passive properties of MTU in parallel with CC and a series elastic component (SEC), resembling the passive structures in series with CC (mostly tendon). There is an angle between CC and SEC, called pennation angle (Figure 4-2). It should be noted that Hill-type model is a phenomenological model, which resembles muscle behavior; therefore, components shown in the model do not have the exact correspondence toreal muscles [175].

The following equation governs the equilibrium among passive and active components of the Hill-type model (Figure 4-2):

$$F_{SEC} = (F_{CC} + F_{PEC})cos(\varphi) \qquad \text{Equation 4-6}$$

Where F_{SEC}, F_{CC}, F_{PEC} and φ are SEC, CC and PEC forces and pennation angle at each instant in time. The following sections explain different elements in Equation 4-6.

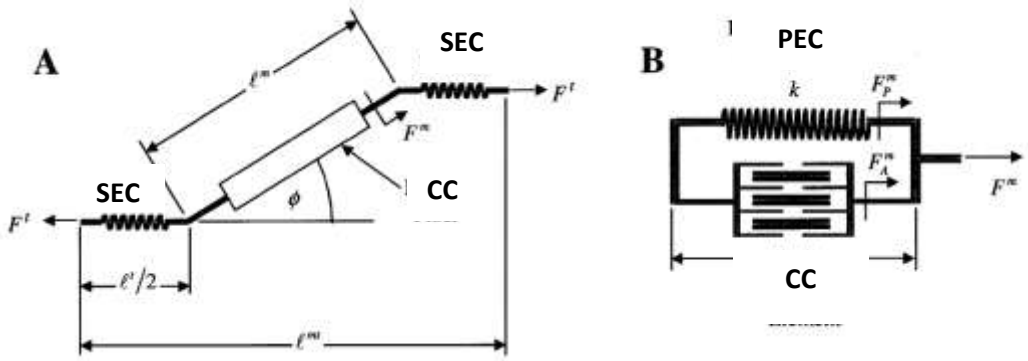

Figure 4-2 A) The Hill-type model, B) the CC and PEC (adapted and modified from [162])

4.3.4 Contractile Component force

The force produced by CC is dependent on its length, velocity and activation. The following equation is used to find the force produced by the CC [103, 162, 169]:

$$F_{cc} = f_A(l)a(t)f_v(v,a)\,F_{0CC} \qquad \text{Equation 4-7}$$

In which $f_A(l)$, $f_v(v,a)$, $a(t)$, and F_{0CC} are normalized active force-length relationship and normalized force-velocity relationship of the muscle, activation, and maximum isometric contraction force of CC, respectively.

4.3.5 Force-length relationship

Force production ability of skeletal muscles is strongly dependent on their CC length. When a muscle has its optimal CC length, it can produce the maximum possible force (F_{0CC}). To model the dependency of the CC force to its length, a second order polynomial was used (Figure 4-3) [176, 177]:

$$f_A(l) = \max(f_{min}, 1 - \left(\frac{l - l_0}{w l_0}\right)^2) \qquad \text{Equation 4-8}$$

Where l is the CC length, l_0 is the optimal CC length, and w is a dimensionless parameter defining the width of force-length relationship (the distance from the optimal length after which the muscle cannot produce any force). A minimum value of 0.05 was used as f_{min} in order to prevent division by zero [177].

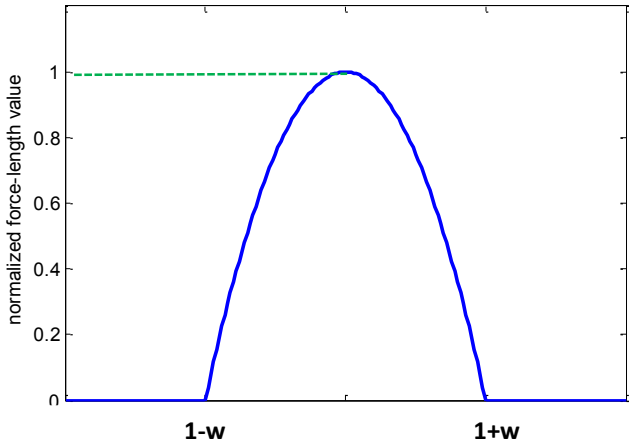

Figure 4-3 Muscle force-length relationship

It has been shown that the optimal CC length of the muscle increases when activation decreases (Figure 4-4) [178]; therefore, the following equation is used to characterize this dependency [177]:

$$l_0^m(t) = l_0^m(\delta(1 - a(t)) + 1)$$ Equation 4-9

A value of 0.15 for δ was chosen, meaning when the muscle has zero activation, the optimal CC length is 0.15 longer than when it is fully activated [103].

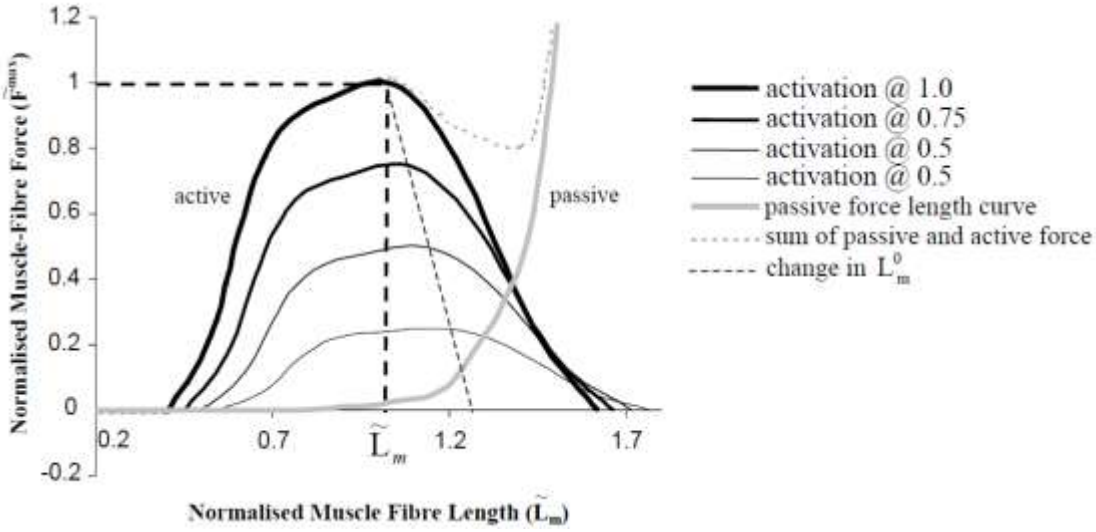

Figure 4-4 Force-length relationship of skeletal muscles and change in the peak active muscle force as a result of activation reduction (adapted from [103])

4.3.6 Parallel Elastic Component Force

Muscles produce high passive forces, when stretched beyond their optimal length [162]. To model this, Schutte proposed an exponential relationship [179]. We used a modified version of this formulation:

$$f_{PEC}(\tilde{l}) = \frac{e^{10(\tilde{l}-1)}}{e^{10w}}$$ Equation 4-10

In which $\tilde{l}$ and f_{PEC} are the normalized CC length (normalized to optimal length) and normalized passive force. This equation means when the muscle CC has a normalized length of 1+w, the produced passive force is equal to maximum isometric muscle force.

The actual passive force of muscle is a function of its maximum isometric force [164], therefore:

$$F_{PEC} = f_{PEC} F_{0CC} \qquad \text{Equation 4-11}$$

4.3.7 Force-velocity relationship

The force-velocity relationship of muscles takes into account the dependency of the muscle force and its contraction velocity. Here, we used a formulation proposed by McLean et al. [177], which assumes the normalized force-velocity relationship of the muscle was independent of the optimal CC length [180, 181]:

$$f_v(v,a) = \begin{cases} d_2\, v + d_2\, v_{max}\, \lambda(a) & v < -v_{max} \\ \dfrac{\lambda(a) v_{max} + v}{\lambda(a) v_{max} - {}^{v}/_{A}} & -v_{max} \le v \le 0 \\ \dfrac{f_{max} v + d_1}{v + d_1} & 0 \le v \le \gamma d_1 \\ d_3 + d_2 v & v > \gamma d_1 \end{cases} \qquad \text{Equation 4-12}$$

Where

$$d_1 = \frac{v_{max} A (f_{max} - 1)}{S(A+1)}$$

$$d_2 = \frac{S(A+1)}{v_{max} A (\gamma + 1)^2}$$

$$d_3 = \frac{\gamma^2 (f_{max} - 1)}{(\gamma + 1)^2} + 1$$

For shortening velocity between maximum contraction velocity, v_{max}, and zero, classic Hill equation was used. Shape parameter A was assumed to be 0.25 and the maximum contraction velocity for the muscle with mixed fast and slow twitch fibers

was assumed to be 10 l_0/s [164]. $\lambda(a)$ was used to take into account the effect of the level of activation a on the force-velocity relationship [177]:

$$\lambda(a) = 1 - e^{-3.82a} + ae^{-3.82} \quad \text{Equation 4-13}$$

For slow lengthening another hyperbolic equation was used. f_{max} the asymptotic value of f_v was assumed to be 1.8 [164] and *S* was set to a value of 2.0 to produce a doubling of slope of the force-velocity curve at zero velocity [176, 177, 182]. For both high lengthening and contraction velocity a linear relationship with the same slope was used to make sure that f_v is invertible. A value of 5.67 for γ was used to approximate correct yielding behavior at high force. The values for other constant of the two lines were obtained based on the continuity of the curve and its first derivative [182].

4.3.8 Pennation angle

To find the pennation angle, it was assumed that h in Figure 4-5 was constant. Therefore, using the following equation, we can find the pennation angle at each instant in time [162, 174]:

$$h = l_0 \sin(\varphi_0) = l \sin(\varphi) \quad \text{Equation 4-14}$$

Where φ_0 is the pennation angle when CC has its optimal length l_0, and φ is the pennation angle corresponding to any other CC length, l.

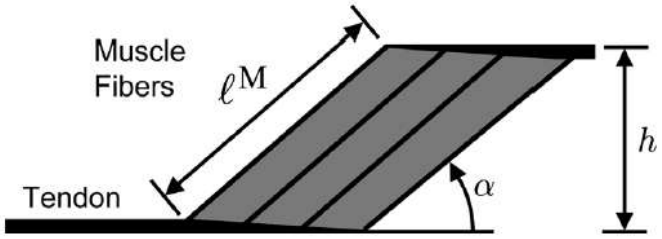

Figure 4-5 Simplified geometric representation of muscle fibers and tendon for musculotendon modeling (adapted from [174])

4.3.9 SEC Force

SEC component is in series with CC and assumed to be a passive structure, transferring the loads produced by CC to the bones. SEC acts like a rubber band, i.e. it does not carry any load when it is shorter than its unloaded length, l_{USEC}; however above this length it transfers high loads to the bones [162]. It was assumed that SEC behaves nonlinearly at small strains and then have a linear relationship with its strain [164], and transfers the force equal to maximum isometric CC force with a strain of %3.3 and fails at %10 strain, when carrying 3.5 maximum isometric CC force [164]:

$$\begin{cases} f_{SEC} = 0 & \varepsilon \leq 0 \\ f_{SEC} = 1480.3\varepsilon^2 & 0 < \varepsilon < 0.0127 \\ f_{SEC} = 37.5\varepsilon - 0.2375 & \varepsilon \geq 0.0127 \end{cases} \quad \text{Equation 4-15}$$

In which f_{SEC} is the normalized SEC force. In additon, ε is the SEC strain calculated as :

$$\varepsilon = \frac{l_{SEC} - l_{USEC}}{l_{USEC}} \quad \text{Equation 4-16}$$

l_{USEC} is the unloaded SEC length after which SEC starts to produce force. To find the tendon force, its normalized force must be multiplied by F_{0CC}.

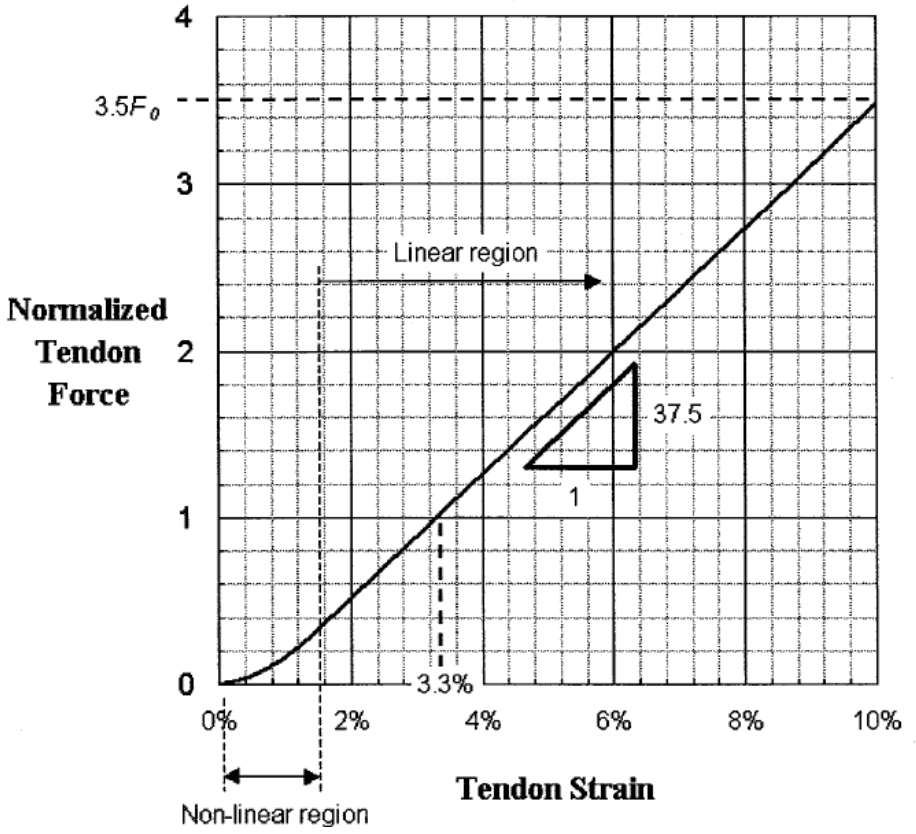

Figure 4-6 Normalized force-length relationship of SEC (adapted from [164])

4.3.10 Putting it all together

Reconsidering Equation 4-6, we can cancel out F_{0CC} from both side of the equation:

$$f_{SEC} = (f_A(l)a(t)f_v(v,a) + f_{PEC}(l))cos(\varphi) \qquad \text{Equation 4-17}$$

This is a first order nonlinear ordinary differential equation (ODE) which should be solved using numerical methods [162, 174]. To solve this ODE the following

parameters must be known: l_0, φ_0, and l_{USEC}, and activation and musculotendon length should be already obtained using the procedure explained in section 4.3.1 and the anatomical model, respectively. Equation 4-17 does not have a unique solution [174]; however, the following equation can be solved to obtain a unique solution [174]:

$$v = f_v^{inv}\left(\frac{f_{SEC}/\cos(\varphi) - f_{PEC}}{f_A(l)a(t)}\right) \quad \text{Equation 4-18}$$

The procedure is as follows [162]:

1- To find the initial CC length, it was assumed that the initial normalized SEC force is equal to initial activation and Equation 4-6 was solved to find the SEC initial length and therefore CC initial length (MTU length is known).

2- Starting with obtained initial CC length, the corresponding pennation angle was found using Equation 4-14.

3- SEC length then was found using the following equation (Figure 4-2);

$$l_{SEC} = l_{mtu} - l\cos(\varphi) \quad \text{Equation 4-19}$$

Therefore, SEC force can be found using Equation 4-15.

4- f_{PEC} and $f_A(l)$ also will be calculated using Equation 4-10 and Equation 4-8, respectively.

5- f_v then can be found and using its inverse the velocity will be calculated. Integration will yield the length of CC at the next time step and the whole loop starts over again.

Equation 4-18 encounters singularities in case of one of the followings [174]:

$$\begin{matrix} a \to 0 \\ f_A \to 0 \\ \varphi \to 90 \end{matrix} \qquad \text{Equation 4-20}$$

Numerical singularities make the integration tedious and slow [174]. In order to avoid this singularities, minimum values of 0.01 and 0.05 was considered for a and f_A, respectively [174, 177]. It was also assumed that the maximum pennation angle is 84.26 degrees ($\cos^{-1} 0.1$) [174]. When the pennation angle reaches its maximum value, CC has its shortest length; therefore, in order to prevent CC length to become unrealistically short the following constraint also was used [174]:

$$v = \begin{cases} 0 & l < l_{min} \; and \; v < 0 \\ v & otherwise \end{cases} \qquad \text{Equation 4-21}$$

In addition to these bounds, a stiff integrator in MATLAB was used to solve the equation.

4.3.11 Calibration

The calibration is done indirectly using the knee joint moment obtained through experiments, i.e. the knee moment, produced by muscle in sagittal plane should be the same as the knee moment obtained using inverse dynamics during self-selected gait of a subject [103, 119, 159]. From the collected trials of the subjects in this study (4.2.2), one was used to calibrate muscle parameters for each subject, and then three trials per subject were used to find the knee joint contact forces and mean values were reported for the muscle and contact forces.

A least square optimization was performed to find a set of muscle parameters that minimized the difference between the moments from inverse dynamics and from the

muscle forces, i.e. the root mean squared error (RMSE) between the two moments, as follows:

$$objective\ function: RMSE = \sqrt{\frac{\sum_{i=1}^{n}(m_i^{ID} - m_i^{EMGd})^2}{n}}$$

Where m_i^{ID} and m_i^{EMGd} are the moments, found using inverse dynamics and EMG-driven model at the ith time step, respectively and n is the total number of data points. Optimization was performed using a global search algorithm that starts with a local gradient based solver (such as fmincon) from multiple start points to sample multiple basins of attraction and find the global optimum. The method was developed based on the work by Ugray et al. [183]; more details can be found in its Matlab documentation page at http://www.mathworks.com/help/gads/how-globalsearch-and-multistart-work.html#bsd946t.

4.3.12 Optimization parameters

Two sets of parameters were calibrated in the optimization process: 10 EMG to activation parameters, and 12 muscle architecture parameters.

For the EMG to activation parameters, it was assumed that each muscle had a different nonlinear shape factor, A (Equation 4-5), constrained to be between -3 to 0 [103, 119]; therefore, a total of 9 shape factors were calibrated (VI was assumed to be the mean of VL and VM). Electromechanical delay also was found through optimization and was assumed to be the same for all the muscles. The bound here was chosen between 30 to 100 milliseconds.

In order to find each muscle force, four parameters should be known, including, optimal CC length, l_0, SEC unloaded length, l_{USEC}, maximum isometric force, F_{0cc}, and pennation angle at optimal length, φ_0. The values for the optimal CC length and corresponding pennation angle were chosen from OpenSim 2392 model. l_{USEC} has huge

effect on the behavior of the muscle; therefore, unloaded SEC lengths was allowed to be adjusted by the optimization process for all 10 muscles. The initial values were obtained from OpenSim 2392 model and l_{USEC} was allowed to vary in a range of ±%20 of the initial values. For the maximum isometric force, the initial values from OpenSim 2392 were used and two global coefficients, α_{flex} for all the flexors and α_{ext} for all the extensors were used to scale the initial values [103]. α_{flex} and α_{ext} were allowed to vary between 0.5 to 2.5 [184].

Optimization does not guarantee realistic solutions for the muscles; therefore, penalty function were used [159]. To prevent unrealistically long CC length, the normalized passive force of MTUs was assumed to be less than 0.06 and otherwise the solution would be penalized based on the difference between the current passive force and 0.06. This was done by adding the absolute difference between the maximum current passive force and 0.06, multiplied by 100 to the objective function, RMSE. Furthermore, for the muscle to be capable of force production when actively contracting during gait, the normalized muscle length should not be less than 0.5 and therefore, the values less than 0.5 would be penalized based on their distance to this value [184]. This was also done by adding the absolute difference between the minimum current normalized CC length and 0.5 multiplied by 100 to the objective function, RMSE.

4.3.13 Mediolateral model to find the contact forces

To find the medial and lateral compartment contact forces, a 2D model in the mediolateral plane was considered [119, 127, 159, 184] (Figure 4-7). Contact forces parallel to the shaft of the tibia were assumed to be the main contributors and the forces perpendicular to this direction were assumed to have negligible effect on joint contact forces [119-121, 127, 159, 184]. It was also assumed that medial and lateral contact forces acted through only one point.

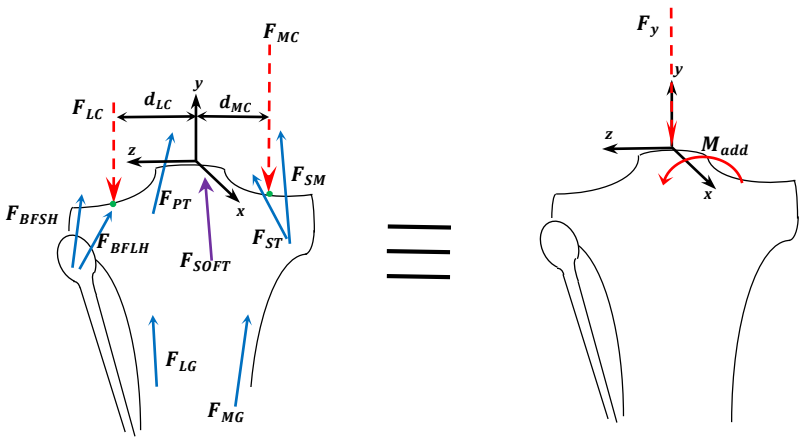

Figure 4-7 Schematics of the loads passing through the medial and lateral compartment of the knee joint and the external knee frontal plane moment; the moment from the external loads about both contact points should be balanced with internal moments of the muscle and contact forces.

To find the medial and lateral contact forces, the frontal plane moment produced internally by muscles, contact forces, and other soft tissues was assumed to be equal to the external adduction moment, obtained through inverse dynamics. This equality referred to as "joint equipollence" [185]. Figure 4-7 shows the muscle and contact forces and forces from other soft tissues (such as ligament, shown as F_{soft}). It was assumed that the action of these soft tissues were negligible during normal gait [119-121, 127, 159]. The following equation was therefore used to yield medial (F_{MC}) and lateral (F_{LC}) contact force (different parameters used are shown in Figure 4-7):

$$F_{MC} = \frac{\sum_{i=1}^{10} r_i^{LC} F_{SECi} - M_{ext}^{LC}}{(d_{LC} + d_{MC})}$$ Equation 4-22

$$F_{LC} = \frac{\sum_{i=1}^{10} r_i^{MC} F_{SECi} - M_{ext}^{MC}}{(d_{LC} + d_{MC})}$$ Equation 4-23

Where

F_{MC}: medial contact force

F_{LC}: lateral contact force

M_{ext}^{LC}: external knee frontal plane moment about the lateral contact point

M_{ext}^{MC}: external knee frontal plane moment about the medial contact point

r_i^{LC}: frontal plane moment arm of the ith MTU about the lateral contact point

r_i^{MC}: frontal plane moment arm of the ith MTU about the medial contact point

d_{LC}: distance between the joint center and the point of the lateral tibial compartment

d_{MC}: distance between the joint center and the mid-point of the lateral tibial compartment

r_i^{LC} and r_i^{MC} were found using OpenSim. $M_{ext}^{LC}$and M_{ext}^{MC} were also found using Visual3D Biomechanics. For the lateral compartment when the force is obtained to be negative, it means that the muscle forces are not sufficient to balance the external moments and the ligament should come to action; in other words, lateral compartment unloading happens when the F_{LC} in Equation 4-23 is negative [103, 121].

4.3.14 Validation of the model against literature

Several parameters were obtained using the EMG-driven model and compared to the existing literature for validation, including root mean squared error (RMSE) of the inverse dynamics sagittal plane moment and the moment predicted by the EMG-driven model, muscle forces, and the patterns of tibiofemoral joint medial, lateral and total contact forces and their peak values.

The results of the model calibration was compared to two EMG-driven modeling studies that stated their RMSE values. In the first study, Lloyd et al. developed an EMG-driven model for healthy individuals to find the distribution of forces among 13 muscles during different tasks, including running, cutting and dynamometer exercises [103]. In the next study, Gerus et al. used an EMG-driven model to find medial, lateral and total knee joint contact forces during walking of a subject, who was implanted with an instrumented prosthesis (11 muscles were modeled) [184].

There was only one EMG-driven modeling study that has reported its obtained muscle forces; however, the study seemed to overestimate the tibiofemoral contact forces due to high muscle forces [119]; therefore, our muscle forces were compared to the results of two other studies that have used optimization to calculate the muscle forces. In the first study Kim et al. predicted tibiofemoral joint contact forces for a subject who was implanted with an instrumented prosthesis. The muscle redundancy problem was solved by minimizing the sum of the squares of the muscle activations [106]. In the second study, Crowninshield and Brand solved the muscle redundancy problem during normal walking by minimizing the sum of the squared stress in 47 muscles in lower limbs [186]. These two studies were chosen to validate the muscle forces, because they obtained muscle forces during normal walking and their force patterns were consistent with measured EMG activity during gait.

The patterns and values of the contact forces were validated against three studies; the first study used an EMG-driven approach to calculate knee joint medial and lateral contact forces for twenty eight subjects [156]; the second study used dynamic optimization method to find the muscle forces and subsequently predict the joint contact forces during normal walking [104]; the last study reported the joint contact force during walking, obtained through using an instrumented prosthesis [187]. These studies were chosen to be able to compare our results to two models which used two different methods, and also experimental data, available through instrumented prosthesis.

4.4 RESULTS

Table 4-1 and Table 4-2 show the characteristics of the three individuals in the study.

Table 4-1 Characteristic of the subjects included in this study

	Mass (Kg)	Height (M)	BMI (Kg/m^2)	Age (years)	Gender
Subject 1	89.0	1.84	26.3	40	Male
Subject 2	101.3	1.84	30.1	53	Male
Subject 3	63.7	1.68	22.6	49	Male

Table 4-2 Stride characteristics of the subjects in the study

	Stride length (m)	Stride time (s)	Stance Time (s)	Stance percent	Speed (m/s)
Subject 1	1.44	1.14	0.73	64.6	1.26
Subject 2	1.42	1.23	0.79	64.4	1.16
Subject 3	1.27	1.16	0.75	64.4	1.09

4.4.1 Validation of the model against literature

This sections shows the results of the simulations performed for subject 1 (Table 4-1, Table 4-2), who was on overweeight asymptomatic 40 year old male, to demonstrate the implementation and validation of the model against existing literature results. Table 4-3 shows the demograhpic information of studies used for the validation of our EMG-driven model.

Table 4-3 Demographic information of the studies used for the validation of the model (NM: not mentioned)

study	Used for the validation of	Mass (Kg)	Height (M)	BMI (Kg/m^2)	Age (years)	Gender	Number of subjects
Current study	-	89.0	1.84	26.3	40	Male	1
Lloyd et al. [103]	RMSE	74.6±8.6	NM	NM	20.5±9.5	Male	6
Kim et al. [106]	Muscle forces	68	1.7	23.5	80	Male	1
Gerus et al. [184]	RMSE	68	1.7	23.5	83	Male	1
Winby et al. [156]	Contact forces	78.4±12.8	1.76±0.08	NM	43±6	NM	28
Crowninshield et al. [186]	Muscle forces	NM	NM	NM	NM	NM	NM
Kutzner et al. [187]	Contact forces	98.3	1.76	NM	65	Male	3
Shelburne et al. [104]	Contact forces	NM	NM	NM	NM	NM	NM

Measured EMG data for subject 1 is shown in Figure 4-8. Muscle forces are shown in Figure 4-9 and their peak values are shown in comparison to two other studies in Table 4-4 [106, 186]. It is seen that the muscles are following the same patterns as the measured EMG activity, which is due to the direct use of EMG to predict the muslce forces. Our peak muscle force values for vasti muscles are consistent with results of the other two studies (Table 4-4), while the maximum force of the RF seems to be small for our subject, which is consistent with its small EMG activity, shown in Figure 4-8. Obtained peak MG is higher than LG, which agrees with its smaller EMG activity (Figure 4-8). The average peak forces of the two muscles are the same as the study performed by Kim et al. [106], while the MG force is higher than the corresponding value in Crowninshield and Brand's study [186]. The average of peak hamstrings muscle forces for subject 1 in our study is almost the same as Kim's study; however, the force distribution among muscles are different from Crowninshield's results. Obtained samll forces for ST and SM are consistent with their small EMG activity (Figure 4-8).

Figure 4-10 shows the internal knee flexion moment during the stance phase of walking obtained through inverse dynamics and through muscle forces, for the trial selected for the calibration. Table 4-5 shows the RMSE for each trial after the model was calibrated for the subject and Table 4-6 compares our mean RMSE for the first subject with two other EMG-driven modeling studies [103, 184], showing agreement among the studies.

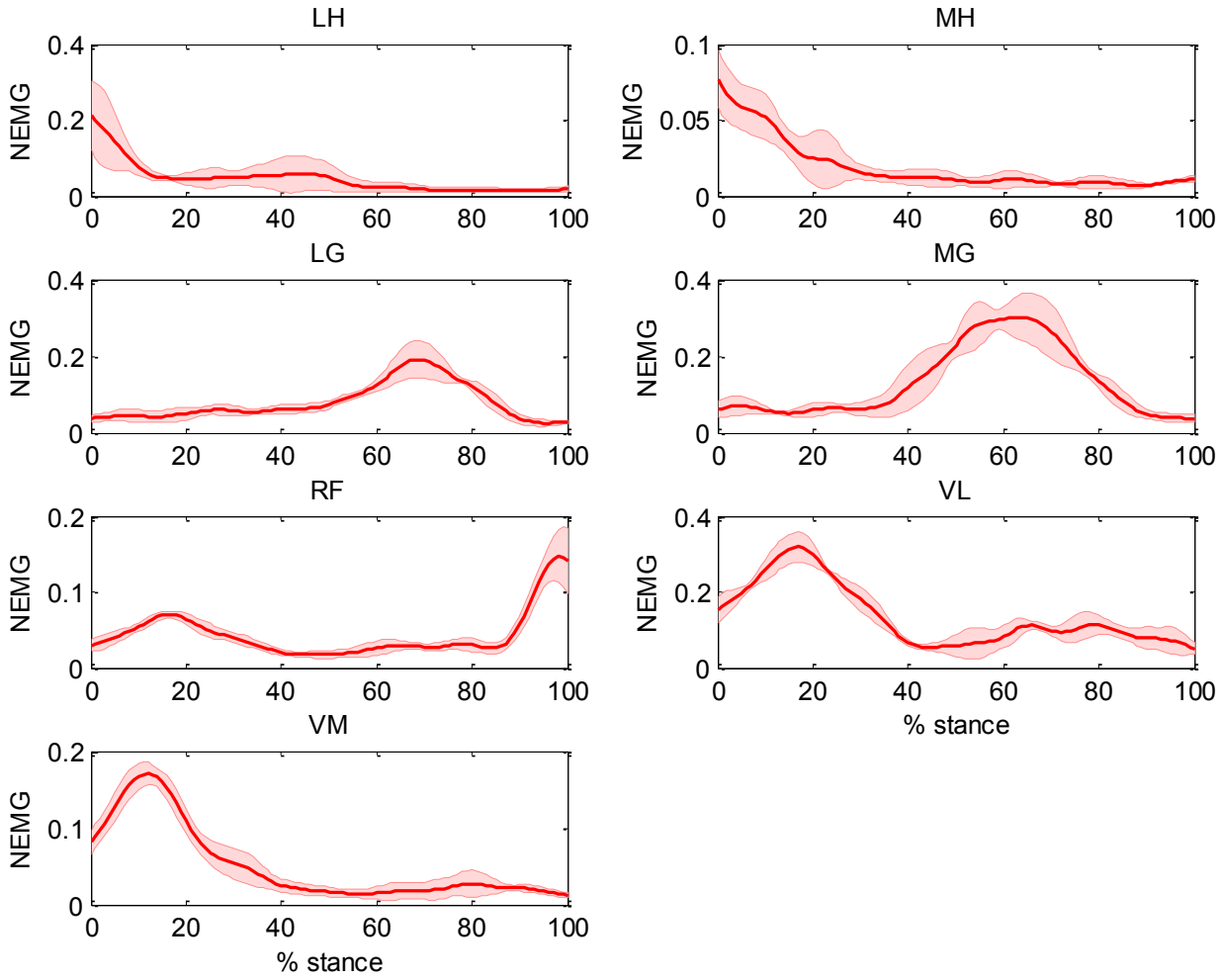

Figure 4-8 Linear enveloped EMG data measured during the stance phase for the first subject (NEMG=Normalized EMG to maximum voluntary isometric contraction; mean ± standard deviations are shown for three trials)

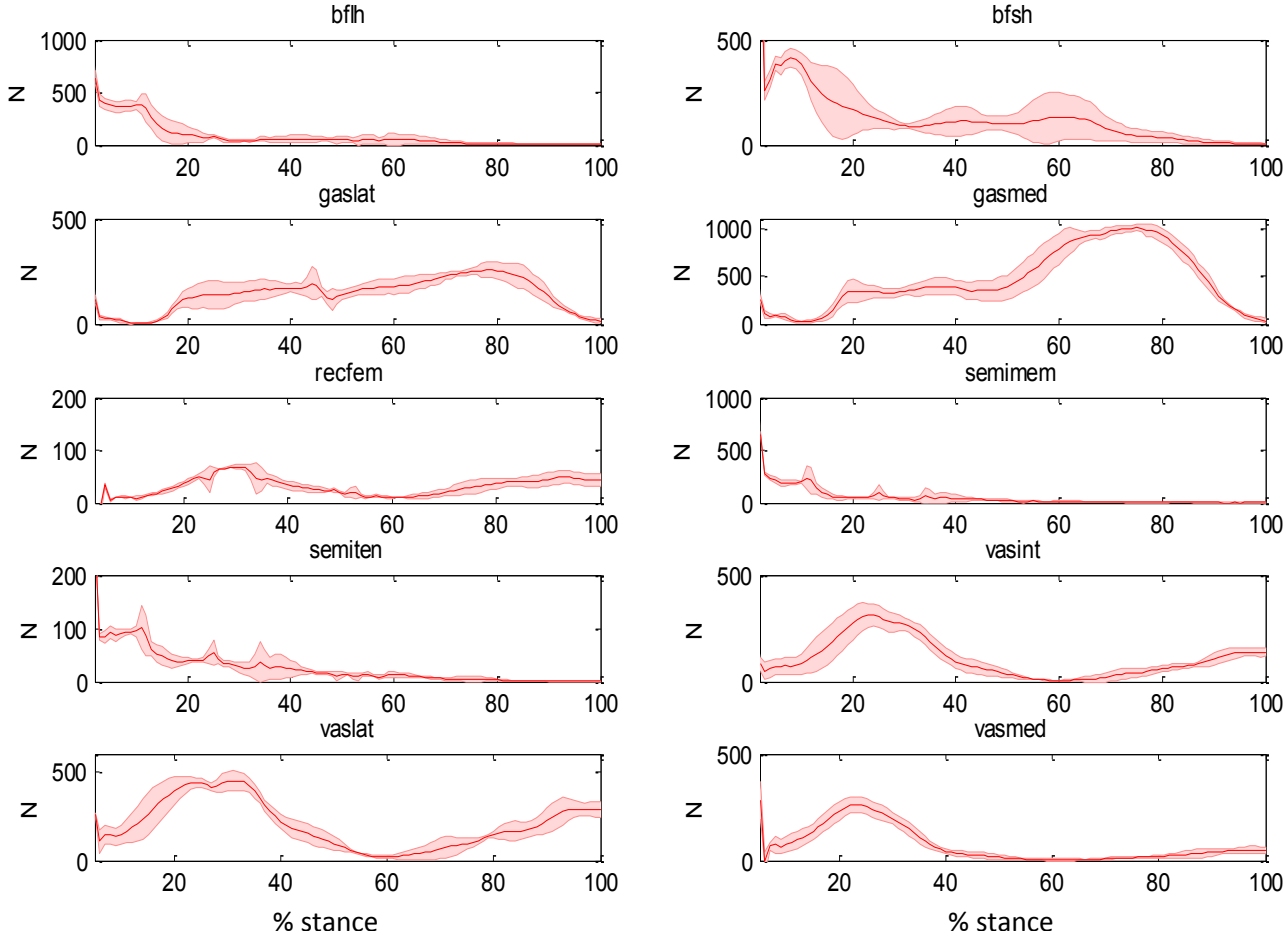

Figure 4-9 Absolute forces of the 10 simulated muscles for the first subject during the stance phase of gait (horizontal axis shows % of the stance phase; mean± standard deviations are shown); the abbreviations used are: bflh=biceps femoris long head, bfsh=biceps femoris short head, gaslat=lateral gastrocnemius, gasmed=medial gastrocnemius, recfem=rectus femoris, semimem=semimembranosus, semiten=semitendinosus, vasint=vastus intermedius, vaslat=vastus lateralis, vasmed=vastus medialis.

Table 4-4 Absolute peak stance phase muscle forces obtained in this study for subject 1 compared to the results from literature

study	Subject 1 (N)	Kim et al [106] (N)	Crownishield and Brand [186] (N)
Mtheod	EMG-driven model	Optimization	Optimization
VL	500	448	550
VM	400		500
VI	300		350
RF	<100	-	300
LG	350	743	450
MG	900		500
BFLH	550	448	650
BFSH	450		350
SM	300		750
ST	100		600

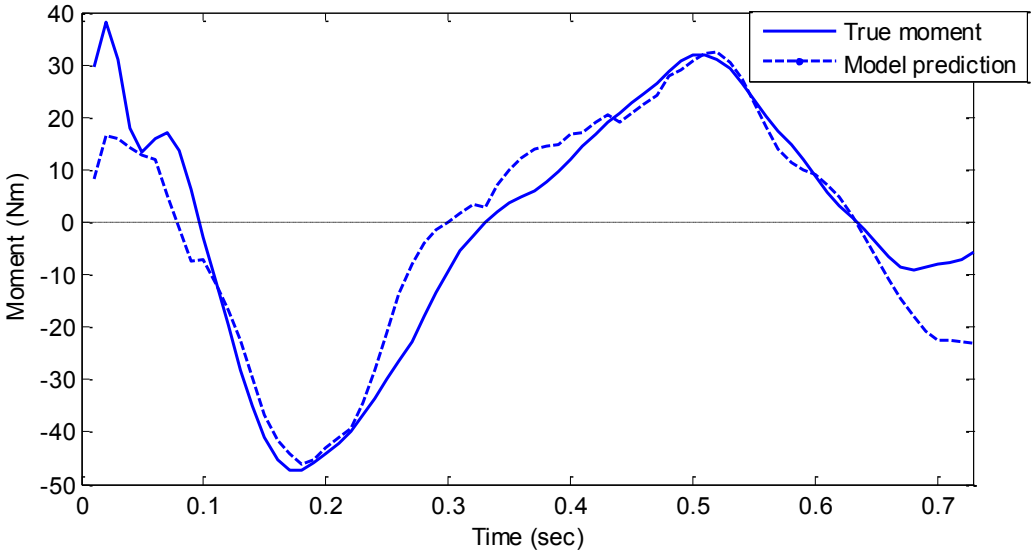

Figure 4-10 The net resultant internal knee sagittal plane moment obtained through inverse dynamics (solid line) and the moment predicted from muscle model (dashed line) during the stance phase for the calibration trial (RMSE=7.15 Nm) for subject 1

Table 4-5 RMSE values of the knee flexion moment, found using muscle model and inverse dynamics for different trials for the first subject during stance phase

	Optimization Trial	Trial 1	Trial 2	Trial 3
RMSE (Nm)	7.14	9.50	9.66	8.19
Normalized RMSE (to body mass, Nm/kg)	0.08	0.11	0.11	0.09

Table 4-6 Mean RMSE obtained in our study compared to two other EMG-driven modeling studies

	Our results	Lloyd et al [103]	Gerus et al [184]
RMSE (Nm)	8.62	9.8-15.88	2.3-17.9
Normalized RMSE (to body mass Nm/kg)	0.10	0.14-0.19	-

Figure 4-11 shows the net resultant knee joint flexion/extension and ab/adduction moments for the subject during the stance phase, calculated from inverse dynamics model. Figure 4-12, Figure 4-13 and Table 4-7 show our results for medial, lateral, and total tibiofemoral joint contact forces during the stance phase of the walking in comparison to three other studies [104, 156, 187]. Our lateral contact force is a little higher than the study which used EMG-driven model [156]; however, it overestimates the values obtained using instrument prosthesis and the other modeling study (Table 4-7). Our medial contact forces are smaller than the EMG-driven study, almost the same as the study which used dynamic optimization, and a little higher than the instrument prosthesis study (Table 4-7). Only the last study stated their average walking speed which was smaller compared to our subject 1's speed. Furthermore, our total contact forces are consistent with the results of the instrumented prosthesis study (Table 4-7). In addition, the patterns of the medial, lateral, and total contact forces for subject 1 is consistent with the results obtained in other studies (Figure 4-12, Figure 4-13).

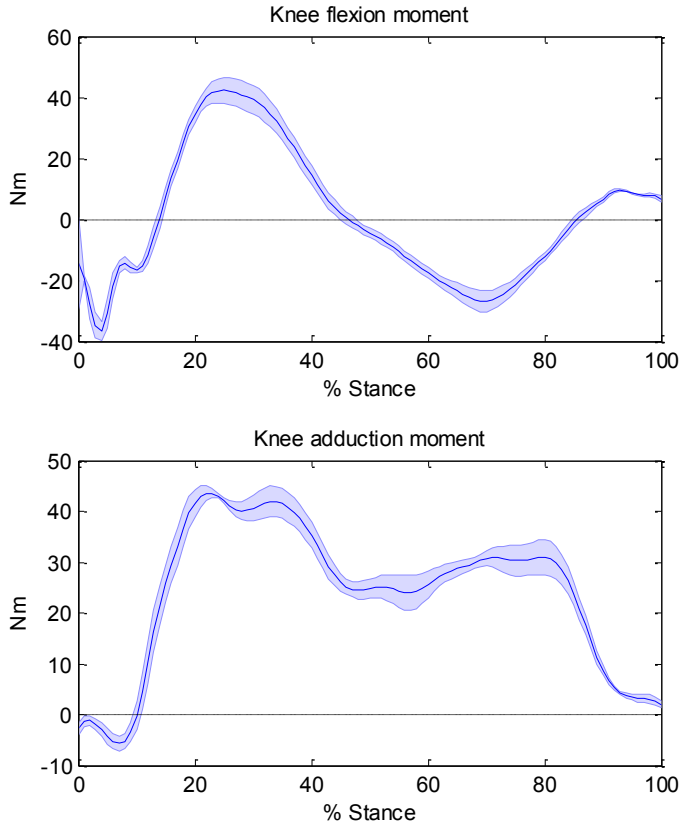

Figure 4-11 Net external resultant knee flexion/extension and ab/adduction moment for subject 1 during the stance phase of the gait (mean± standard deviations are shown)

Table 4-7 Normalized (xBW) peak stance phase values of medial, leteral, and total tibiofemoral contact forces for subject 1 compared to literature studies

study	**Method**	**Walking Speed** (m/s)	**Lateral**		**Medial**		**Total**	
			1st Peak (BW)	2nd Peak (BW)	1st Peak (BW)	2nd Peak (BW)	1st Peak (BW)	2nd Peak (BW)
Subject 1	EMG-driven model	1.26	1.33±0.08	0.31±0.04	2.24±0.05	2.14±0.04	2.56±0.09	2.34±0.13
Winby et al [156]	EMG-driven model	-	1.63± 0.53	-	2.54±0.48	-	-	-
Shelburne et al [104]	Dynamic Optimization	-	0.45	0.61	2.30	2.14	2.66	2.47
Kutzner et al [187]	Instrumented prosthesis	1.18	0.5-0.9		1.5-2.0		2.1-2.5	

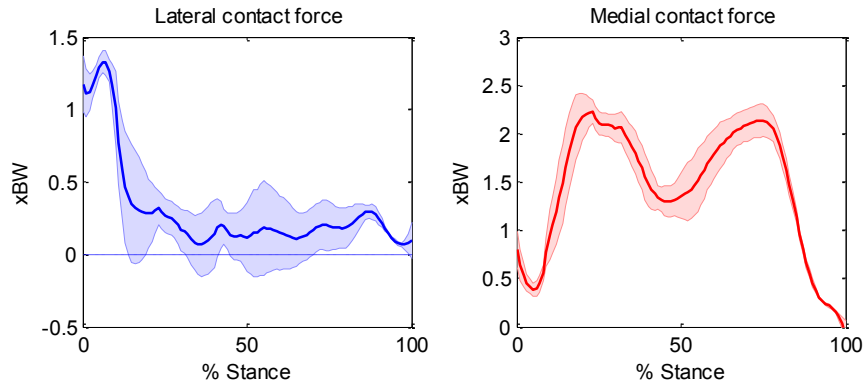

(a)

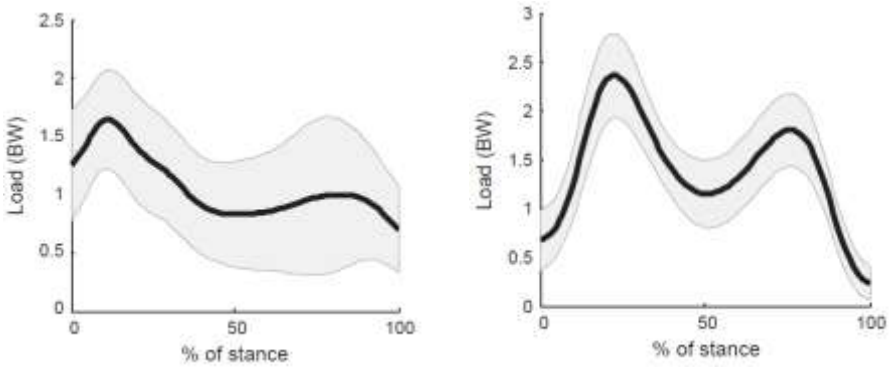

(b)

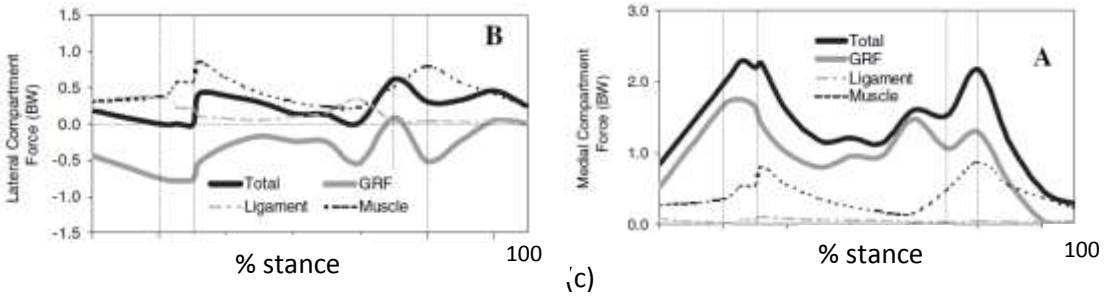

(c)

Figure 4-12 Normalized tibiofemoral joint medial and lateral contact forces during the stance phase: (a) our results for subject 1 (mean ± standard deviations), (b) Winby et al [156], (c) Kim et al [106] (the thick black lines are the knee compartmental forces)

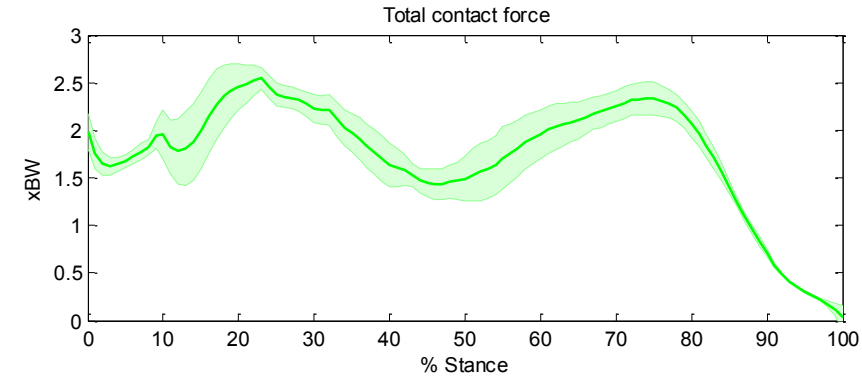

(a)

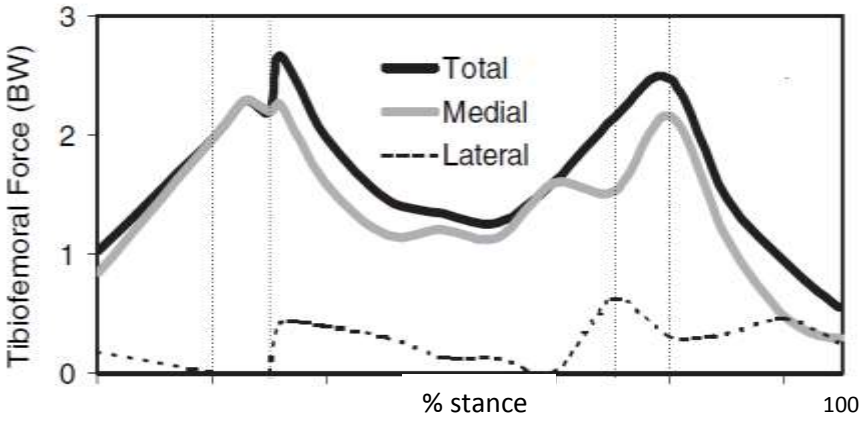

(b)

Figure 4-13 Normalized (xBW) total tibiofemoral joint total contact forces during the stance phase (a) our results for subject 1 (mean ± standard deviations) (c) Kim et al [106] (the thick black line is the total contact force)

4.4.2 Comparison of tibiofemoral joint contact force between the healthy weight and obese subjects

This sections reports the results obtained for subject 2 and subject 3 (Table 4-1, Table 4-2), who were obese and healthy weight asymptomatic subjects, respectively. The mean calibration RMSE of the EMG-driven model for the obese and healthy weight subjects were 7.83±1.26 Nm, and 4.64±0.29 Nm. Linear enveloped EMG activity, net resultant knee moments, absolute muscle forces, and tibiofemoral joint contact forces are shown in Figure 4-14, Figure 4-15, Figure 4-16, and Figure 4-17 for both subjects, respectively. The obese subject has higher EMG activity for all muscles compared to the healthy weight individual. This does not translate to the muscle forces, as the muscle forces for the vasti muscles are almost the same between the two subject (Figure 4-16).

The obese subject had higher first and second peak of all medial, lateral, and total absolute contact forces, and higher absolute knee flexion and adduction moments compared to the healthy weight subject (Table 4-8). This table also shows the difference between the peak values, obtained relative to subject 3 using the following:

$$percent\ difference = \frac{x_{obes} - x_{healthyweigh}}{x_{healthyweigh}} \times 100$$

X can be any of the parameters in the first colum of the Table 4-8. If the percent difference is positive it means obese subject had a higher value and vice versa.

Table 4-8 Absolute peak force and moment values for the obese and healthy weigh subjects

parameter	Subject 2 (obese)		Subject 3 (healthy weight)		Percent difference	
	1st peak	2nd peak	1st peak	2nd peak	1st peak	2nd peak
Lateral contact force (N)	1388±242	471±6	363±46	149±30	282%	216%
Medial contact force (N)	1795±121	1521±21	1448±82	1090±41	24%	40%
Total contact force (N)	2017±146	1887±60	1448±82	1090±41	39%	73%
Flexion moment (Nm)	57.5±6.2	-15.7±2.2	29.2±1.9	-8.0±0.6	97%	86%
Adduction moment (Nm)	47.4±1.3	34.7±1.7	30.2±1.1	26.8±1.2	57%	29%

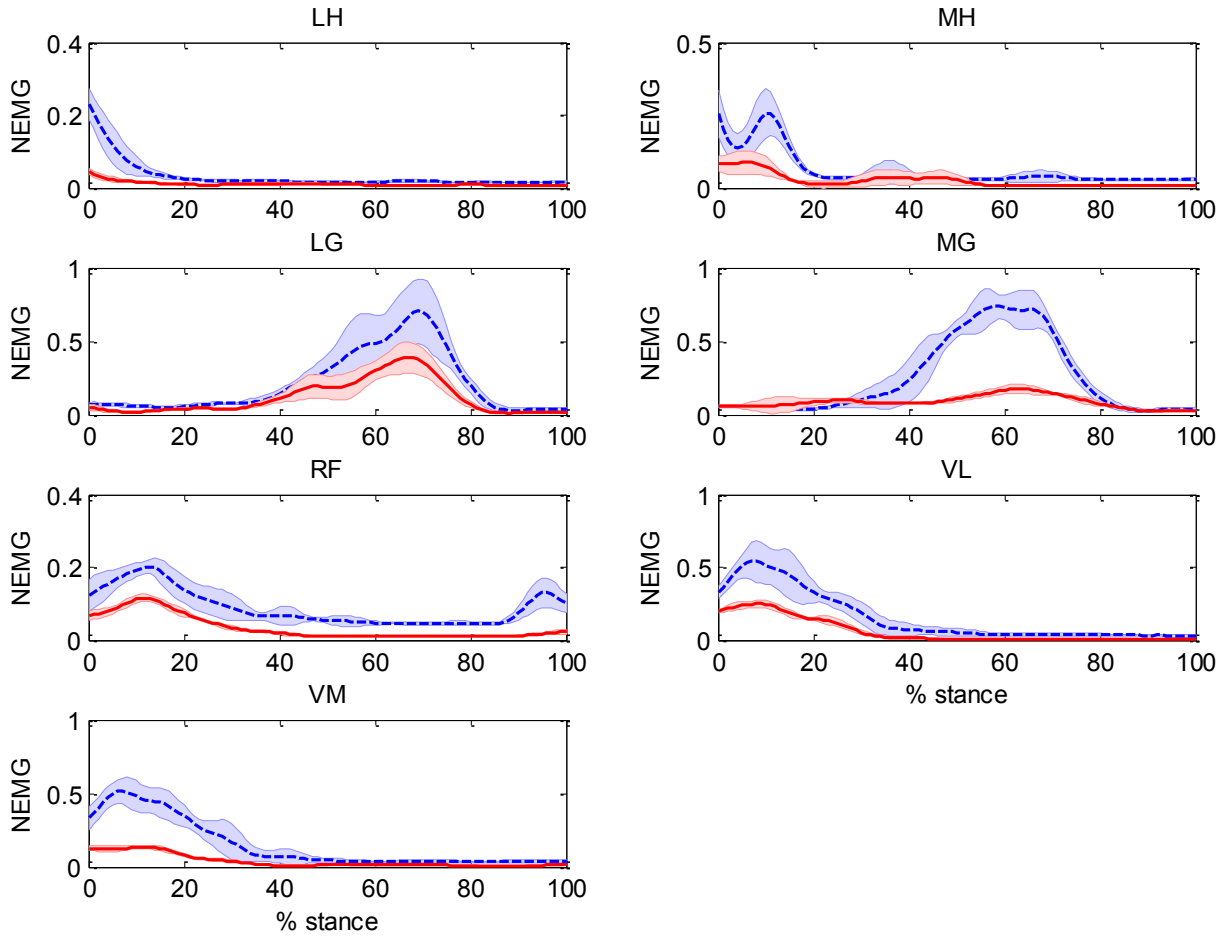

Figure 4-14 Linear enveloped EMG data measured during the stance phase for the obese (blue dashed line) and healthy weight (red solid line) subjects (NEMG=Normalized EMG; mean ± standard deviations are shown)

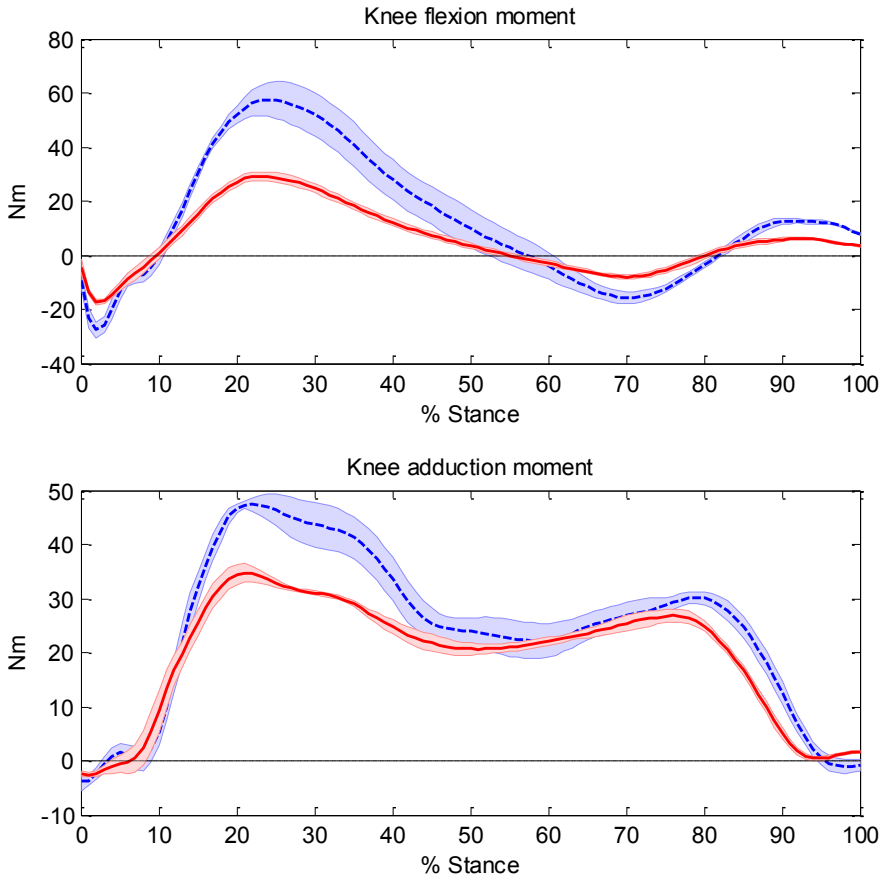

Figure 4-15 Knee flexion and adduction moments for the healthy weight (red solid line) and obese (blue dashed line) subjects during the stance phase (mean ± standard deviations are shown.)

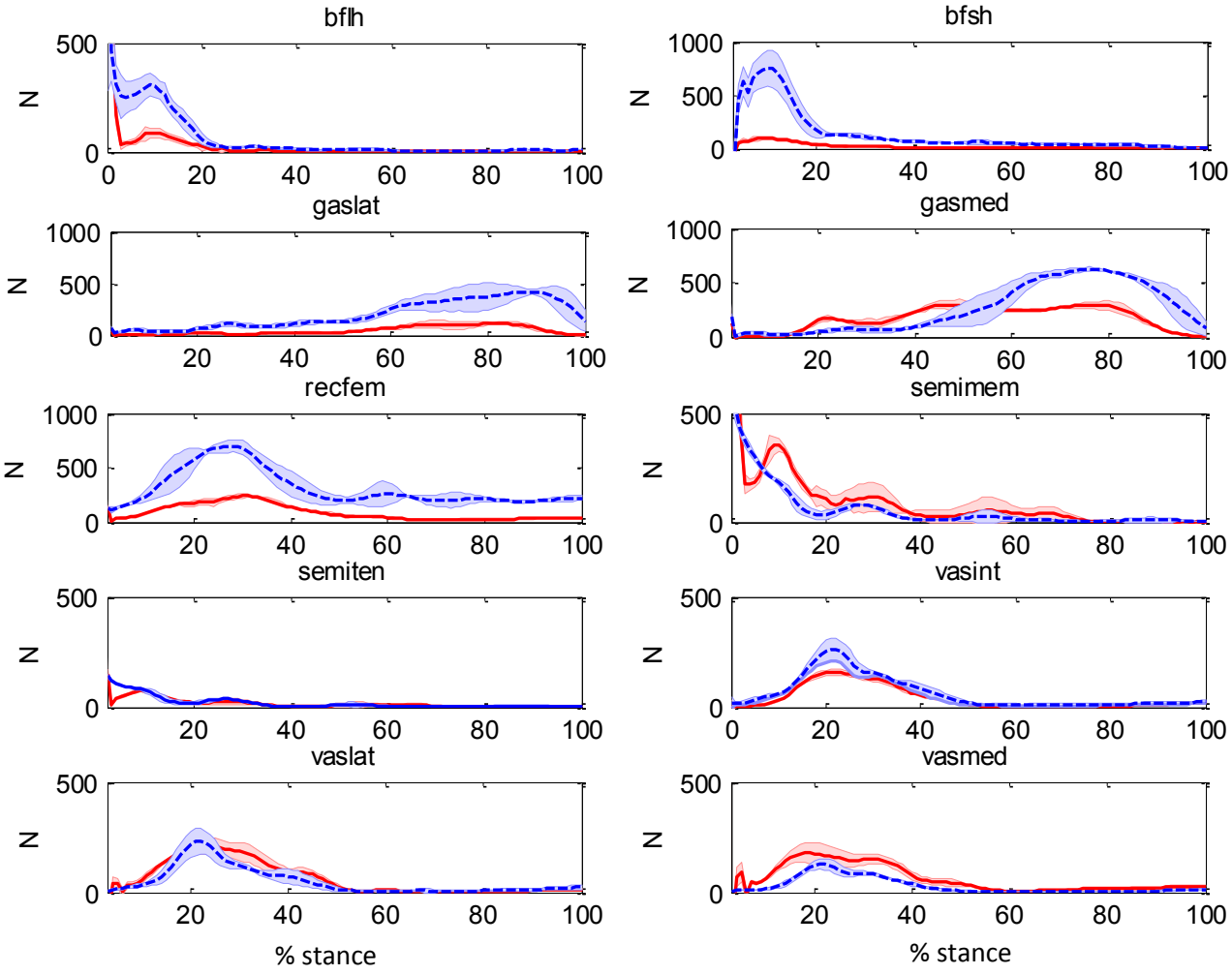

Figure 4-16 Absolute muscle forces for the healthy weight (red solid line) and obese (blue dashed line) subjects during the stance phase (mean ± standard deviations are shown.) ; the abbreviation used are: bflh=biceps femoris long head, bfsh=biceps femoris short head, gaslat=lateral gastrocnemius, gasmed=medial gastrocnemius, recfem=rectus femoris, semimem=semimembranosus, semiten=semitendinosus, vasint=vastus intermedius, vaslat=vastus lateralis, vasmed=vastus medialis.

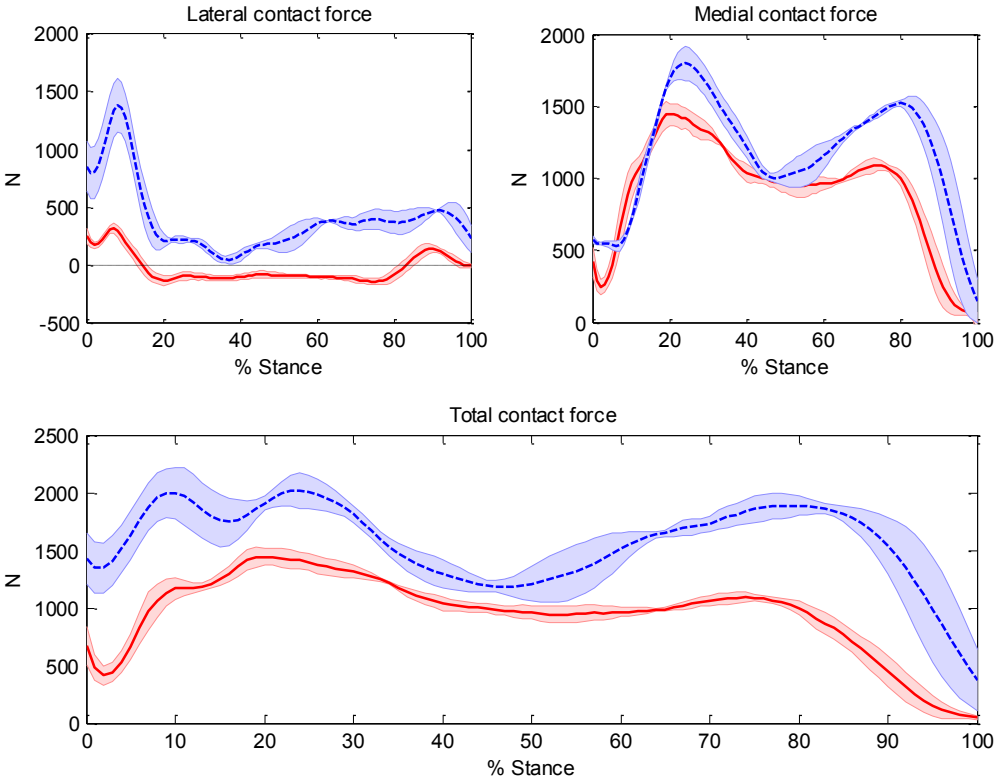

Figure 4-17 Absolute medial, lateral, and total tibiofemoral joint contact forces for the healthy weight (red solid line) and obese (blue dashed line) subjects during the stance phase (mean ± standard deviations are shown.)

Normalized muscle forces, tibiofemoral joint contact forces, and net resultant knee moments are shown in Figure 4-18, Figure 4-19, and Figure 4-20, respectively. The obese subject had higher first and second peak lateral normalized contact forces; however, in contrast to absolute values, the healthy weight subject had higher first peak of both medial and total normalized contact forces (Figure 4-19, Table 4-9). In addition, the obese subject had higher normalized knee flexion and smaller adduction moments (Figure 4-20, Table 4-9).

Table 4-9 Normalized peak contact forces and moment values for the obese and healthy weight subjects

parameter	Subject 2 (obese)		Subject 3 (healthy weight)		Percent difference	
	1st peak	2nd peak	1st peak	2nd peak	1st peak	2nd peak
Lateral contact force (xBW)	1.40±0.24	0.47±0.02	0.51±0.72	0.24±0.05	175%	96%
Medial contact force (xBW)	1.81±0.12	1.53±0.02	2.32±0.13	1.79±0.11	-22%	-15%
Total contact force (xBW)	2.03±0.23	1.90±0.05	2.32±0.13	1.79±0.11	-12%	6%
Flexion moment (Nm/kg)	0.57±0.06	-0.16±0.02	0.46±0.02	-0.13±0.01	24%	23%
Adduction moment (Nm/kg)	0.47±0.01	0.30±0.01	0.55±0.03	0.42±0.02	-15%	-29%

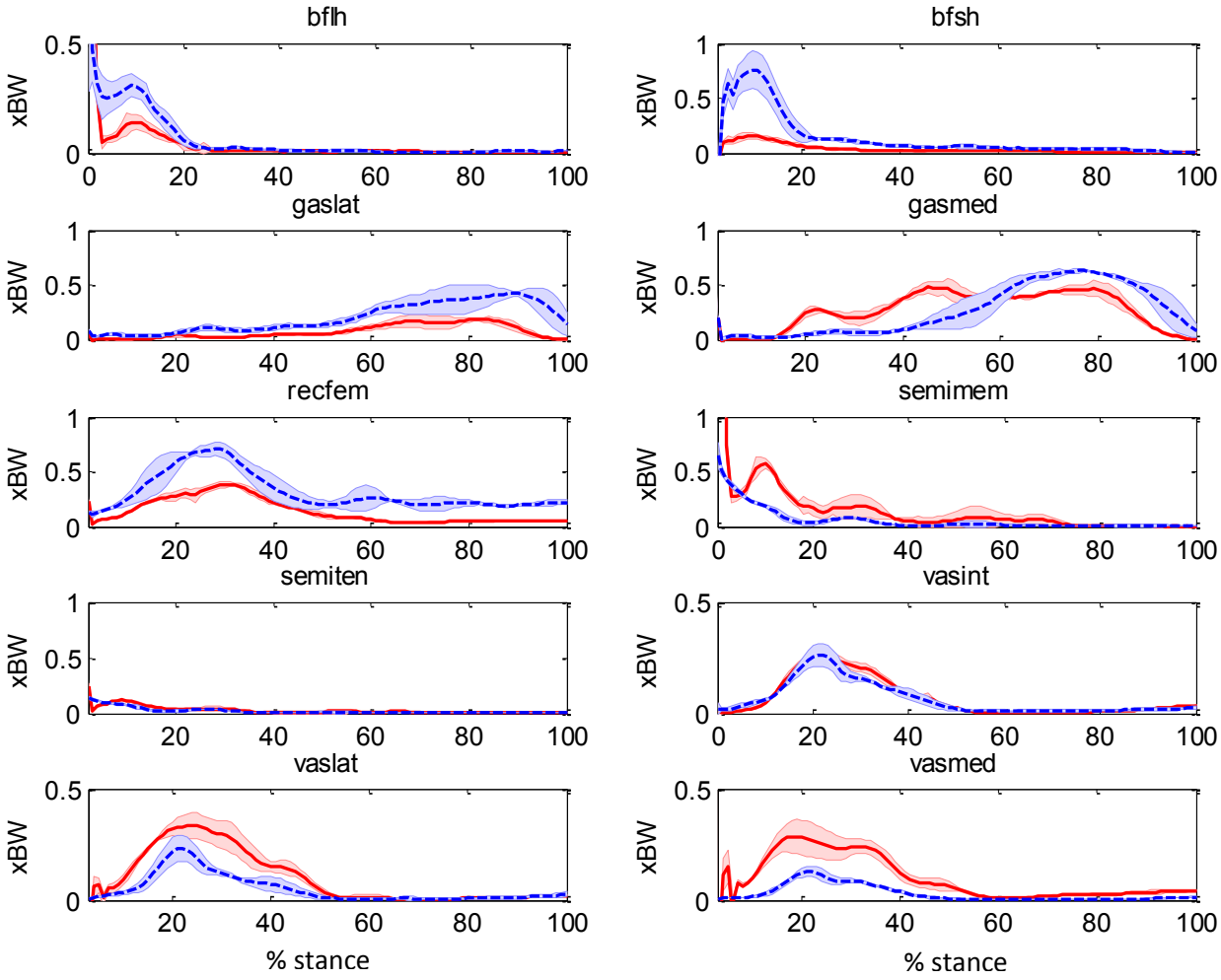

Figure 4-18 Muscle forces normalized to BW for the healthy weight (red solid line) and obese (blue dashed line) subjects during the stance phase (mean ± standard deviations are shown.); the abbreviation used are: bflh=biceps femoris long head, bfsh=biceps femoris short head, gaslat=lateral gastrocnemius, gasmed=medial gastrocnemius, recfem=rectus femoris, semimem=semimembranosus, semiten=semitendinosus, vasint=vastus intermedius, vaslat=vastus lateralis, vasmed=vastus medialis.

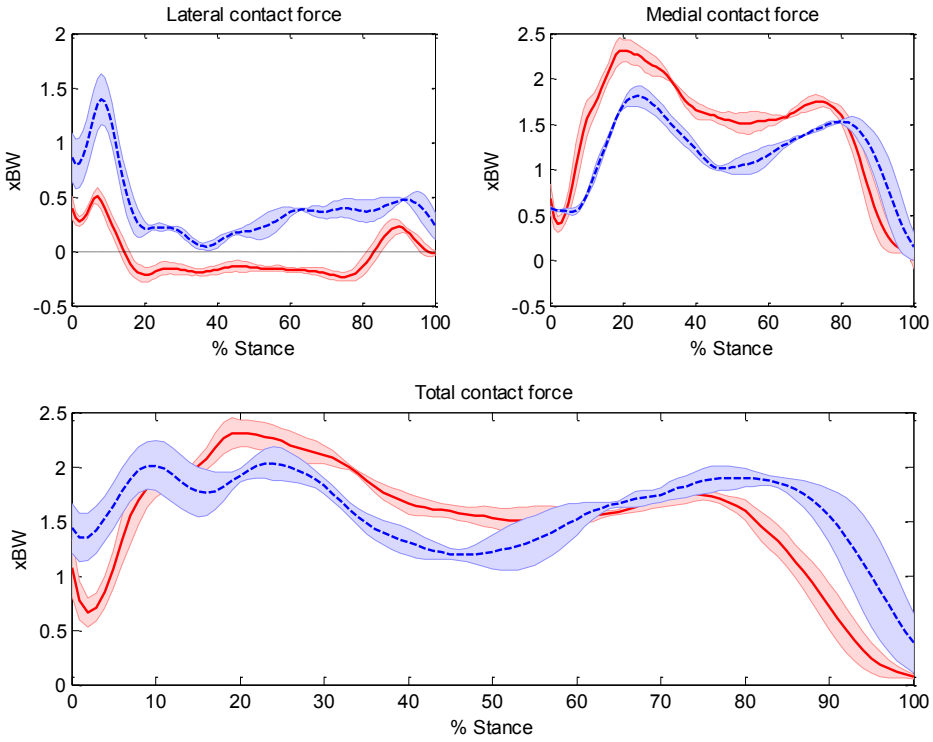

Figure 4-19 Medial, lateral, and total tibiofemoral joint contact forces normalized to BW for the healthy weight (red solid line) and obese (blue dashed line) subjects during the stance phase (mean ± standard deviations are shown.)

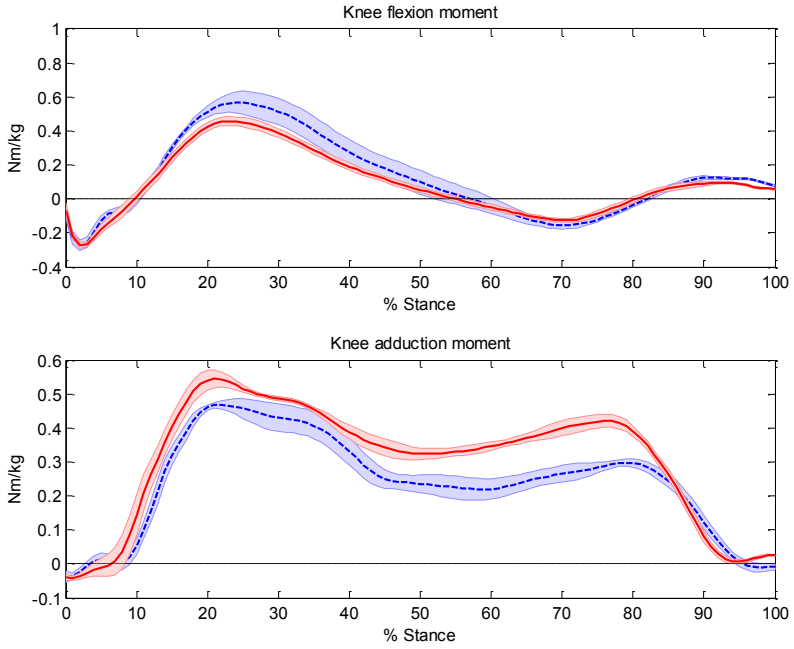

Figure 4-20 Normalized knee flexion and adduction moments for the healthy weight (red solid) and obese (blue dashed) subjects during the stance phase (mean ± standard deviations are shown.)

4.5 DISCUSSION

4.5.1 Validation of the model against literature

Obtained medial and total contact forces for the overweight subject (subject 1) followed similar patterns compared to literature studies, reporting contact forces from an instrumented prosthesis (Figure 4-12, Figure 4-13) [187] and modeling [106, 114, 156]. The patterns of the lateral contact force also agrees with previous EMG-driven studies [119, 159, 184]. The values of the maximum medial and total contact forces were 2.24 and 2.56 BW for subject 1 (Table 4-7), which are also consistent with data reported through the use of instrumented prosthesis by Kutzner et al. [187], showing medial and total contact forces in the range of 1.5-2.0 and 2.1-2.5 BW, respectively (Table 4-7). It should be noted that the data reported by Kutzner, the average walking speed of the subjects were 1.18 m/s which was smaller than the subject 1's speed, 1.26 m/s; therefore, higher contact forces in our study were expected. The peak contact forces are also consistent with the results of the modeling study by Shelburne et al. [104] and the EMG-driven model by Winby et al. [156] (Table 4-7). The small differences that exists between our results and other studies are probably due to differences of speeds, which are not mentioned in two out of three chosen studies (Table 4-4).

Obtained contact forces also confirmed the fact that a greater portion of the contact force passed through the medial compartment of the knee joint for subject 1 (Figure 4-12, Table 4-7) [104, 156]. High knee adduction moments during the stance phase of normal gait tend to unload the lateral compartment of the knee [108]. This could be prevented by a combination of muscle actions and pretention in the passive structures of the joint [108], and it was reported that individuals who have joint laxity produce higher muscle forces to compensate for the lost function of the ligaments and other passive structure [108]. Several modeling studies have examined this issue and some of them reported lateral joint unloading during gait [104, 127, 159, 188] and some found that muscles have the ability to counteract the external knee adduction moment and prevent lateral joint unloading [119, 189]. Here we see for subject 1 for half of the

stance phase lateral contact force is close to zero (Figure 4-12). This means that the ligaments should come into action to provide joint stability and prevent joint opening; consistent with previous studies hamstrings and quadriceps during early stance and gastrocnemius during late stance are the main stabilizers of the joint, which also agrees with the EMG activity of the muscles (Figure 4-8) [104, 112].

A combination of values of muscle parameters, reported in the literature [103, 161, 171, 190] were used to find the allowable ranges in the calibration process. RMSE for different walking trials are in the range of previous EMG-driven modeling studies (Table 4-5) [103, 184]. Lloyd et al reported RMSE of 9.08 to 15.88 Nm and normalized RMSE of 0.137 to 0.192 Nm/Kg for a set of running, cutting and dynamometer tasks for 6 asymptomatic individuals [103] (Table 4-6). Gerus et al reported RMSE values between 2.3 to 17.9 Nm during the stance phase of walking trials of a male subject implanted with an instrumented prosthesis [184] (Table 4-6). Here we found RMSE of 7.14 to 9.66 Nm and normalized RMSE of 0.08 to 0.11 Nm/Kg for subject 1 (Table 4-5), showing the accuracy of our optimization approach. Higher RMSE values seen in Lloyd et al. compared to our study probably were obtained due to the fact that they calibrated their model over a range of different tasks and this resulted in higher RMSE while giving their model better prediction ability and also more confidence in the values they obtained for the muscle parameters. Furthermore, as shown in Figure 4-10, the moments are different at the beginning and end of the stance phase. This probably has happened due to possible errors of the inverse dynamics output and therefore, the optimization was not able to match the two moments at these two intervals. It should be noted that optimization methods, which try to find a set of activations or muscle forces to replicate moments from inverse dynamics are easier to perform than EMG-driven models because they can choose muscle forces or activations in a relatively big range. In EMG-driven modelling, the solutions are constrained to a set of activations, obtained from experimental EMG, to reproduce the inverse dynamic moments. Furthermore, optimization methods are very sensitive to the formulation of the problem, i.e. the selection of the objective function and constraints may result in two completely different set of muscle forces, while

producing almost the same contact forces and inverse dynamic moments [114]. However, using EMG-driven models we can be more confident about the patterns of the muscle forces and the relative distribution of forces among muscle in different instances, because these are all dictated by amplitude and pattern of EMG.

Obtained muscle forces for subject 1 were consistent with previous studies [106, 114]. Our obtained values for VL, VI, and VM muscle for subject 1 were approximately 500, 400 and 300 N (Table 4-4, Figure 4-9), which were consistent with the results by Crowninshield and Brand [186], and Kim et al. [106]. Winby et al., who used an EMG-driven model reported a value of approximately 18 Nm/kg for the whole quadriceps (normalized to body mass) [119], while our obtained average value for normalized quadriceps is approximately 4 Nm/kg. It should be noted that this EMG-driven model study is different from the one used to validate the knee joint contact forces. This is the only EMG-driven model study reporting its muscle forces. Although they did not mention their moment arms, this may be due to difference in the moment arms that resulted in much higher muscle force in the study performed by Winby et al. [119]. Furthermore, the average obtained contact forces in that study were approximately 4 BW during the stance phase of walking, which are higher than the values usually reported for individuals implanted with instrumented knee prosthesis [89, 158, 187, 191], ranging from 1.8 to 3.0 BW. This may be in part due to the large quadriceps muscle forces predicted [119], considering that the muscle are responsible for a large portion of the observed contact forces (quadriceps are contributing to the first peak of contact forces) [90, 109].

Crowninshield and Brand reported values of approximately 450 N for LG and 550 for MG [186], respectively. Kim et al also reported an average value of 743 N for gastrocnemius [106]. Our values for subject 1 were approximately 350 and 900 N for LG and MG, respectively (Table 4-4, Figure 4-9). It should be noted that MG has a physiological cross sectional area (PCSA) which is almost twice as large as the PCSA of LG [31]; therefore, with the same amount of activation it is expected that MG force would be twice as large as LG force. In addition, for subject 1 the EMG activity of the

MG was almost twice as high as the LG activation (Figure 4-8), which again resulted in approximately twice larger force. Altogether, this resulted in a force for MG around three to four times higher than LG force. Therefore, the result found through optimization for MG seems to be correct. As a matter of fact, this seems to be a strength of EMG-driven approach that can distinguish between the muscles in a group with same function and distribute forces based on measured EMG. This is important, because as seen in Figure 4-10 the first peak of the knee adduction moment was higher than the second peak. However, the both peaks of the medial contact force were obtained to be almost the same. This was the result of large MG force, captured using the real EMG of the muscles (Figure 4-8), and shows that knee adduction moment cannot be used alone to assess the medial knee joint contact forces.

Subject 1's lateral hamstrings forces are consistent with the results reported by Crowninshield and Brand, while his medial hamstrings forces are smaller (Figure 4-9, Table 4-4). This small force values for SM and ST from our model were the results of low EMG activity (MH in Figure 4-8).

Obtained muscle forces demonstrated the ability of our implemented EMG-driven approach to solve the muscle redundancy problem in a way which was consistent with measured activation patterns of the muscle. Comparing muscle forces and their corresponding EMG-activity showed that both patterns and amplitude feature, seen in the EMG (Figure 4-8) were reflected into muscle forces (Figure 4-9) (i.e. higher EMG activity corresponded to higher muscle forces and vice versa (for an individual)). It may be argued that this model is a curve fitting exercise with the possibility of being over-determined. First, it should be noted that this model was developed based on real physiological phenomena that happen in the muscle, and the interaction between SEC force and CC force in a MTU constraint the way that the muscles are behaving [103]. Furthermore, the argument of being over-determined can be raised if the parameters which are candidates for the calibration, were adjusted without any constraint. However, in the calibration step all the parameters were allowed to vary in small, physiological ranges. Furthermore, the penalty functions kept the passive and active

forces within bounds expected during walking. Moreover, the number of data points used to calibrate the muscle parameters were well above the number of calibrated parameters, which was 22.

There are still some limitations with the EMG-driven method utilized in this study. The search space for the muscle parameters is large and therefore the solution to estimate absolute muscle force values is not unique [184]. One improvement could be to use a full lower limb model accompanied by sufficient experimental data during different tasks, which would improve the training of EMG-driven model (with more certainty of estimated muscle forces). In addition, the anatomical model used was a generic model whose limbs and muscles and corresponding attachment points were scaled uniformly to match the subject in the study and not measured directly. This may have introduced some errors in the obtained results because the muscle force prediction in the model is very sensitive to the obtained MTU length. Second, due to small moment arms for the muscles and relatively large knee joint moment, a small deviation from the real moment arm may result in high change in the predicted muscle force. This is specifically the case if we want to calibrate our model using maximum voluntary isometric contractions (MVIC). In this study we tried to calibrate the model using our MVIC trials; however, because accurate kinematics of the knee, hip, and ankle were not available, the results were not satisfactory and this happened due to error in the MTU length and moment arms due to lack of kinematic data during MVICs. Therefore, model results are very sensitive to moment arm lengths and therefore future models may want to incorporate more subject-specific information at this step. Furthermore, inherent errors due to unwanted skin movement of the markers during gait, propagated through inverse kinematic calculations, may result in some errors in the estimated MTU moment arms and lengths.

Regarding the contact forces, we decided to validate our model against existing literature and our values and patterns agreed well with the results of similar previous studies. It may be argued that considering the availability of the data published by "Grand Challenge Competition to Predict In-Vivo Knee Loads", the model should be

validated against these data (https://simtk.org/home/kneeloads). However, there are many parameters in the model that can be adjusted until a satisfactory match with the contact forces is obtained, which does not necessarily mean the model has good prediction ability. More importantly, due to variability seen among different individuals, ability of the model to estimate the contact forces for one subject does not guarantee that the same model can predict the contact forces for other subjects with the same accuracy. Furthermore, the data published for the grand challenge are for older individuals, implanted with instrumented knee prosthesis, who may have altered anatomical characteristics, so optimizing parameters of the model to match grand challenge's data would not prove the accuracy of the model for use with other individuals.

4.5.2 Comparison of tibiofemoral joint contact force between the healthy weight and obese subjects

The two subjects were walking with almost the same speeds (healthy weigh 1.09 m/s and 49 years vs. obese: 1.16 m/s and 53 years), while their BMI were different (22.6 vs. 30.1 kg/m^2). There may, however, be an effect of the small velocity difference between the subjects in the result. It should also be noted that the healthy weight subject, although not diagnosed with knee OA, walked slowly for a 49 year old asymptomatic individual, and also had EMG and knee net resultant moment patterns more characteristic of an individual with OA than asymptomatic. However, the purpose of the two-subject comparison was not to draw any definite conclusions regarding obesity and the potential development of knee OA, but to demonstrate the added utility of the EMG-driven model in defining and interpreting differences in the mechanical loading environment of the knee joint between two individuals (which could then be extended to between groups in future work), rather than results of an inverse dynamics technique alone or in combination with measured EMG data not used as input into such a model.

The mean RMSE of the calibration for the obese subject was higher than the healthy weight subject (7.83±1.26 Nm vs. 4.64±0.29 Nm), which was expected due to the fact

that the obese subject walked with higher knee sagittal plane moment (although, when normalized they are almost the same: 0.08 vs. 0.07 Nm/kg). This could also be attributed to more variations in the EMG of the obese subject (Figure 4-14).

Obtained results showed that obese subject walked with higher absolute medial, lateral, and total joint contact forces than the healthy weight individual (Figure 4-17, Table 4-8). Furthermore, the obese subject walked with higher absolute gastrocnemius and lateral hamstrings forces, while the medial hamstrings, and quadriceps forces are almost the same between the same subjects (Figure 4-16). Obtained results can be explained as follows:

Quadriceps are important contributors to the first peak of the medial contact force. Higher quadriceps EMG activity for the obese compared to the healthy weight subject (Figure 4-14) and larger knee flexion moment in the first half of the gait cycle, may suggest that obese individual should have higher quadriceps forces; however, the obese subject also had larger quadriceps moment arms; therefore, the results of the calibration yielded almost the same quadriceps forces for both subjects, showing higher EMG activity did not necessarily mean higher forces (between two individuals). Furthermore, the obese subject's first peak of the knee adduction moment was 57% higher than the other subject; therefore, it was expected that obese subject should have had a first peak of the medial joint contact force that was also 57% higher (due to the same quadriceps muscle forces and 57% higher knee adduction moment); however, the knee joint medial contact force was 24% higher than the healthy weight subject (Table 4-8). Therefore, the relationship between the knee adduction moment and peak contact force was not linear, even when the muscles had approximately the same forces. This happened due to the fact that the smaller body size of the healthy weight subject resulted in smaller distance between the contact points on the head of the tibia, meaning smaller moment arms for the medial contact force compared to the obese individual and therefore, even with the same quadriceps force and same knee adduction moment, the medial contact force was higher for the healthy weight subject. It should be also noted consistent with our findings in the last chapter, RF had a prolonged EMG activity for the obese subject

(Figure 4-14), which was reflected in the quadriceps force (Figure 4-16) due to the use of an EMG-driven model.

The medial gastrocnemius force and the net external knee adduction moment are responsible for the second peak of the knee medial contact force [104, 119]. In the second half of the stance phase, the obese subject walked with a higher net external knee extension moment compared to the healthy weight individual, while the muscle moment arms were almost the same between the two subjects. This necessitates the production of higher gastrocnemius forces, which was consistent with the higher EMG activity of gastrocnemius muscle for the obese subject (Figure 4-14). The obese individual walked with a second peak absolute adduction moment which was 29% higher than the healthy weight subject; however, higher medial gastrocnemius force for the obese subject, added to the knee adduction moment, causing the second peak of medial contact force to increase to a higher percent of 40% (Table 4-8).

Muscle forces for the obese individual also balanced a larger net external knee adduction moment (Table 4-8) potentially preventing the lateral joint from unloading, while for the healthy weight subject smaller muscle forces, seemingly did not have the ability to counteract external adduction moment and this suggest that there was a need for pretension in the lateral ligaments to prevent joint opening [108]. These results were consistent with the results obtained by Harding et al., showing higher absolute muscle and contact forces due to obesity [2], although in their study, obesity did not have a significant effect on the overall magnitude of the knee flexion and adduction moment. Aaboe et al [86] and Messier et al [88] also reported each pound of weight loss induced a reduction of the total knee joint compressive forces of 2 and 4 pounds, respectively. This may suggest that higher BMI is associated with higher absolute joint contact forces, as we have demonstrated here just with two representative cases.

These findings show that we should be cautions when we draw conclusions based on traditional gait data, including EMG and net resultant moments calculated from an inverse dynamics procedure. First, neither the EMG activity nor the knee moments

necessarily determine the muscle forces and musculoskeletal models with accurate representation of the muscles and bone geometry are needed to more accurately examine muscle force distribution through the knee joint. Second, the knee adduction moment is one important factor, but muscle forces and also the geometry of the joint, specifically the location of the contact points, can have significant effects of the calculated contact forces. Therefore, care should be take when examining the knee adduction moment, which is usually assumed to be correlated with the knee joint medial contact forces. As a matter of fact, it was shown that in medial thrust gait which results in a reduction in knee adduction moment, the medial knee joint contact force increased for a subject implanted with an instrumented prosthesis [89]. Interestingly, Manal and Buchanan used an EMG-driven model to examine the medial joint contact forces for this subject during his medial thrust gait and were able to show the unexpected increase in the medial joint contact force [159]. EMG-driven model, as shown here, is able to solve the muscle redundancy problem in line with the real activity of muscles, which makes it a powerful tool when we are dealing with individuals with altered muscle activities due to some kind of pathology, such as knee OA [31]. In our study, this method could address the force distribution between the medial and lateral gastrocnemius, which is an important factor in determining the medial knee joint contact forces in the second half of the stance phase. This is important, because the two muscles have the same function in the sagittal plane; however, higher medial gastrocnemius force results in higher medial knee joint contact forces, and this distribution was nicely solved using measured EMG. Furthermore, prolonged EMG activity of the RF, which was shown in chapter 3, was captured by our EMG-driven model, showing promise for the model to capture the alterations seen in the activity of the muscles due to knee OA (increased co-contraction) and obesity (prolonged activations, shown in the last chapter).

On the other hand, our results showed that the healthy weight subject walked with higher first normalized peak medial and total contact forces, while the second peak of the normalized medial contact force were almost the same between the two subjects (Figure 4-19, Table 4-9). The second peak of the normalized total contact force was

higher for the obese subject. Furthermore, healthy weight subject walked with increased normalized quadriceps muscle forces (except RF) (Figure 4-18), which resulted in the higher first peak of the medial contact force compared to the obese individual; while for the second half, the interaction is a little more complicated: the external normalized knee adduction moment about the lateral contact points are almost the same for both subject (not shown here), accompanied by higher normalized gastrocnemius moment for the obese subject compared to the healthy weight individual (Figure 4-20); however, the moment arm for the medial contact force (about the lateral contact point) is smaller for the healthy weight subject; therefore, this interaction results in almost the same normalized joint contact forces (Figure 4-19). Our results for the normalized forces are different from the findings of Harding et al., showing no difference in normalized muscle forces with increasing BMI category [2].

There are some limitations with this study. First, EMG measurement are usually subject to cross talk [35], which can be even amplified in the case of obese individuals, the EMG signals for each muscle can be contaminated by adjacent muscles. To minimize the cross talk, electrodes were placed on the muscle bellies based on standard protocols [31] and isolated resistance testing was performed for different muscle to make sure that the cross talk is minimized. Second, finding the activation of VI using activation of VM and VL and difficulty in separating the EMG activity of SM and ST and BFLH and BFSH may have introduced some errors in the results. Third, it was assumed that the contact forces are acting on articular surfaces only through one point, located at the midpoint of each compartment. However, the contact points were reported to be moving approximately around 3 mm in anteroposterior and mediolateral directions [192, 193]. Sensitivity analysis showed that change up to 10 mm results in less than 5% change in predicted contact loads [119]. It was assumed only forces parallel to the shaft of tibia contribute to the contact forces of articular surfaces and shear forces were neglected; although, Shelburne et al reported that the influence of shear forces in total knee joint contact forces are small [104]. Only one healthy weight and one obese subjects were included in the study. Currently, we are using our model to find the tibiofemoral joint contact forces for more individuals and the data will be used to

examine the effect of obesity (in order to draw stronger conclusions). Finally, although EMG-driven model helps us capture the real patterns of muscle activities during different tasks, still the search space for muscle parameters is big and the results may not reflect the real values of muscle forces [184]. Finding the real muscle parameters were also harder in our study, due to the fact that we did not have the experimental data for different tasks such as running, medial thrust gait, etc, which would make the search space more constrained.

4.6 CONCLUSIONS

In conclusion, the EMG-driven model implemented in this chapter has the ability to solve the muscle redundancy problem in an effective way based on the real activation patterns of the muscle. Specifically when dealing with new gait patterns and pathologies, EMG-driven model may give us realistic muscle forces which then can be used to find biomechanical variables of interest which are not readily possible to measure using more traditional biomechanical analysis techniques such as inverse dynamics, and in our case tibiofemoral joint contact forces. Furthermore, our case study demonstrated that muscle forces may have a significant effect on the medial joint contact forces, implicated to be involved in the progression of knee OA. Our future aim is to apply our model to a gait database of individuals with asymptomatic and symptomatic knees with a range of BMIs to examine how altered muscle activity, and possibly other changed kinematic and kinetic variables may change the knee joint contact loading and relate this information to knee OA development and progression longitudinally.

CHAPTER 5 Conclusions

5.1 THESIS SUMMARY

Obesity is known as a major risk factor for the development and progression of knee OA [54, 55]. It has been proposed to affect the joint through linked mechanical and metabolic factors [55]. However, its precise role in the pathomechanics of the disease is still not well understood [60]. Given the importance of altered mechanical environment in both initiation and progression of knee OA [10], it is crucial to examine if and how obesity may affect the joint mechanically, and this probably gives us the ability to manage conservative treatment options to slow the progression of the disease or even prevent it.

This thesis is a continuing work of our group on the role obesity and its influence on joint mechanics. Previous work in our group showed that obese individuals walk with altered pattern of the loading of the knee joint [1] and furthermore, obesity may expose the joint to higher absolute contact forces found through an inverse dynamics model [2]. Following the previous work on obesity by our group, in this thesis we aimed to analyze the influence of obesity and its interaction with knee OA on the activation patterns of major knee muscles, and then implement an EMG-driven model, which was capable of incorporating real measured activity of knee muscles to find the muscle forces, validate the model against existing results in the literature, and finally show the utility of the model to examine the knee joint contact forces through a case study, which included one obese and one healthy weight asymptomatic subject.

Two primary objective were addressed in this thesis. First, the interacting role of obesity and moderate knee osteoarthritis on activation patterns of the periarticular knee musculature during self-selected gait were examined. The EMG activity of 295 individuals with and without knee OA were analyzed using PCA, to examine the patterns of the muscle activities rather than only looking at peak and mean parameters

of the EMG waveforms. The results of this study, described in Chapter 3, revealed that in contrast to the results of the previous studies in the literature [128, 130], obese individuals walk with altered knee joint muscle activity that includes delayed and prolonged activation of gastrocnemius, and also sustained activity of quadriceps.

Given the important role of the muscles in tibiofemoral joint contact forces [90], altered activity of the gastrocnemius and quadriceps suggest that obesity may result in altered contact forces, which may be responsible for joint degeneration. However, it is not possible to assess the muscle forces based on their EMG, as many factors are involved in the force produced by muscles. Therefore, there was a need to obtain the knee joint contact forces, using real activation patterns of the muscles to assess if obesity influences the tibiofemoral joint contact forces or not. Following our first study, we implemented an EMG-driven model, working based on the measured experimental gait data, including 3D motion and ground reaction force data and also electromyography. The model was validated against the existing results in literature. The EMG-driven model then was used to conduct a case study in which the knee joint contact forces of an obese and a healthy weight subject with asymptomatic knees were compared in order to show the utility of the model and its potential to be used for further studying the populations with altered gait and muscle activation patterns. The results of our case study showed that the obese individual walked with higher absolute knee joint contact forces compared to the healthy weight subject, and this happened due to a combination of higher absolute muscle forces and higher net external knee adduction moment. Furthermore, the model was able to predict the muscle forces, consistent with their measured EMG. Specifically, prolonged activations seen in the activity of the RF for the obese subject, was reflected in the force profile, and contributed to tibiofemoral contact force that was not reflected in the net external moments from inverse dynamics.

5.2 IMPLICATIONS OF THESIS RESULTS

The results of this thesis have implications for the management of knee osteoarthritis. Our first study showed that obese individuals walk with prolonged activity of the knee joint major muscles. This implies that the muscle activity may result in the sustained application of the force on the knee articular surfaces, which may lead to the degeneration of the joint [194]. Our study was cross-sectional in nature, and therefore difficult to draw conclusions regarding the effect of weight loss on neuromuscular control. However, if the same relationships held for weight loss, then it is possible that weight loss could contribute to a more favorable joint mechanical environment.

Our second study which was performed on one obese and one asymptomatic individual, showed that the obese subject walked with increased absolute knee joint medial and lateral contact forces, from contributions from both a larger knee adduction moment and higher muscle forces. This result for the one obese individual in this study, with higher absolute knee joint contact forces, was consistent with the population-based statistical results found by Harding et al. using a two-dimensional contact force model without EMG input [2]. Because there is variability in EMG profiles of obese individuals (Chapter 3), the EMG-driven model implemented in Chapter 4 should be used to examine a larger cohort in order to be able to draw conclusions regarding tibiofemoral contact forces during gait with and without obesity. It was demonstrated in chapter 4 that gait waveforms, including net resultant joint moments obtained using inverse dynamics, and linear enveloped EMG, may not accurately reflect real tibiofemoral joint contact forces, and there is a need for more detailed models, taking into account musculoskeletal geometry, external and muscle forces and their interactions at the same time.

Furthermore, in chapter 4 it was demonstrated that the EMG-driven model is capable of finding the distribution of the muscle forces corresponding to the directly measured activation patterns of the muscle. This is specifically important when we are dealing with populations with some kind pathology such as knee OA, which has been shown to

be associated with increased co-contraction of the muscles [31] or prolonged activation as shown in the case of obese individuals in chapter 3 of this thesis. In addition, EMG-driven model was able to distinguish between muscles with the same function based on their activations, and as demonstrated for the particular cases highlighted in chapter 4, this was most important in the second half of the gait cycle when the gastrocnemii are responsible for the propulsion of the body. The distribution of the force between the medial and lateral gastrocnemius is important in determining accurate peak of the knee joint medial contact forces in the second half of the stance phase. Overall, the results show promise for the implemented EMG-driven model for further investigation of different risk factors that may result in alteration in knee joint loading and progression of disease, such as knee osteoarthritis.

5.3 LIMITATIONS

The limitations in this thesis are associated with the limitations of the experimental gait data collection, the assumptions in the development of the EMG-driven model, and the small number of the subjects used to examine the influence of obesity on knee joint contact forces. First, EMG measurement is prone to cross talk. Although in our lab, individuals are usually asked to perform resistant isolated exercises in order to minimize this effect, due to the amount of adipose tissue in the case of obese individuals, cross talk can be amplified and as a result, measured EMG signals may be contaminated by activity and signals from adjacent muscles. Therefore, this limitation in the data collection may have introduced some errors in our analysis in Chapter 3. More specifically, cross talk would act primarily to amplify the signal, and therefore the first PC for each muscle group may be most affected by the cross talk, because this PC usually shows the overall amplitude of the waveforms. However, for other PCs which are showing the relative activity of muscles in different points of gait, we can be more confident that the effect of cross talk is almost canceled by the relative nature of those PCs. Furthermore, the EMG-driven model uses these EMG activities as an input, which may also cause some error in the muscle force estimation problem.

Second, errors in the inverse dynamics model due to some assumptions, such as ones made for measuring the inertial properties of the segment and also excess skin marker movement in obese individuals [195], may introduce some errors both in the calibration of the EMG-driven model and also in the calculation of tibiofemoral joint contact forces using sagittal and frontal plane knee moment from inverse dynamics model. Furthermore, the errors propagated into inverse kinematics calculation due to the skin movement of the markers also can have a significant effect on the EMG-driven model [159], as the MTU lengths and moment arms are solely a function of inverse kinematics and error in the measurement of the movement will be translated to these variables and therefore, may introduce some error to the obtained muscle forces. In addition, the problem of error in the measurement of the muscle moment arms due to inaccurate musculoskeletal geometry as a result of uniform scaling of generic musculoskeletal models to match a subject of interest may results in error in muscle forces.

There are limitations as well with the implemented EMG-driven model. First, although the model is a powerful tool to solve the muscle redundancy problem, especially when we are dealing with pathologies and atypical gait patterns, the search space for the muscle parameters is large and therefore there is not a unique solution. It is possible, then, that the calibrated muscle parameters do not reflect their real values and therefore, real muscle forces [184]. Experimental motion and EMG data during different tasks accompanied by a more detailed lower limb model, which benefits from subject specific muscle parameters, obtained using imaging techniques such as MRI may improve our model. In addition, the assumptions made to find the activation of the muscles such as VI, may have introduced some error in the obtained muscle forces.

Finally, the contact model assumes that the location contact points are almost constant at the middle of the each aspect of the tibia; however, this may not be true [192]. This is important, because the ratio of muscle and contact force values to their corresponding frontal plane moment arms about medial and lateral contact points are large; therefore,

small deviations in the contact point locations may result in big changes in the obtained contact forces.

Obtained results in our case study were based on the comparison of only two subjects with different BMI, and almost the same walking speeds. Therefore, it only gives us a demonstration of the potential utility of the model and how obesity may influence the joint forces. Therefore, strong conclusions regarding the role of the obesity in the joint contact loading may not be drawn and the model should be applied to more individuals with a range of BMI to be able to make stronger statements about the obesity and how it changes joint mechanical loading.

Finally, the method of validation used here, i.e. validation against existing results in literature is not perfect. The problem is that there is not still any perfect method for validating the models which are developed to calculate knee joint contact forces. In addition, even validating the model against the knee grand challenged does not guarantee the accuracy of the model for other cases, due to the variability among different individuals.

5.4 FUTURE DIRECTIONS

The case study using the implemented EMG-driven model in chapter 4 demonstrated the potential ability of the model to capture differences in the tibiofemoral articular loading of the two subjects with different body mass indices. In the future, the model should be used for more subjects with different levels of BMI and in the presence of knee OA in order to be able to draw statistically strong conclusions, regarding the effect of obesity and knee OA and their interactions on knee articular contact loading. This will be necessary to understand if there is a biomechanical role of obesity implicated in knee OA initiation and progression.

It has been proposed that weight loss in obese individuals may result in the reduction of the knee joint contact forces [88]; However, due to improvement in the joint function after weight loss, walking speed may increase and this may cause the knee joint contact forces to increase [196]. Therefore, weight loss studies for obese individuals should be performed, while the joint contact loading before and after weight loss are monitored using the EMG-driven model to assess if the weight loss is a viable treatment strategy for obese individuals for the reduction of knee joint contact forces. Furthermore, the model should be used in longitudinal studies to examine the effect of tibiofemoral joint contact forces at baseline on the progression of the knee OA.

More efforts should be made to improve the implemented EMG-driven model to predict the knee joint contact forces with more certainty for individuals. One improvement could be to use a full lower limb model accompanied by sufficient experimental data during different tasks, which would improve the training of EMG-driven model for more certainty of estimated muscle forces. In addition, the use of subject specific muscle parameters using MRI may improve the ability of the model to solve the muscle redundancy problem. Furthermore, new techniques should be developed in order to determine more accurate articular contact points and their movement during gait to find the medial and lateral knee joint contact forces with more accuracy. One of the interesting applications of the EMG-driven model is its ability to be used for online purposes after it is calibrated. Therefore, the model can be used for the purpose of training individuals with obesity and knee OA to learn new gait patterns in order to reduce their joint contact loading and therefore, probably decrease the rate of the progression of knee OA.

In conclusion, this thesis demonstrated that higher body mass index was associated with altered activation patterns of major knee periarticular muscles during gait. Following this finding, a considerable amount of work was performed to implement an electromyography driven model in order to incorporate the real activation patterns of muscles in solving the muscle redundancy problem. Obtained muscle forces then were used for determining the tibiofemoral joint medial, lateral, and total contact forces. The

model was calibrated for a few subjects, validated against existing literature and used to demonstrate its potential utility to examine how obesity may contribute to the alteration of the mechanical environment of the knee joint. Future work aims at the use of the model with large cohort with varying levels of BMI in order to draw statistical conclusions regarding the role of obesity on tibiofemoral joint contact forces during walking.

Bibliography

1. Harding, G.T., et al., *Body mass index affects knee joint mechanics during gait differently with and without moderate knee osteoarthritis.* Osteoarthritis Cartilage, 2012. **20**(11): p. 1234-42.
2. Harding, G., *OBESITY, MODERATE KNEE OSTEOARTHRITIS, AND KNEE JOINT DYNAMICS*, in *School of biomedical engineering*. 2012, Dalhousie university.
3. Das, S.K. and A. Farooqi, *Osteoarthritis.* Best Pract Res Clin Rheumatol, 2008. **22**(4): p. 657-75.
4. Felson, D.T., et al., *Osteoarthritis: new insights. Part 1: the disease and its risk factors.* Ann Intern Med, 2000. **133**(8): p. 635-46.
5. Hunter, D.J., *Risk stratification for knee osteoarthritis progression: a narrative review.* Osteoarthritis Cartilage, 2009. **17**(11): p. 1402-7.
6. Perruccio, A.V., J.D. Power, and E.M. Badley, *The relative impact of 13 chronic conditions across three different outcomes.* J Epidemiol Community Health, 2007. **61**(12): p. 1056-61.
7. Coleman, R., *The cost of chronic disease in Nova Scotia.* Health Canada, Population and Public Health Branch, Atlantic Region, 2002.
8. Andriacchi, T.P., et al., *A framework for the in vivo pathomechanics of osteoarthritis at the knee.* Ann Biomed Eng, 2004. **32**(3): p. 447-57.
9. Kuettner, K.G., VM. Introduction. In: Kuettner K, Goldberg VM, editors., *Osteoarthritic disorders.* . Rosemont (IL): American Academy of Orthopaedic Surgeons;, 1995: p. xxi–v.
10. Brandt, K.D., P. Dieppe, and E.L. Radin, *Etiopathogenesis of osteoarthritis.* Rheum Dis Clin North Am, 2008. **34**(3): p. 531-59.
11. Brandt, K.D., et al., *Yet more evidence that osteoarthritis is not a cartilage disease.* Ann Rheum Dis, 2006. **65**(10): p. 1261-4.
12. Burr, D.B. and M.B. Schaffler, *The involvement of subchondral mineralized tissues in osteoarthrosis: quantitative microscopic evidence.* Microsc Res Tech, 1997. **37**(4): p. 343-57.

13. Andriacchi, T.P. and A. Mundermann, *The role of ambulatory mechanics in the initiation and progression of knee osteoarthritis.* Curr Opin Rheumatol, 2006. **18**(5): p. 514-8.
14. Winter, D.A., *Biomechanics and Motor Control and Human Movement*. second ed. 1990: Wiley, New York, .
15. Ying, N. and W. Kim, *Use of dual Euler angles to quantify the three-dimensional joint motion and its application to the ankle joint complex.* J Biomech, 2002. **35**(12): p. 1647-57.
16. Woltring, H.J., *Representation and calculation of 3-D joint movement.* Human Movement Science, 1991. **10**(5): p. 603-616.
17. Buckwalter, J.A., et al., *The increasing need for nonoperative treatment of patients with osteoarthritis.* Clin Orthop Relat Res, 2001(385): p. 36-45.
18. Felson, D.T., et al., *The prevalence of knee osteoarthritis in the elderly. The Framingham Osteoarthritis Study.* Arthritis Rheum, 1987. **30**(8): p. 914-8.
19. Sharma, L., et al., *Knee adduction moment, serum hyaluronan level, and disease severity in medial tibiofemoral osteoarthritis.* Arthritis Rheum, 1998. **41**(7): p. 1233-40.
20. Guccione, A.A., *Arthritis and the process of disablement.* Phys Ther, 1994. **74**(5): p. 408-14.
21. Kaufman, K.R., et al., *Gait characteristics of patients with knee osteoarthritis.* J Biomech, 2001. **34**(7): p. 907-15.
22. Astephen, J.L., et al., *Biomechanical changes at the hip, knee, and ankle joints during gait are associated with knee osteoarthritis severity.* J Orthop Res, 2008. **26**(3): p. 332-41.
23. Messier, S.P., et al., *Osteoarthritis of the knee: effects on gait, strength, and flexibility.* Arch Phys Med Rehabil, 1992. **73**(1): p. 29-36.
24. Hurwitz, D.E., et al., *The knee adduction moment during gait in subjects with knee osteoarthritis is more closely correlated with static alignment than radiographic disease severity, toe out angle and pain.* J Orthop Res, 2002. **20**(1): p. 101-7.

25. Miyazaki, T., et al., *Dynamic load at baseline can predict radiographic disease progression in medial compartment knee osteoarthritis.* Annals of the Rheumatic Diseases, 2002. **61**: p. 617-22.
26. Weidenhielm, L., et al., *Adduction moment of the knee compared to radiological and clinical parameters in moderate medical osteoarthrosis of the knee.* Ann Chir Gynaecol, 1994. **83**(3): p. 236-42.
27. Vincent, K.R., et al., *The pathophysiology of osteoarthritis: a mechanical perspective on the knee joint.* Pm r, 2012. **4**(5 Suppl): p. S3-9.
28. Landry, S.C., et al., *Knee biomechanics of moderate OA patients measured during gait at a self-selected and fast walking speed.* J Biomech, 2007. **40**(8): p. 1754-61.
29. Mundermann, A., C.O. Dyrby, and T.P. Andriacchi, *Secondary gait changes in patients with medial compartment knee osteoarthritis: increased load at the ankle, knee, and hip during walking.* Arthritis Rheum, 2005. **52**(9): p. 2835-44.
30. Hubley-Kozey, C., K. Deluzio, and M. Dunbar, *Muscle co-activation patterns during walking in those with severe knee osteoarthritis.* Clin Biomech (Bristol, Avon), 2008. **23**(1): p. 71-80.
31. Hubley-Kozey, C.L., et al., *Neuromuscular alterations during walking in persons with moderate knee osteoarthritis.* J Electromyogr Kinesiol, 2006. **16**(4): p. 365-78.
32. Hubley-Kozey, C.L., et al., *Alterations in neuromuscular patterns between pre and one-year post-total knee arthroplasty.* Clin Biomech (Bristol, Avon), 2010. **25**(10): p. 995-1002.
33. Hubley-Kozey, C.L., et al., *Co-activation differences in lower limb muscles between asymptomatic controls and those with varying degrees of knee osteoarthritis during walking.* Clin Biomech (Bristol, Avon), 2009. **24**(5): p. 407-14.
34. Konard, P., *The ABC of EMG*. 2005.
35. GL., S., *Selected topics in surface electromyography for use in the occupational setting: expert perspectives.* . 1992: Washington, DC: US Department of Health and Human Services, US National Institute for Occupational Safety and Health.

36. Ivanenko, Y.P., R.E. Poppele, and F. Lacquaniti, *Five basic muscle activation patterns account for muscle activity during human locomotion.* J Physiol, 2004. **556**(Pt 1): p. 267-82.
37. Carr, L.J., et al., *Patterns of central motor reorganization in hemiplegic cerebral palsy.* Brain, 1993. **116 (Pt 5)**: p. 1223-47.
38. Unnithan, V.B., et al., *Cocontraction and phasic activity during GAIT in children with cerebral palsy.* Electromyogr Clin Neurophysiol, 1996. **36**(8): p. 487-94.
39. Childs, J.D., et al., *Alterations in lower extremity movement and muscle activation patterns in individuals with knee osteoarthritis.* Clin Biomech (Bristol, Avon), 2004. **19**(1): p. 44-9.
40. Mills, K., et al., *A systematic review and meta-analysis of lower limb neuromuscular alterations associated with knee osteoarthritis during level walking.* Clin Biomech (Bristol, Avon), 2013. **28**(7): p. 713-24.
41. Lewek, M.D., et al., *Stride-to-stride variability of knee motion in patients with knee osteoarthritis.* Gait Posture, 2006. **23**(4): p. 505-11.
42. Hortobagyi, T., et al., *Altered hamstring-quadriceps muscle balance in patients with knee osteoarthritis.* Clin Biomech (Bristol, Avon), 2005. **20**(1): p. 97-104.
43. Schmitt, L.C. and K.S. Rudolph, *Influences on knee movement strategies during walking in persons with medial knee osteoarthritis.* Arthritis Rheum, 2007. **57**(6): p. 1018-26.
44. Heiden, T.L., D.G. Lloyd, and T.R. Ackland, *Knee joint kinematics, kinetics and muscle co-contraction in knee osteoarthritis patient gait.* Clin Biomech (Bristol, Avon), 2009. **24**(10): p. 833-41.
45. Liikavainio, T., et al., *Gait and muscle activation changes in men with knee osteoarthritis.* Knee, 2010. **17**(1): p. 69-76.
46. Astephen, J.L., et al., *Gait and neuromuscular pattern changes are associated with differences in knee osteoarthritis severity levels.* J Biomech, 2008. **41**(4): p. 868-76.

47. Rudolph, K.S., L.C. Schmitt, and M.D. Lewek, *Age-related changes in strength, joint laxity, and walking patterns: are they related to knee osteoarthritis?* Phys Ther, 2007. **87**(11): p. 1422-32.
48. Rutherford, D.J., et al., *Neuromuscular alterations exist with knee osteoarthritis presence and severity despite walking velocity similarities.* Clin Biomech (Bristol, Avon), 2011. **26**(4): p. 377-83.
49. Felson, D.T., *Risk factors for osteoarthritis: understanding joint vulnerability.* Clin Orthop Relat Res, 2004(427 Suppl): p. S16-21.
50. *Obesity: preventing and managing the global epidemic. Report of a WHO consultation.* World Health Organ Tech Rep Ser, 2000. **894**: p. i-xii, 1-253.
51. M., T., *Adult obesity in canada: Measured height and weight.* Statistics Canada, 2004.
52. Wang, Y. and T. Lobstein, *Worldwide trends in childhood overweight and obesity.* Int J Pediatr Obes, 2006. **1**(1): p. 11-25.
53. Must, A. and R.S. Strauss, *Risks and consequences of childhood and adolescent obesity.* Int J Obes Relat Metab Disord, 1999. **23 Suppl 2**: p. S2-11.
54. Davis, M.A., W.H. Ettinger, and J.M. Neuhaus, *Obesity and osteoarthritis of the knee: evidence from the National Health and Nutrition Examination Survey (NHANES I).* Semin Arthritis Rheum, 1990. **20**(3 Suppl 1): p. 34-41.
55. Felson, D.T., *The epidemiology of knee osteoarthritis: results from the Framingham Osteoarthritis Study.* Semin Arthritis Rheum, 1990. **20**(3 Suppl 1): p. 42-50.
56. Hochberg, M.C., et al., *The association of body weight, body fatness and body fat distribution with osteoarthritis of the knee: data from the Baltimore Longitudinal Study of Aging.* J Rheumatol, 1995. **22**(3): p. 488-93.
57. Sturmer, T., K.P. Gunther, and H. Brenner, *Obesity, overweight and patterns of osteoarthritis: the Ulm Osteoarthritis Study.* J Clin Epidemiol, 2000. **53**(3): p. 307-13.
58. Sonne-Holm, S. and S. Jacobsen, *[Osteoarthritis and obesity]*. Ugeskr Laeger, 2006. **168**(2): p. 187-90.

59. Felson, D.T., et al., *Risk factors for incident radiographic knee osteoarthritis in the elderly: the Framingham Study.* Arthritis Rheum, 1997. **40**(4): p. 728-33.
60. Manninen, P., et al., *Overweight, gender and knee osteoarthritis.* Int J Obes Relat Metab Disord, 1996. **20**(6): p. 595-7.
61. Oliveria, S.A., et al., *Body weight, body mass index, and incident symptomatic osteoarthritis of the hand, hip, and knee.* Epidemiology, 1999. **10**(2): p. 161-6.
62. Dougados, M., et al., *Longitudinal radiologic evaluation of osteoarthritis of the knee.* J Rheumatol, 1992. **19**(3): p. 378-84.
63. Wolfe, F. and N.E. Lane, *The longterm outcome of osteoarthritis: rates and predictors of joint space narrowing in symptomatic patients with knee osteoarthritis.* J Rheumatol, 2002. **29**(1): p. 139-46.
64. Dieppe, P.A., J. Cushnaghan, and L. Shepstone, *The Bristol 'OA500' study: progression of osteoarthritis (OA) over 3 years and the relationship between clinical and radiographic changes at the knee joint.* Osteoarthritis Cartilage, 1997. **5**(2): p. 87-97.
65. Niu, J., et al., *Is obesity a risk factor for progressive radiographic knee osteoarthritis?* Arthritis Rheum, 2009. **61**(3): p. 329-35.
66. Felson, D.T., et al., *The effect of body weight on progression of knee osteoarthritis is dependent on alignment.* Arthritis Rheum, 2004. **50**(12): p. 3904-9.
67. Sharma, L., et al., *The mechanism of the effect of obesity in knee osteoarthritis: the mediating role of malalignment.* Arthritis Rheum, 2000. **43**(3): p. 568-75.
68. Moyer, R.F., et al., *Alignment, body mass and their interaction on dynamic knee joint load in patients with knee osteoarthritis.* Osteoarthritis Cartilage, 2010. **18**(7): p. 888-93.
69. Lee, R. and W.F. Kean, *Obesity and knee osteoarthritis.* Inflammopharmacology, 2012. **20**(2): p. 53-8.
70. Grotle, M., et al., *Obesity and osteoarthritis in knee, hip and/or hand: an epidemiological study in the general population with 10 years follow-up.* BMC Musculoskelet Disord, 2008. **9**: p. 132.

71. Pottie, P., et al., *Obesity and osteoarthritis: more complex than predicted!* Ann Rheum Dis, 2006. **65**(11): p. 1403-5.
72. Browning, R.C., et al., *Effects of obesity and sex on the energetic cost and preferred speed of walking.* J Appl Physiol (1985), 2006. **100**(2): p. 390-8.
73. Hortobagyi, T., et al., *Massive weight loss-induced mechanical plasticity in obese gait.* J Appl Physiol (1985), 2011. **111**(5): p. 1391-9.
74. McGraw, B., et al., *Gait and postural stability in obese and nonobese prepubertal boys.* Arch Phys Med Rehabil, 2000. **81**(4): p. 484-9.
75. Messier, S.P., *Osteoarthritis of the knee and associated factors of age and obesity: effects on gait.* Med Sci Sports Exerc, 1994. **26**(12): p. 1446-52.
76. Spyropoulos, P., et al., *Biomechanical gait analysis in obese men.* Arch Phys Med Rehabil, 1991. **72**(13): p. 1065-70.
77. Gushue, D.L., J. Houck, and A.L. Lerner, *Effects of childhood obesity on three-dimensional knee joint biomechanics during walking.* J Pediatr Orthop, 2005. **25**(6): p. 763-8.
78. Michał Plewa, J.C.Ś., Bogdan Bacik, Barbara Zahorska-Markiewicz, Andrzej Markiewicz, Janusz W. Błaszczyk, *Effects of the Weight loss Treatment on Selected Kinematic Gait Parameters in Obese Women.* Journal of Human Kinetics, 2007. **18**: p. 3-14.
79. Larsson, U.E. and E. Mattsson, *Influence of weight loss programmes on walking speed and relative oxygen cost (%VO2max) in obese women during walking.* J Rehabil Med, 2003. **35**(2): p. 91-7.
80. Browning, R.C. and R. Kram, *Effects of obesity on the biomechanics of walking at different speeds.* Med Sci Sports Exerc, 2007. **39**(9): p. 1632-41.
81. Griffin, T.M., T.J. Roberts, and R. Kram, *Metabolic cost of generating muscular force in human walking: insights from load-carrying and speed experiments.* J Appl Physiol (1985), 2003. **95**(1): p. 172-83.
82. Stephen R Messier, W.H.E., Jr., Thomas E. Doyle, Timothy Morgan, Margaret K. James, Mary L. O'Toole, and Robert Burns, *Obesity: Effects on Gait in an Osteoarthritic Population.* JOURNAL OF APPLIED BIOMECHANICS, 1996. **12**: p. 161-1 72.

83. DeVita, P. and T. Hortobagyi, *Obesity is not associated with increased knee joint torque and power during level walking.* J Biomech, 2003. **36**(9): p. 1355-62.
84. Foti, T., J.R. Davids, and A. Bagley, *A biomechanical analysis of gait during pregnancy.* J Bone Joint Surg Am, 2000. **82**(5): p. 625-32.
85. Quesada, P.M., et al., *Biomechanical and metabolic effects of varying backpack loading on simulated marching.* Ergonomics, 2000. **43**(3): p. 293-309.
86. Aaboe, J., et al., *Effects of an intensive weight loss program on knee joint loading in obese adults with knee osteoarthritis.* Osteoarthritis Cartilage, 2011. **19**(7): p. 822-8.
87. Messier, S.P., et al., *Weight loss reduces knee-joint loads in overweight and obese older adults with knee osteoarthritis.* Arthritis Rheum, 2005. **52**(7): p. 2026-32.
88. Messier, S.P., et al., *Does high weight loss in older adults with knee osteoarthritis affect bone-on-bone joint loads and muscle forces during walking?* Osteoarthritis Cartilage, 2011. **19**(3): p. 272-80.
89. Fregly, B.J., et al., *Grand challenge competition to predict in vivo knee loads.* J Orthop Res, 2012. **30**(4): p. 503-13.
90. Herzog, W., D. Longino, and A. Clark, *The role of muscles in joint adaptation and degeneration.* Langenbecks Arch Surg, 2003. **388**(5): p. 305-15.
91. Erdemir, A., et al., *Model-based estimation of muscle forces exerted during movements.* Clin Biomech (Bristol, Avon), 2007. **22**(2): p. 131-54.
92. Finni, T., P.V. Komi, and J. Lukkariniemi, *Achilles tendon loading during walking: application of a novel optic fiber technique.* Eur J Appl Physiol Occup Physiol, 1998. **77**(3): p. 289-91.
93. Dennerlein, J.T., *Finger flexor tendon forces are a complex function of finger joint motions and fingertip forces.* J Hand Ther, 2005. **18**(2): p. 120-7.
94. Komistek, R.D., et al., *Mathematical model of the lower extremity joint reaction forces using Kane's method of dynamics.* J Biomech, 1998. **31**(2): p. 185-9.
95. Lu, T.W., et al., *Validation of a lower limb model with in vivo femoral forces telemetered from two subjects.* J Biomech, 1998. **31**(1): p. 63-9.

96. Crowninshield, R.D., *A physiologically based criterion for muscle force predictions on locomotion.* Bull Hosp Jt Dis Orthop Inst, 1983. **43**(2): p. 164-70.
97. Glitsch, U. and W. Baumann, *The three-dimensional determination of internal loads in the lower extremity.* J Biomech, 1997. **30**(11-12): p. 1123-31.
98. Herzog, W. and P. Binding, *Predictions of antagonistic muscular activity using nonlinear optimization.* Math Biosci, 1992. **111**(2): p. 217-29.
99. McLean, S.G., et al., *Sagittal plane biomechanics cannot injure the ACL during sidestep cutting.* Clin Biomech (Bristol, Avon), 2004. **19**(8): p. 828-38.
100. Erdemir, A. and S.J. Piazza, *Changes in foot loading following plantar fasciotomy: a computer modeling study.* J Biomech Eng, 2004. **126**(2): p. 237-43.
101. Piazza, S.J. and S.L. Delp, *The influence of muscles on knee flexion during the swing phase of gait.* J Biomech, 1996. **29**(6): p. 723-33.
102. Amarantini, D. and L. Martin, *A method to combine numerical optimization and EMG data for the estimation of joint moments under dynamic conditions.* J Biomech, 2004. **37**(9): p. 1393-404.
103. Lloyd, D.G. and T.F. Besier, *An EMG-driven musculoskeletal model to estimate muscle forces and knee joint moments in vivo.* J Biomech, 2003. **36**(6): p. 765-76.
104. Shelburne, K.B., M.R. Torry, and M.G. Pandy, *Contributions of muscles, ligaments, and the ground-reaction force to tibiofemoral joint loading during normal gait.* J Orthop Res, 2006. **24**(10): p. 1983-90.
105. Thambyah, A., B.P. Pereira, and U. Wyss, *Estimation of bone-on-bone contact forces in the tibiofemoral joint during walking.* Knee, 2005. **12**(5): p. 383-8.
106. Kim, H.J., et al., *Evaluation of predicted knee-joint muscle forces during gait using an instrumented knee implant.* J Orthop Res, 2009. **27**(10): p. 1326-31.
107. Heller, M.O., et al., *The influence of alignment on the musculo-skeletal loading conditions at the knee.* Langenbecks Arch Surg, 2003. **388**(5): p. 291-7.
108. Schipplein, O.D. and T.P. Andriacchi, *Interaction between active and passive knee stabilizers during level walking.* J Orthop Res, 1991. **9**(1): p. 113-9.

109. Kuster, M.S., et al., *Joint load considerations in total knee replacement.* J Bone Joint Surg Br, 1997. **79**(1): p. 109-13.
110. Morrison, J.B., *The mechanics of the knee joint in relation to normal walking.* J Biomech, 1970. **3**(1): p. 51-61.
111. Mikosz, R.P., T.P. Andriacchi, and G.B. Andersson, *Model analysis of factors influencing the prediction of muscle forces at the knee.* J Orthop Res, 1988. **6**(2): p. 205-14.
112. Shelburne, K.B., M.R. Torry, and M.G. Pandy, *Muscle, ligament, and joint-contact forces at the knee during walking.* Med Sci Sports Exerc, 2005. **37**(11): p. 1948-56.
113. Seireg, A. and Arvikar, *The prediction of muscular lad sharing and joint forces in the lower extremities during walking.* J Biomech, 1975. **8**(2): p. 89-102.
114. Lin, Y.C., et al., *Simultaneous prediction of muscle and contact forces in the knee during gait.* J Biomech, 2010. **43**(5): p. 945-52.
115. Taylor, W.R., et al., *Tibio-femoral loading during human gait and stair climbing.* J Orthop Res, 2004. **22**(3): p. 625-32.
116. Wimmer, M.A. and T.P. Andriacchi, *Tractive forces during rolling motion of the knee: implications for wear in total knee replacement.* J Biomech, 1997. **30**(2): p. 131-7.
117. Lundberg, H.J., K.C. Foucher, and M.A. Wimmer, *A parametric approach to numerical modeling of TKR contact forces.* J Biomech, 2009. **42**(4): p. 541-5.
118. Wehner, T., L. Claes, and U. Simon, *Internal loads in the human tibia during gait.* Clin Biomech (Bristol, Avon), 2009. **24**(3): p. 299-302.
119. Winby, C.R., et al., *Muscle and external load contribution to knee joint contact loads during normal gait.* J Biomech, 2009. **42**(14): p. 2294-300.
120. Kumar, D., K.S. Rudolph, and K.T. Manal, *EMG-driven modeling approach to muscle force and joint load estimations: case study in knee osteoarthritis.* J Orthop Res, 2012. **30**(3): p. 377-83.
121. Kumar, D., K.T. Manal, and K.S. Rudolph, *Knee joint loading during gait in healthy controls and individuals with knee osteoarthritis.* Osteoarthritis Cartilage, 2013. **21**(2): p. 298-305.

122. Catalfamo, P.F., et al., *Anterior Cruciate Ligament Injury: Compensation during Gait using Hamstring Muscle Activity.* Open Biomed Eng J, 2010. **4**: p. 99-106.
123. van Baar, M.E., et al., *Effectiveness of exercise therapy in patients with osteoarthritis of the hip or knee: a systematic review of randomized clinical trials.* Arthritis Rheum, 1999. **42**(7): p. 1361-9.
124. Anandacoomarasamy, A., et al., *Weight loss in obese people has structure-modifying effects on medial but not on lateral knee articular cartilage.* Ann Rheum Dis, 2012. **71**(1): p. 26-32.
125. Zhang, W., *Risk factors of knee osteoarthritis--excellent evidence but little has been done.* Osteoarthritis Cartilage, 2010. **18**(1): p. 1-2.
126. Rutherford, D.J., C.L. Hubley-Kozey, and W.D. Stanish, *The neuromuscular demands of altering foot progression angle during gait in asymptomatic individuals and those with knee osteoarthritis.* Osteoarthritis Cartilage, 2010. **18**(5): p. 654-61.
127. Brandon, S.C., et al., *Selective lateral muscle activation in moderate medial knee osteoarthritis subjects does not unload medial knee condyle.* J Biomech, 2014. **47**(6): p. 1409-15.
128. Hills, A.P. and A.W. Parker, *Electromyography of walking in obese children.* Electromyogr Clin Neurophysiol, 1993. **33**(4): p. 225-33.
129. Blakemore, V.J., et al., *Mass affects lower extremity muscle activity patterns in children's gait.* Gait Posture, 2013. **38**(4): p. 609-13.
130. de Carvalho, F.R., A.T. Figueira Martins, and A.M. Teixeira, *Analyses of gait and jump tasks in female obese adolescents.* Pediatr Exerc Sci, 2012. **24**(1): p. 26-33.
131. Simpson, K.M., B.J. Munro, and J.R. Steele, *Backpack load affects lower limb muscle activity patterns of female hikers during prolonged load carriage.* J Electromyogr Kinesiol, 2011. **21**(5): p. 782-8.
132. Han KH, H.E., Frykman P, Johnson M, Russell F, Rosentein M., *Load carriage: the effects of walking speed on gait timing, kinetics, and muscle*

activity. Medicine and Science in Sports and Exercise, 1992. **24**(5 Supplement:S129.).

133. Harman E, H.K., Frykman P, Johnson M, Russell F, Rosentein M. , *The effects on gait timing, kinetics and muscle activity of various loads carried on the back.* Medicine and Science in Sports and Exercise, 1992. **24**: p. 5 Supplement:S129.
134. Ghori, G.M. and R.G. Luckwill, *Responses of the lower limb to load carrying in walking man.* Eur J Appl Physiol Occup Physiol, 1985. **54**(2): p. 145-50.
135. Brandon, S.C., et al., *Interpreting principal components in biomechanics: representative extremes and single component reconstruction.* J Electromyogr Kinesiol, 2013. **23**(6): p. 1304-10.
136. Jackson, J.E., *A User's Guide to Principal Components*. 2005: John Wiley & Sons.
137. Chau, T., *A review of analytical techniques for gait data. Part 1: Fuzzy, statistical and fractal methods.* Gait Posture, 2001. **13**(1): p. 49-66.
138. Deluzio, K.J. and J.L. Astephen, *Biomechanical features of gait waveform data associated with knee osteoarthritis: an application of principal component analysis.* Gait Posture, 2007. **25**(1): p. 86-93.
139. O'Connor, K.M. and M.C. Bottum, *Differences in cutting knee mechanics based on principal components analysis.* Med Sci Sports Exerc, 2009. **41**(4): p. 867-78.
140. Kirkwood, R.N., et al., *Application of principal component analysis on gait kinematics in elderly women with knee osteoarthritis.* Rev Bras Fisioter, 2011. **15**(1): p. 52-8.
141. Patla, A.E., *Some characteristics of EMG patterns during locomotion: implications for the locomotor control process.* J Mot Behav, 1985. **17**(4): p. 443-61.
142. Kellgren, J.H. and J.S. Lawrence, *Radiological assessment of osteo-arthrosis.* Ann Rheum Dis, 1957. **16**(4): p. 494-502.
143. B. Leveau, G.B.J.A., , U.S. Department of Health and Human Services,, *Output Forms: Data Analysis and Applications, in: G.L. Soderberg (Ed.), Selected*

topics in surface electromyography for use in the occupational setting: Expert perspectives. 1992: p. 69–102.

144. Shiavi, R., H.J. Bugle, and T. Limbird, *Electromyographic gait assessment, Part 1: Adult EMG profiles and walking speed.* J Rehabil Res Dev, 1987. **24**(2): p. 13-23.

145. Winter, D.A., A.J. Fuglevand, and S.E. Archer, *Crosstalk in surface electromyography: Theoretical and practical estimates.* J Electromyogr Kinesiol, 1994. **4**(1): p. 15-26.

146. Rutherford, D.J., C.L. Hubley-Kozey, and W.D. Stanish, *Maximal voluntary isometric contraction exercises: a methodological investigation in moderate knee osteoarthritis.* J Electromyogr Kinesiol, 2011. **21**(1): p. 154-60.

147. Menegoni, F., et al., *Gender-specific effect of obesity on balance.* Obesity (Silver Spring), 2009. **17**(10): p. 1951-6.

148. Bennell, K.L., et al., *Update on the role of muscle in the genesis and management of knee osteoarthritis.* Rheum Dis Clin North Am, 2013. **39**(1): p. 145-76.

149. Slemenda, C., et al., *Quadriceps weakness and osteoarthritis of the knee.* Ann Intern Med, 1997. **127**(2): p. 97-104.

150. Maly, M.R., *Abnormal and cumulative loading in knee osteoarthritis.* Curr Opin Rheumatol, 2008. **20**(5): p. 547-52.

151. Hurley, M.V. and D.L. Scott, *Improvements in quadriceps sensorimotor function and disability of patients with knee osteoarthritis following a clinically practicable exercise regime.* Br J Rheumatol, 1998. **37**(11): p. 1181-7.

152. Hurley, M.V., *Muscle dysfunction and effective rehabilitation of knee osteoarthritis: what we know and what we need to find out.* Arthritis Rheum, 2003. **49**(3): p. 444-52.

153. Harman E, H.K., Frykman P, Pandorf CE. , *The effects of backpack weight on the biomechanics of load carriage.* Natick, USA. U.S. Army Research Institute of Environmental Medicine, 2000: p. 1–71.

154. Kuiken, T.A., M.M. Lowery, and N.S. Stoykov, *The effect of subcutaneous fat on myoelectric signal amplitude and cross-talk.* Prosthet Orthot Int, 2003. **27**(1): p. 48-54.
155. Bartuzi, P., T. Tokarski, and D. Roman-Liu, *The effect of the fatty tissue on EMG signal in young women.* Acta Bioeng Biomech, 2010. **12**(2): p. 87-92.
156. Winby, C.R., et al., *Correlation between EMG-based co-activation measures and medial and lateral compartment loads of the knee during gait.* Clin Biomech (Bristol, Avon), 2013. **28**(9-10): p. 1014-9.
157. Meyer, A.J., et al., *Are external knee load and EMG measures accurate indicators of internal knee contact forces during gait?* J Orthop Res, 2013. **31**(6): p. 921-9.
158. Kutzner, I., et al., *Knee adduction moment and medial contact force--facts about their correlation during gait.* PLoS One, 2013. **8**(12): p. e81036.
159. Manal, K. and T.S. Buchanan, *An electromyogram-driven musculoskeletal model of the knee to predict in vivo joint contact forces during normal and novel gait patterns.* J Biomech Eng, 2013. **135**(2): p. 021014.
160. Kinney, A.L., et al., *Update on grand challenge competition to predict in vivo knee loads.* J Biomech Eng, 2013. **135**(2): p. 021012.
161. Gordon Robertson, G.C., Joseph Hamill and Gary Kamen, *Research methods in biomechanics*. 2013: Champaign, Illinois: Human Kinetics.
162. Buchanan, T.S., et al., *Neuromusculoskeletal modeling: estimation of muscle forces and joint moments and movements from measurements of neural command.* J Appl Biomech, 2004. **20**(4): p. 367-95.
163. Corcos, D.M., et al., *Electromechanical delay: An experimental artifact.* J Electromyogr Kinesiol, 1992. **2**(2): p. 59-68.
164. Zajac, F.E., *Muscle and tendon: properties, models, scaling, and application to biomechanics and motor control.* Crit Rev Biomed Eng, 1989. **17**(4): p. 359-411.
165. Milner-Brown, H.S., R.B. Stein, and R. Yemm, *Changes in firing rate of human motor units during linearly changing voluntary contractions.* J Physiol, 1973. **230**(2): p. 371-90.

166. Herzog, W., et al., *EMG-force relation in dynamically contracting cat plantaris muscle.* J Electromyogr Kinesiol, 1998. **8**(3): p. 147-55.
167. Woods, J.J. and B. Bigland-Ritchie, *Linear and non-linear surface EMG/force relationships in human muscles. An anatomical/functional argument for the existence of both.* Am J Phys Med, 1983. **62**(6): p. 287-99.
168. Lawrence, J.H. and C.J. De Luca, *Myoelectric signal versus force relationship in different human muscles.* J Appl Physiol Respir Environ Exerc Physiol, 1983. **54**(6): p. 1653-9.
169. Manal, K., et al., *A real-time EMG-driven virtual arm.* Comput Biol Med, 2002. **32**(1): p. 25-36.
170. Arnold, E.M., et al., *A model of the lower limb for analysis of human movement.* Ann Biomed Eng, 2010. **38**(2): p. 269-79.
171. Delp, S.L., et al., *OpenSim: open-source software to create and analyze dynamic simulations of movement.* IEEE Trans Biomed Eng, 2007. **54**(11): p. 1940-50.
172. Ward, S.R., et al., *Are current measurements of lower extremity muscle architecture accurate?* Clin Orthop Relat Res, 2009. **467**(4): p. 1074-82.
173. Walker, P.S., J.S. Rovick, and D.D. Robertson, *The effects of knee brace hinge design and placement on joint mechanics.* J Biomech, 1988. **21**(11): p. 965-74.
174. Matthew Millard, T.U., Ajay Seth, and Scott L. Delp, *Flexing Computational Muscle: Modeling and Simulation of Musculotendon Dynamics.* J Biomech Eng., 2013. **135**(2).
175. Hill, A.V., *The heat of shortening and the dynamic constants of muscle.* Proceedingsof the Royal Society of London Series B. **126**: p. 136-195.
176. van Soest, A.J. and M.F. Bobbert, *The contribution of muscle properties in the control of explosive movements.* Biol Cybern, 1993. **69**(3): p. 195-204.
177. McLean, S.G., A. Su, and A.J. van den Bogert, *Development and validation of a 3-D model to predict knee joint loading during dynamic movement.* J Biomech Eng, 2003. **125**(6): p. 864-74.

178. Huijing, P.A., *Important experimental factors for skeletal muscle modelling: non-linear changes of muscle length force characteristics as a function of degree of activity.* Eur J Morphol, 1996. **34**(1): p. 47-54.
179. Schutte, L.M., *Using musculoskeletal models to explore strategies for improving performance in electrical stimulation-induced leg cycle ergometry.* . 1992, Stanford University.
180. Edman, K.A.P., *The Velocity of Unloaded Shortening and its Relation to Sarcomere Length and Isometric Force in Vertebrate Muscle Fibers.* J. Physiol., 1979. **291**: p. 143–159.
181. Petrofsky, J.S. and C.A. Phillips, *The influence of temperature initial length and electrical activity on the force-velocity relationship of the medial gastrocnemius muscle of the cat.* J Biomech, 1981. **14**(5): p. 297-306.
182. Katz, B., 1939,, *The Relation Between Force and Speed in Muscular Contraction.* J. Physiol. , 1939. **96**: p. 45–64.
183. Ugray, Z., Leon Lasdon, John C. Plummer, Fred Glover, James Kelly, and Rafael Martí, *Scatter Search and Local NLP Solvers: A Multistart Framework for Global Optimization.* INFORMS Journal on Computing, 2007. **16**(3): p. 328–340.
184. Gerus, P., et al., *Subject-specific knee joint geometry improves predictions of medial tibiofemoral contact forces.* J Biomech, 2013. **46**(16): p. 2778-86.
185. Crowninshield, R.D. and R.A. Brand, *The prediction of forces in joint structures; distribution of intersegmental resultants.* Exerc Sport Sci Rev, 1981. **9**: p. 159-81.
186. Crowninshield, R.D. and R.A. Brand, *A physiologically based criterion of muscle force prediction in locomotion.* J Biomech, 1981. **14**(11): p. 793-801.
187. Kutzner, I., et al., *The effect of valgus braces on medial compartment load of the knee joint - in vivo load measurements in three subjects.* J Biomech, 2011. **44**(7): p. 1354-60.
188. Hurwitz, D.E., et al., *Dynamic knee loads during gait predict proximal tibial bone distribution.* J Biomech, 1998. **31**(5): p. 423-30.

189. Sritharan, P., Y.C. Lin, and M.G. Pandy, *Muscles that do not cross the knee contribute to the knee adduction moment and tibiofemoral compartment loading during gait.* J Orthop Res, 2012. **30**(10): p. 1586-95.
190. Anderson, F.C. and M.G. Pandy, *A Dynamic Optimization Solution for Vertical Jumping in Three Dimensions.* Comput Methods Biomech Biomed Engin, 1999. **2**(3): p. 201-231.
191. D'Lima, D.D., et al., *Knee joint forces: prediction, measurement, and significance.* Proc Inst Mech Eng H, 2012. **226**(2): p. 95-102.
192. Iwaki, H., V. Pinskerova, and M.A. Freeman, *Tibiofemoral movement 1: the shapes and relative movements of the femur and tibia in the unloaded cadaver knee.* J Bone Joint Surg Br, 2000. **82**(8): p. 1189-95.
193. Hamai, S., et al., *Knee kinematics in medial osteoarthritis during in vivo weight-bearing activities.* J Orthop Res, 2009. **27**(12): p. 1555-61.
194. Hatfield, G., *DO LOWER EXTREMITY BIOMECHANICS DURING GAIT PREDICT PROGRESSION TO TOTAL KNEE ARTHROPLASTY?* . 2013, Dalhousie University.
195. Matrangola, S.L., et al., *Changes in body segment inertial parameters of obese individuals with weight loss.* J Biomech, 2008. **41**(15): p. 3278-81.
196. Henriksen, M., et al., *Is increased joint loading detrimental to obese patients with knee osteoarthritis? A secondary data analysis from a randomized trial.* Osteoarthritis Cartilage, 2013. **21**(12): p. 1865-75.

APPENDIX A Mean EMG waveforms of all groups

Figure 5A-5-1 Mean EMG waveforms for the 6 groups in chapter 3shows the mean EMG waveforms of the 6 groups included in our study presented in chapter 3.

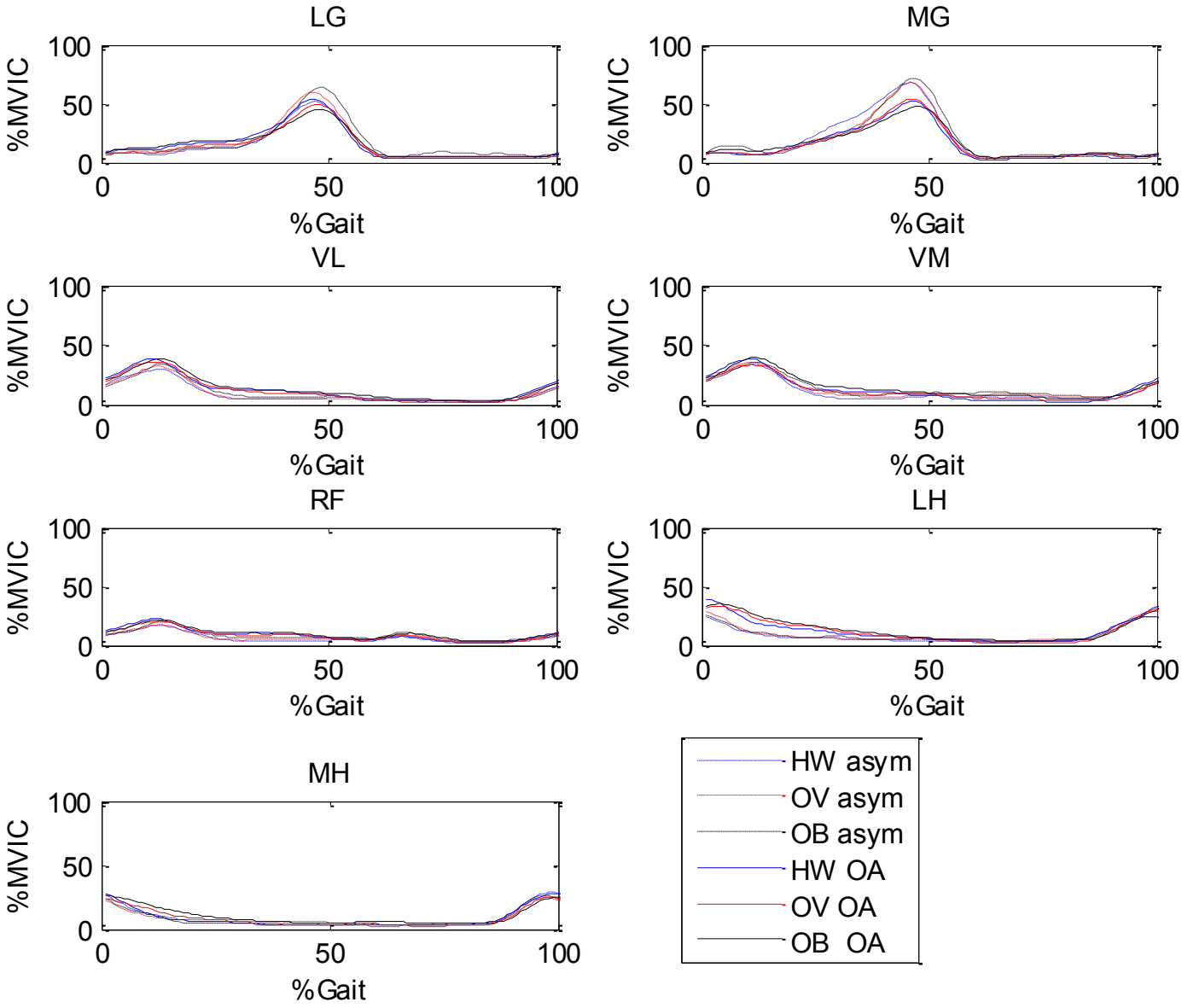

Figure 5A-5-1 Mean EMG waveforms for the 6 groups in chapter 3

APPENDIX B Histograms of Z-scores

Error! Reference source not found. Figure B-1 shows the histograms of the Z-scores obtained to test the normality of the data presented in chapter 3.

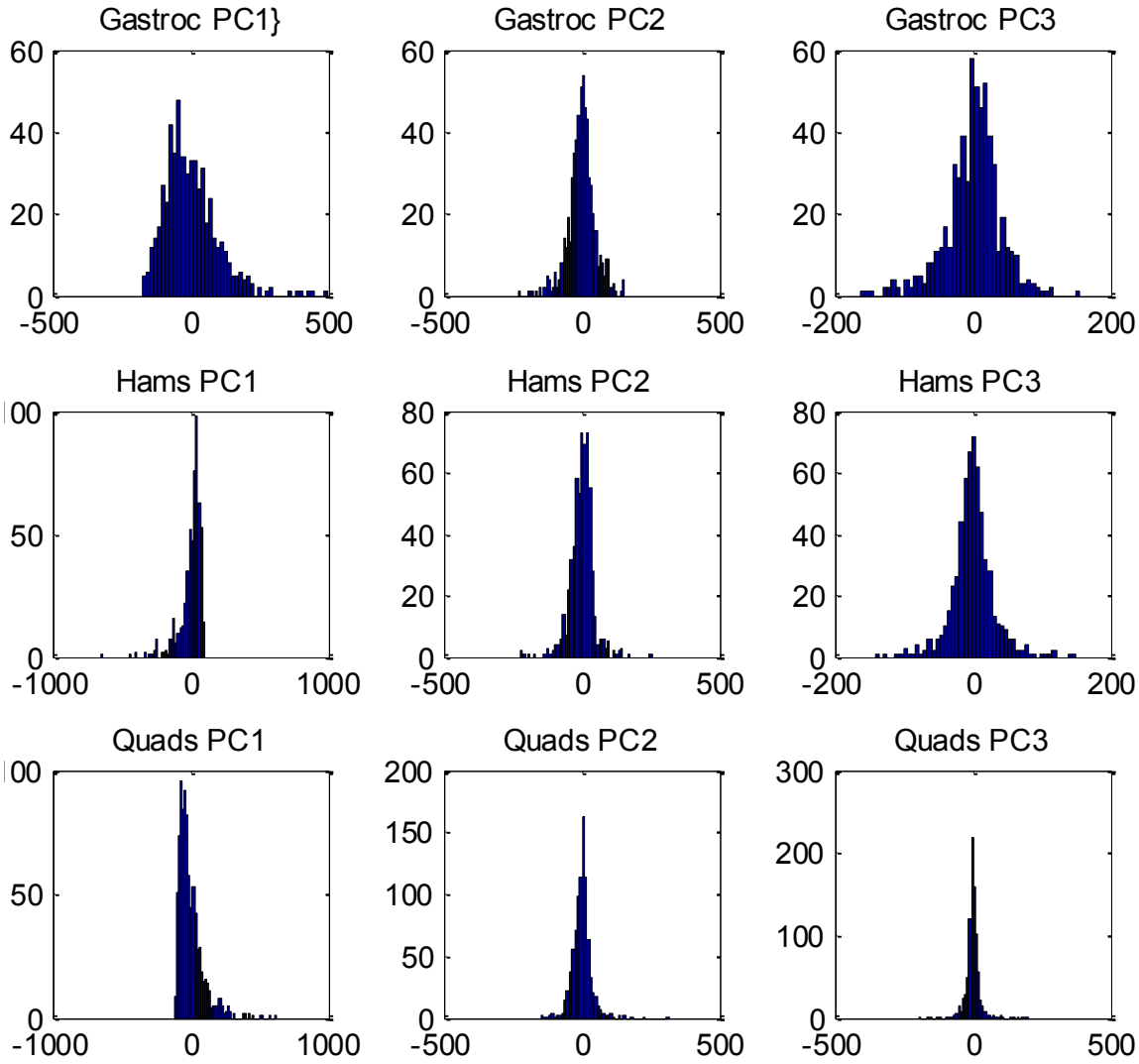

Figure B-1 Histograms for the Z-scores corresponding to the first 3 PCs for each muscle group

APPENDIX C Reconstructed EMG waveform

Figure C-1 to Figure C-7 show the mean EMG waveforms in chapter 3 and the reconstructed waveforms using the first three PCs for each group.

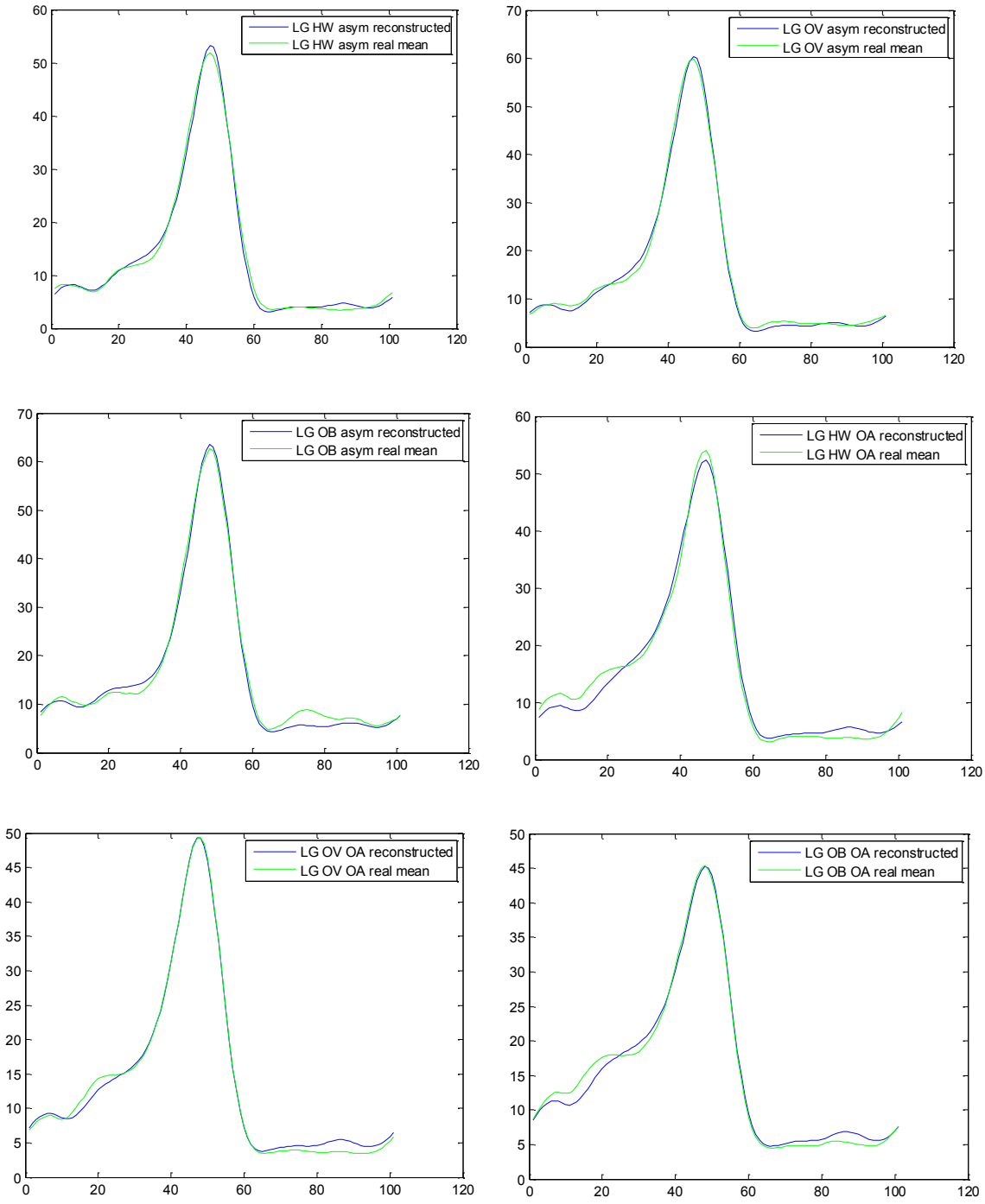

Figure C-1 Lateral gastrocnemius reconstructed wavefomrs

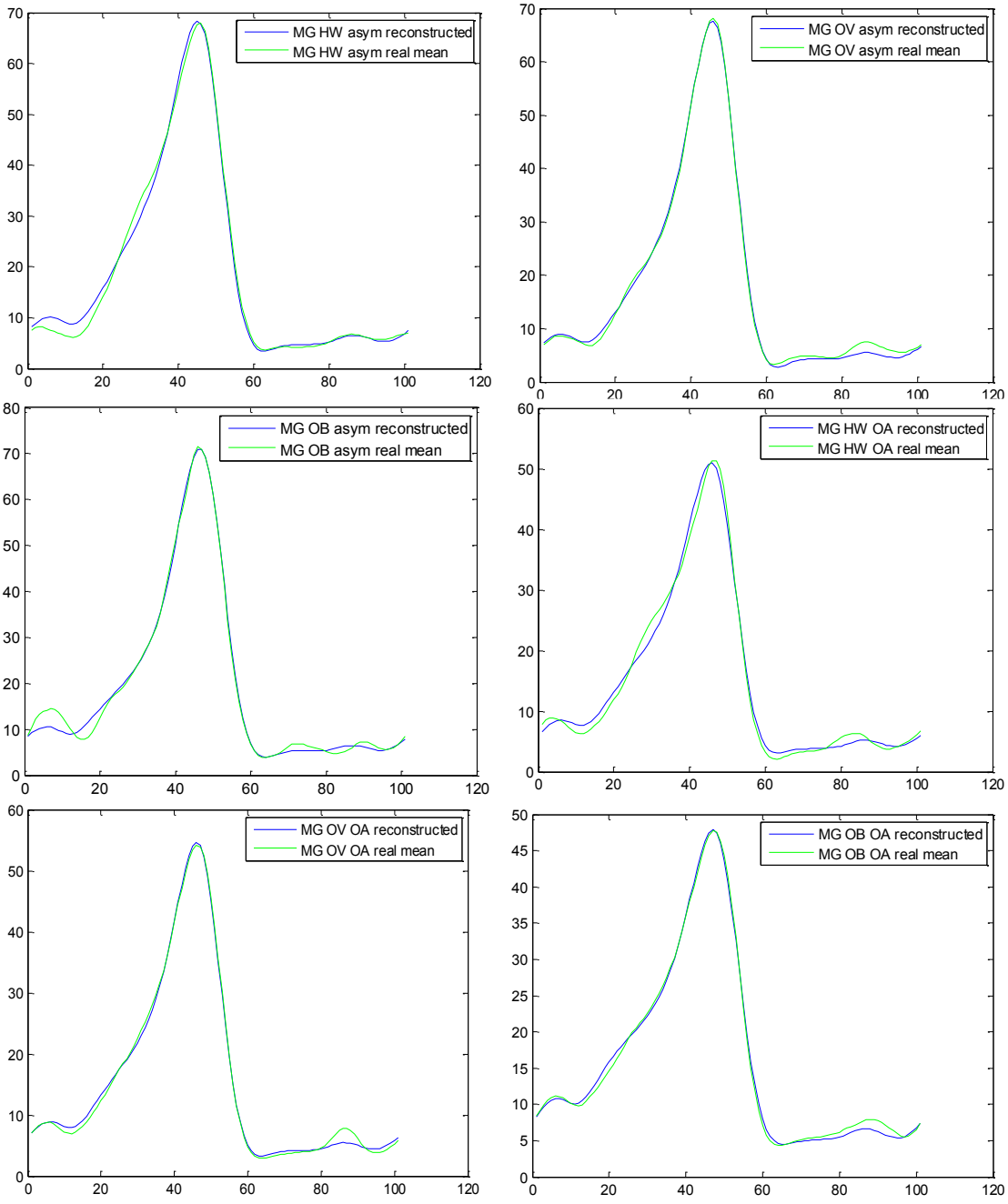

Figure C-2 Medial gastrocnemius reconstructed wavefomrs

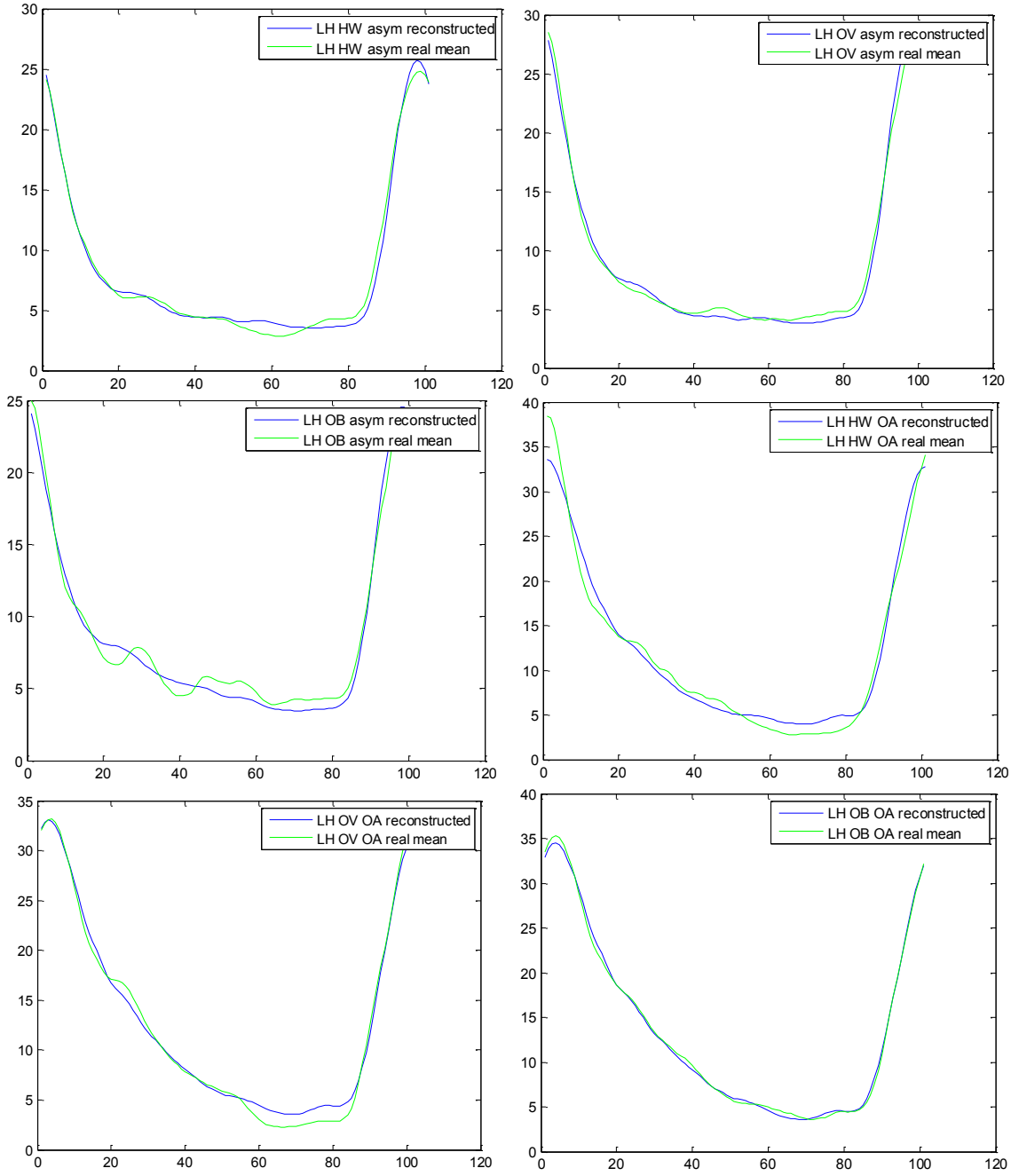

Figure C-3 Lateral hamstrings reconstructed wavefomrs

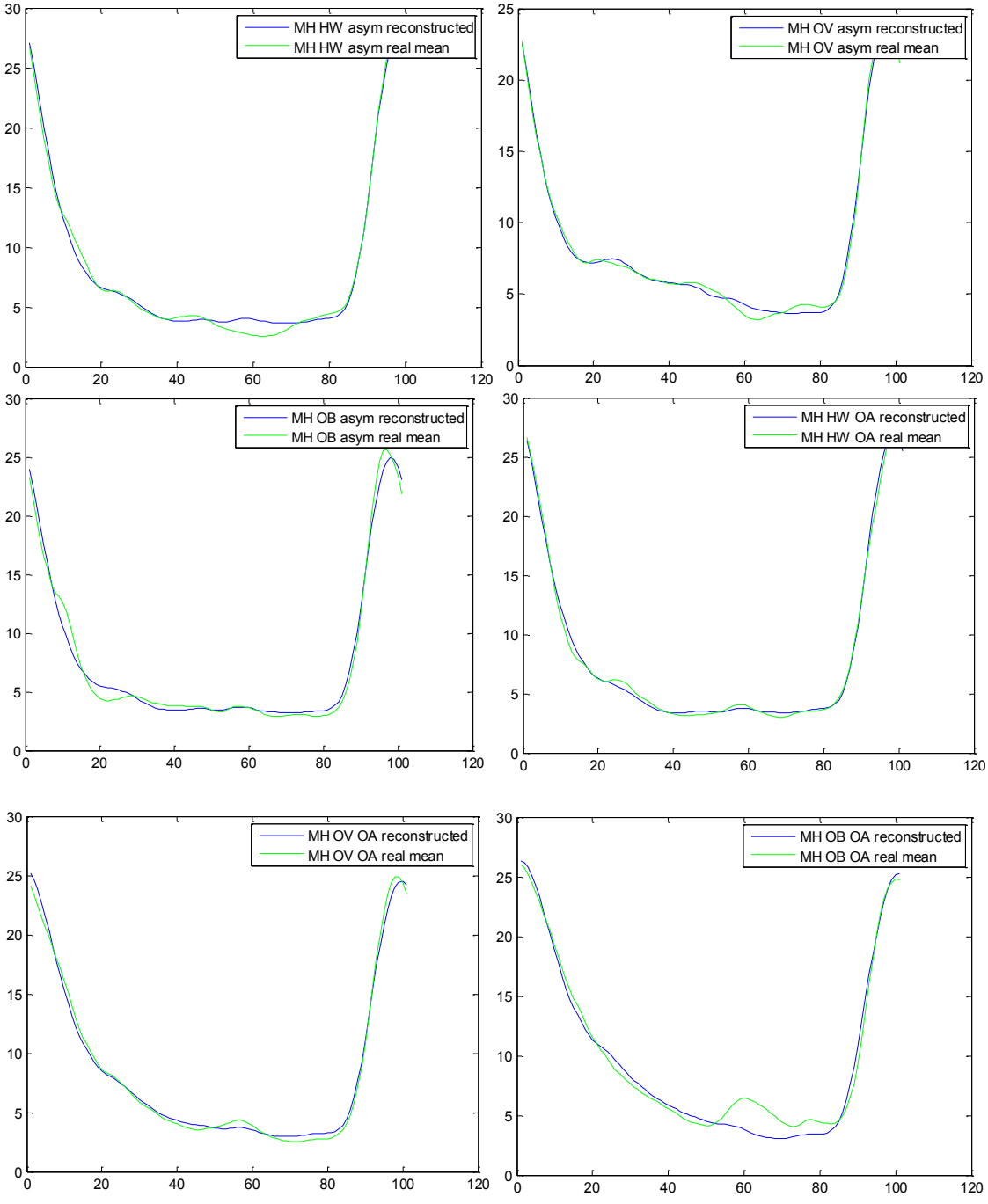

Figure C-4 Medial hamstrings reconstructed wavefomrs

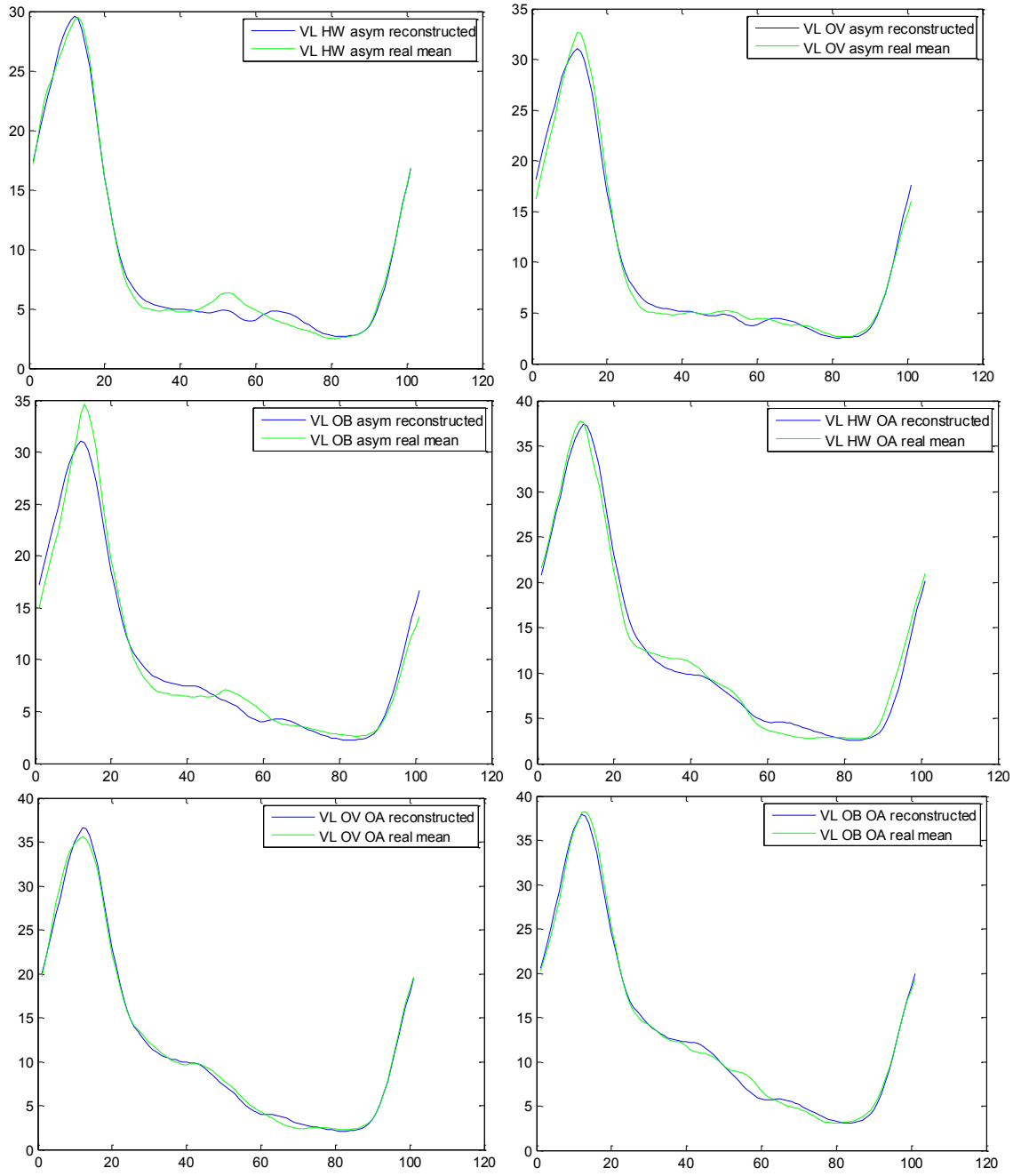

Figure C-5 Vastus lateralis reconstructed wavefomrs

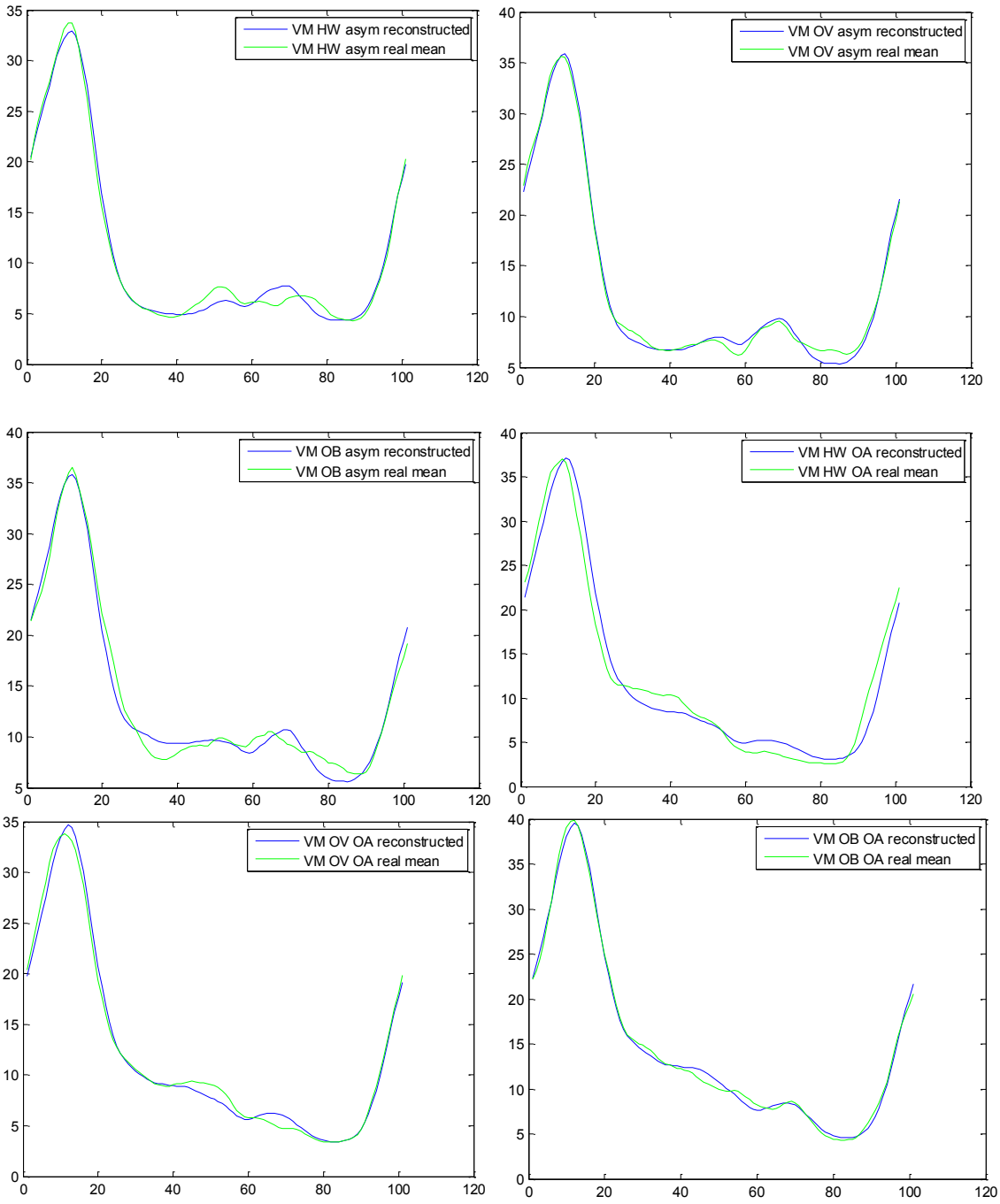

Figure C-6 Vastus medialis reconstructed wavefomrs

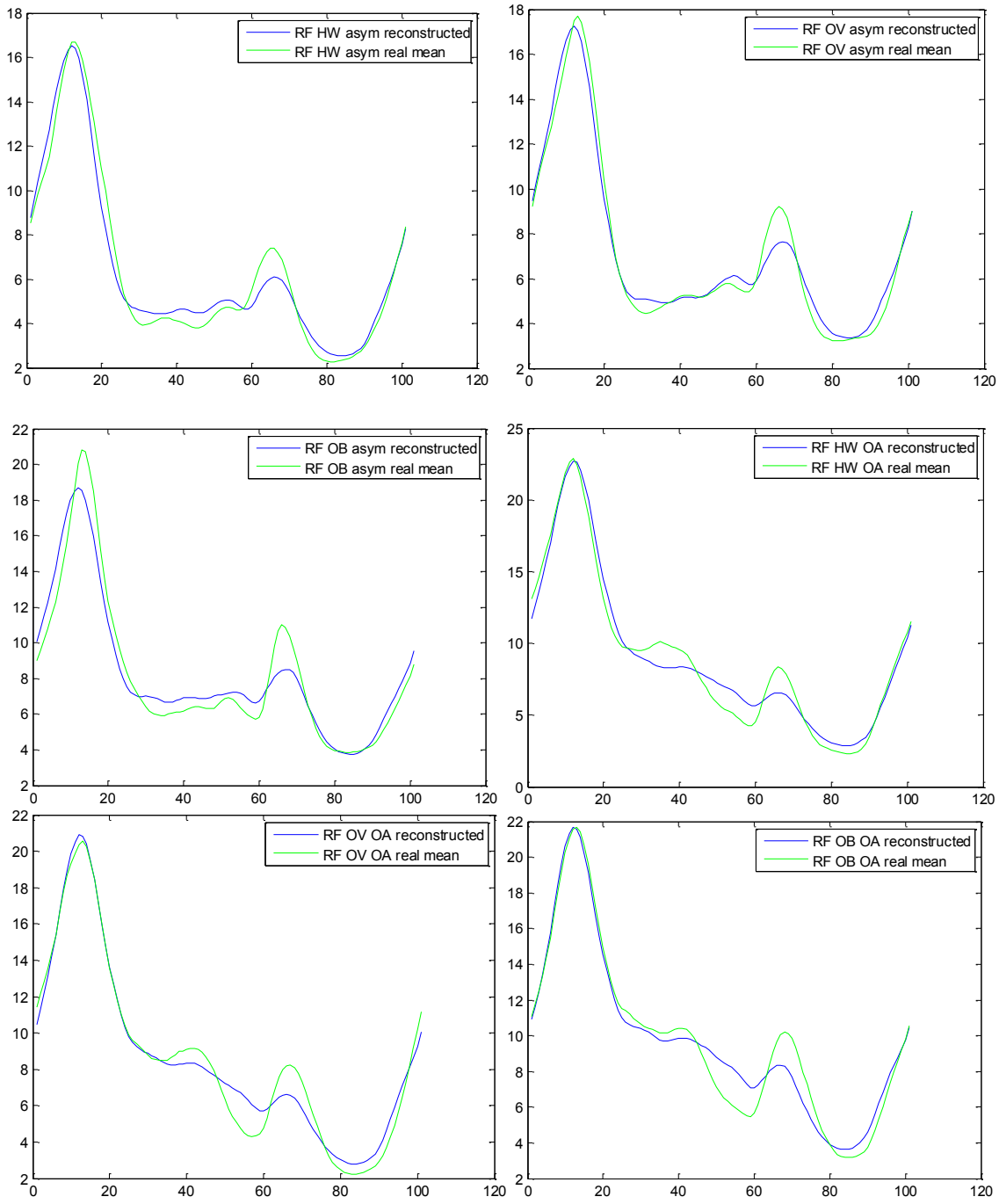

Figure C-7 Rectus femoris reconstructed wavefomrs

APPENDIX D Mean Z-scores of the EMG waveforms

Table D-1 Shows the Z-scores obtained for different groups' EMG waveforms in chapter 3.

Table D-1 Mean Z-scores corresponding to different groups in chapter 3 (values in parenthesis show standard deviations).

		Gastrocnemius			Hamstrings			Quadriceps		
		PC_1	PC_2	PC_3	PC_1	PC_2	PC_3	PC_1	PC_2	PC_3
Asym	HW	19.3 (103.7)	8.2 (56.1)	10.4 (36.7)	-24.0 (66.1)	-11.3 (34.3)	8.3 (23.4)	-22.4 (71.9)	-8.7 (24.2)	7.9 (21.4)
	OV	23.2 (112.4)	-1.9 (52.0)	16.8 (40.0)	-21 (51.9)	-7.6 (33.1)	11.5 (32.6)	-13.0 (74.6)	-6.3 (34.6)	9.9 (26.2)
	OB	33.1 (106.8)	-31.3 (55.7)	5.4 (39.3)	-26.1 (56.9)	-5.8 (31.4)	7.9 (27.4)	-5.2 (75.3)	5.3 (28.0)	6.3 (24.3)
OA	HW	-5.8 (87.1)	11.7 (52.1)	1.9 (35.3)	3.7 (71.5)	-9.8 (40.8)	-1.4 (24.0)	10.8 (82.2)	-4.2 (34.6)	-6.7 (18.9)
	OV	-12.6 (87.5)	0.1 (48.3)	3.4 (33.1)	9.8 (92.4)	4.8 (49.7)	-6.2 (33.5)	2.2 (101.7)	-0.7 (34.1)	-6.6 (31.1)
	OB	-19.5 (83)	-0.9 (38.8)	-20.4 (41.0)	23.4 (96.4)	10.9 (50.6)	-7.6 (33.5)	19.7 (117.8)	10.0 (43.9)	-4.7 (35.0)